



Universiteit
Leiden
The Netherlands

Gaining control of lipid-based nanomedicine by understanding the nano-bio interface

Pattipeiluhu, R.

Citation

Pattipeiluhu, R. (2021, December 9). *Gaining control of lipid-based nanomedicine by understanding the nano-bio interface*. Retrieved from <https://hdl.handle.net/1887/3245795>

Version: Publisher's Version

License: [Licence agreement concerning inclusion of doctoral thesis in the Institutional Repository of the University of Leiden](#)

Downloaded from: <https://hdl.handle.net/1887/3245795>

Note: To cite this publication please use the final published version (if applicable).

Appendix 1

Supplementary Information to Chapter 2

1. Supplementary Figures and Tables

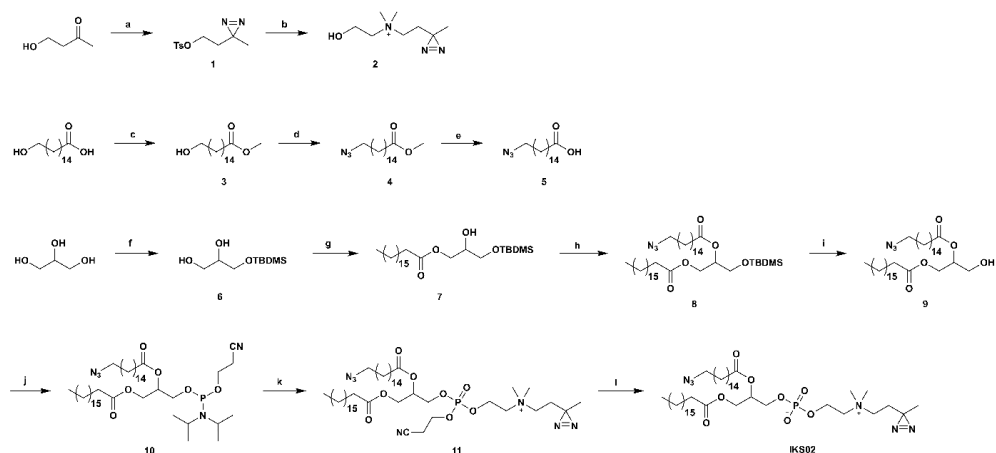


Figure S1. Synthesis scheme of the PAL probe IKS02. Reagents and conditions: (a) 1. 7N NH₃ in methanol; 2. NH₂OSO₃H; 3. I₂, Et₃N; 4. TsCl, pyridine, 20% over 4 steps; (b) DMEA, acetone, quant.; (c) AcCl, MeOH, 92%; (d) 1. MsCl, Et₃N, DCM; 2. NaN₃, DMF, 70 °C, 91% over 2 steps; (e) 4M NaOH, dioxane, 95%; (f) tBDMSCl, imidazole, DCM:DMF (1:1), -18 °C, 34%; (g) Stearic acid, DCC, DMAP, DCM, 76%; (h) 5, DCC, DMAP, DCM, 64%; (i) Et₃N·3HF, THF, quant.; (j) PCl(OCH₂CH₂CN)(NiPr₂), Et₃N, DCM, 74%; (k) 1. 2, imidazole, DCM; 2. tBuOOH, DCM, 10% over 2 steps; (l) tBuNH₂, DCM, 48%. Detailed procedures are described in the Chemical Synthesis section of the Supplementary Information.

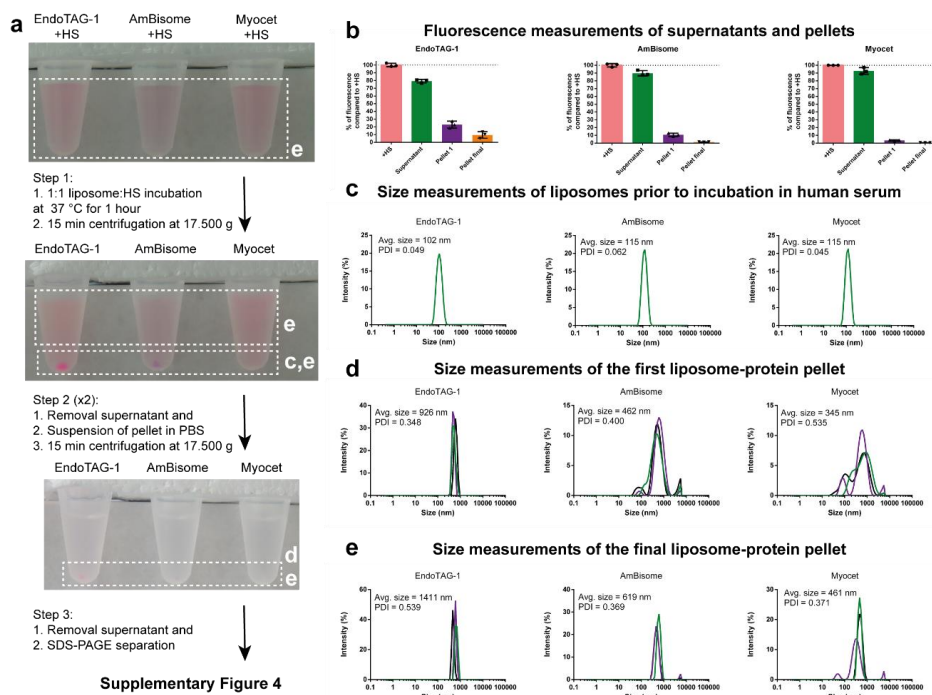


Figure S2. Sedimentation of liposome-protein complexes. **(a)** Liposomes containing 1 mol% fluorescent lipid (DOPE-LR) were incubated in human serum at a 1:1 ratio, followed by centrifugation for 15 minutes at 17,500 g. The supernatant was removed, the pellet was resuspended in PBS and the centrifugation and wash step repeated twice. After the last removal of the supernatant, the liposome-protein complexes were resolved on SDS-PAGE as shown in Figure S7. **(b)** Fluorescence measurements of supernatant and pellet from the steps described in a. Pellets were resuspended in PBS. All samples were performed in triplicate. Fluorescence of DOPE-LR (560 ex./583 em.) was determined using a fluorescence plate reader (Tecan M200, Tecan Life Sciences). **(c)** Dynamic Light Scattering (DLS) size measurements of the extruded liposomes prior to incubation in human serum. **(d)** DLS size measurements of the liposome-protein pellet after the first centrifugation step. **(e)** DLS size measurements of the liposome-protein pellet after the final centrifugation step. Pellets were resuspended in PBS (100 μ L) for DLS measurements.

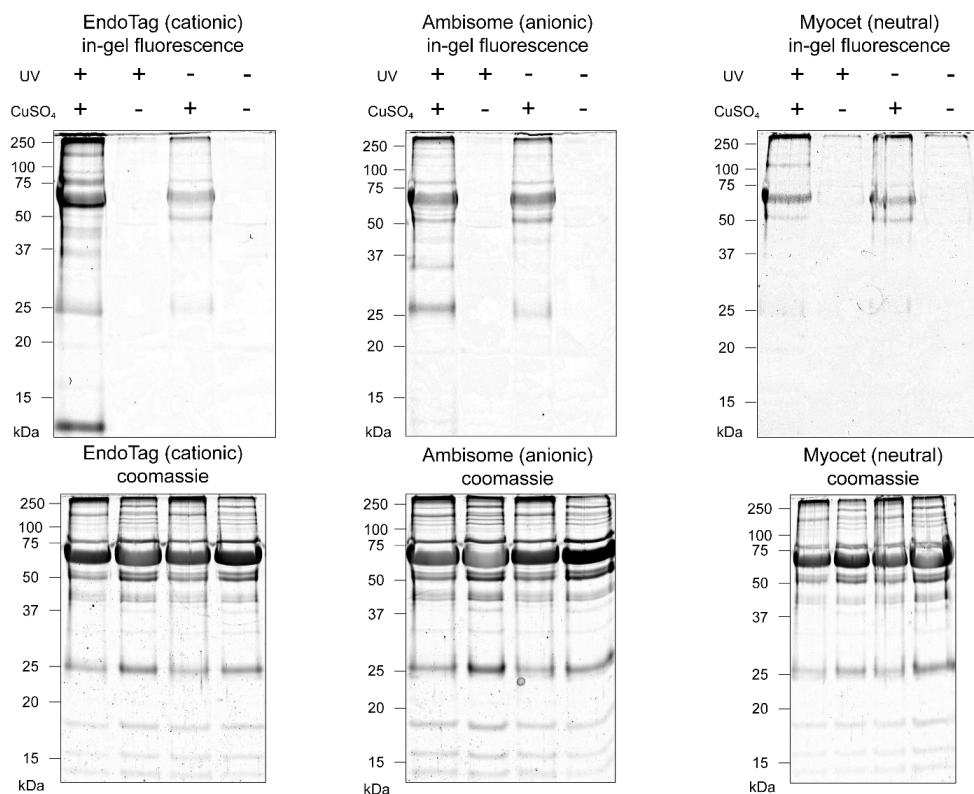
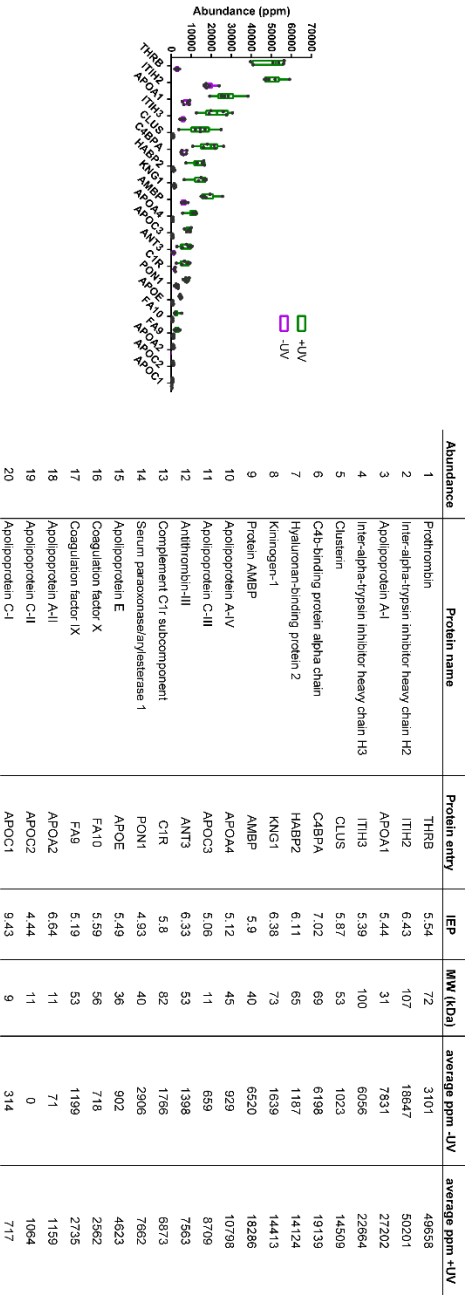
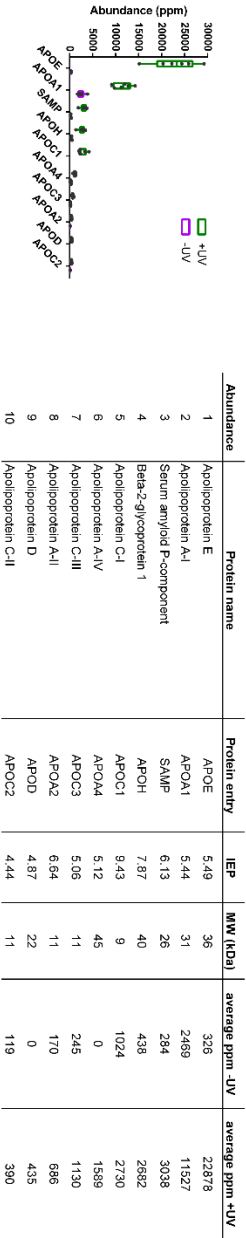


Figure S3. In-gel fluorescence and Coomassie stained SDS-PAGE gels for the photoaffinity method, displaying the fluorescently labelled protein corona (in-gel fluorescence) and the total protein content (Coomassie Blue). 10 µg total protein was loaded in each lane, as determined by BCA assay. Gels were run on a 10% polyacrylamide gel as described in the Biological Methods & Proteomics section.

EndoTAG-1



AmBisome



Myocet

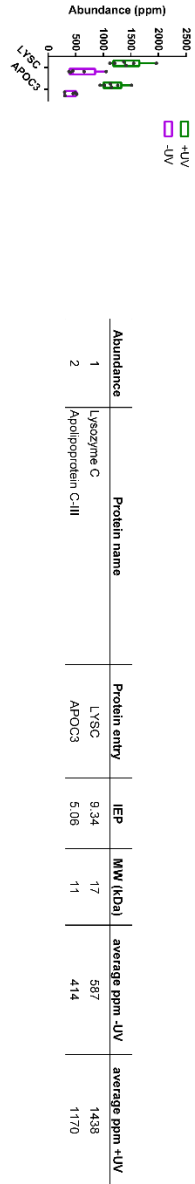


Figure S4. Abundance profiles for proteins meeting the selection criteria. Displayed as plots, showing the protein entry and abundance in both +UV and -UV samples, as well as in table format.

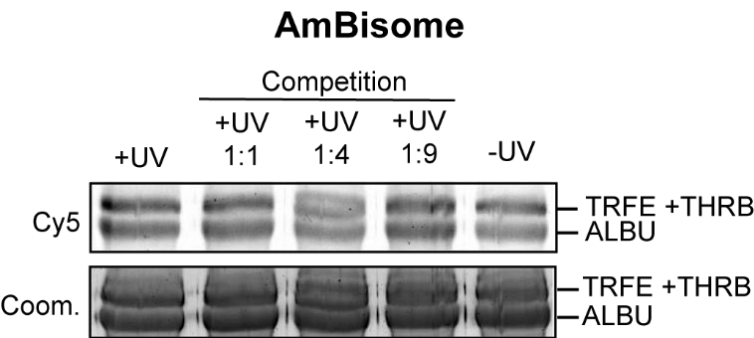


Figure S5. Competitive binding of human serum albumin (ALBU), transferrin (TRFE) and prothrombin (THRB). Increasing concentrations (1:1 to 1:9 molar ratios) of unlabeled AmBisome liposomes were incubated, together with AmBisome liposomes containing IKS02 (5 mol%), in a predefined mixture of purified human serum proteins (see Figure 4). Captured proteins were separated by SDS-PAGE and visualized by in-gel fluorescence (Cy5). Protein loading determined by Coomassie Blue (coom.).

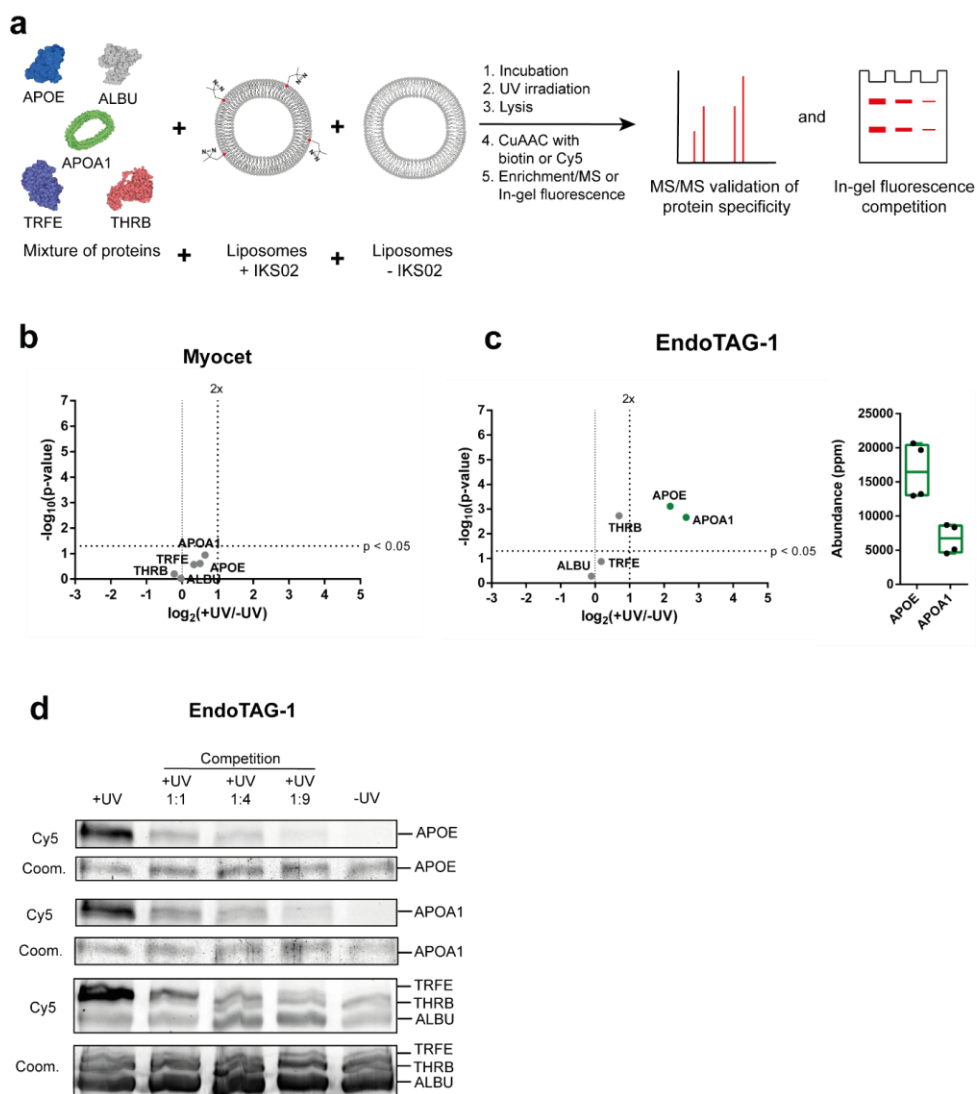


Figure S6. Validation of apolipoprotein E and A1 binding to Myocet and EndoTAG-1 liposomes. **(a)** Liposomes, containing 5 mol% IKS02, were incubated in a mixture of purified human serum proteins consisting of apolipoprotein E (APOE, 2 $\mu\text{g mL}^{-1}$), serum albumin (ALBU, 25 $\mu\text{g mL}^{-1}$), apolipoprotein A-I (APOA1, 2 $\mu\text{g mL}^{-1}$), transferrin (TRFE, 10 $\mu\text{g mL}^{-1}$) and prothrombin (THR, 2 $\mu\text{g mL}^{-1}$). **(b,c)** Volcano plot of protein enrichment over background ($\log_2(+UV/-UV)$) plotted against the statistical significance of this comparison ($-\log_{10}(p\text{-value})$). Proteins meeting all selection criteria labelled in green. For EndoTAG-1, abundance plot of apoE and apoA1 within the +UV samples. **(d)** Competition assay of apolipoprotein E and A1 binding. Increasing concentrations (1:1 to 1:9 molar ratios) of

unlabelled EndoTAG-1 liposomes were incubated, together with EndoTAG-1 liposomes containing IKSo₂ (5 mol%), in the above predefined mixture of purified human serum proteins. Captured apoE and apoA1 on the surface of IKSo₂-labeled EndoTAG-1 liposomes were separated by SDS-PAGE and visualized by in-gel fluorescence (Cy5). Protein loading determined by Coomassie Blue (coom.). Protein structures were obtained from the protein data bank (PDB): APOE: 2L7B, APOA1: 1AV1, ALBU: 1E78, THRB: 6C2W, TRFE: 1D3K). Illustrations were generated using Illustrate.

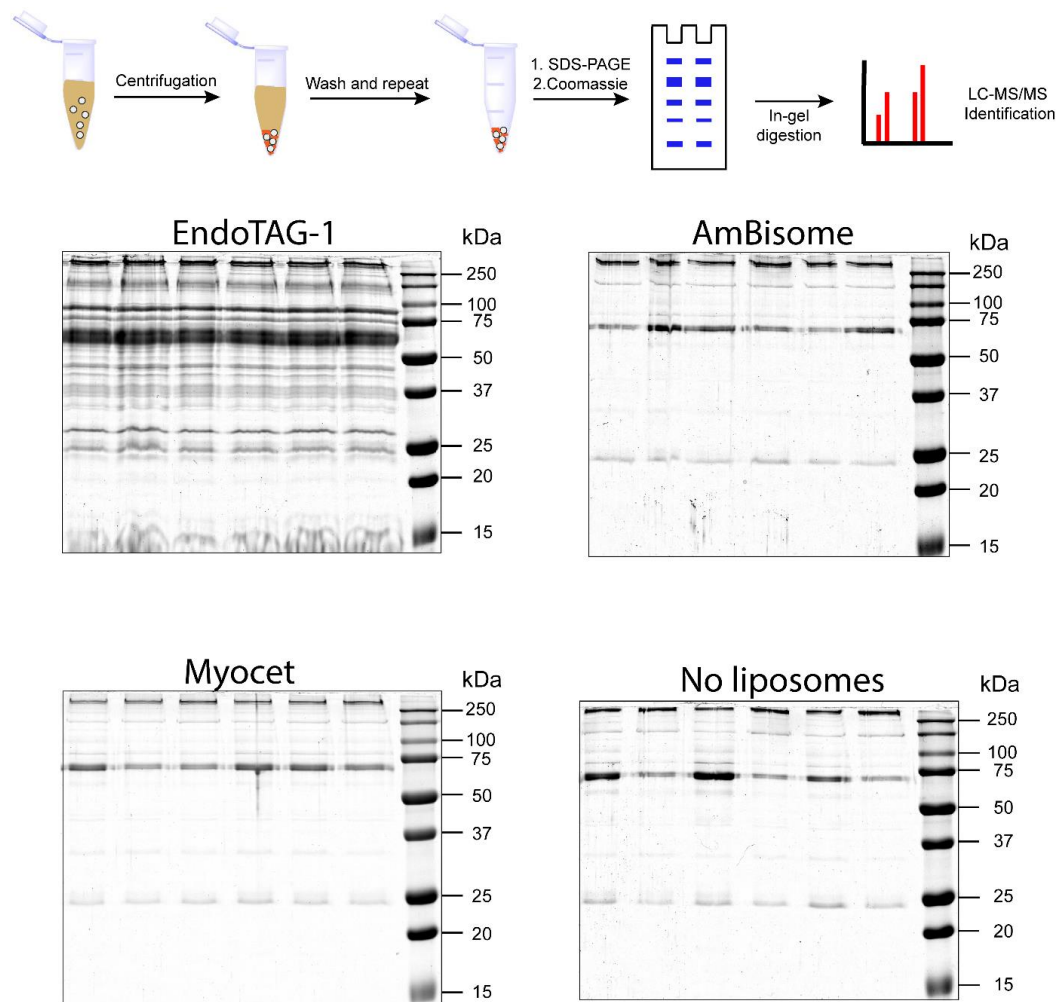


Figure S7. Gel electrophoresis (SDS-PAGE) of protein coronas isolated via centrifugation, displaying Coomassie Blue stained replicates (n=6) used for in-gel digestion. The total amount of liposome-protein complexes isolated by centrifugation were loaded in each lane without correction. Gels were run on a 10% polyacrylamide gel as described in the Biological Methods & Proteomics section.

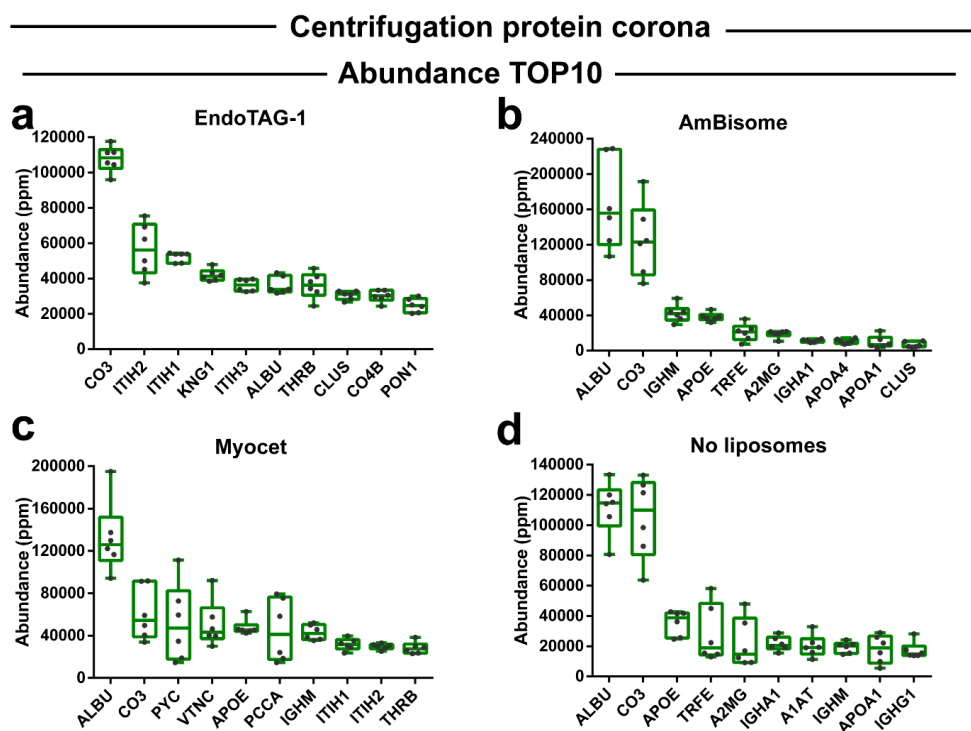


Figure S8. Top 10 most abundant proteins in the corona determined by the centrifugation method for each formulation as well as the negative control in which buffer without liposomes was added to the serum. Complete abundancy lists can be found as table format in Tables S4-7.

Formulation name	Lipid composition (mol%)	Size avg. (nm)	PDI	Zeta Potential (mV)
Myocet	55% POPC : 45% Cholesterol	105.3	0.034	-7.4 ± 2.1
AmBisome	53% DSPC : 21% DSPG : 26% Cholesterol	107.2	0.087	-24.5 ± 3.2
EndoTAG-1	51.5% DOTAP : 48.5% DOPC	101.4	0.044	+41.6 ± 4.6
Myocet + IKS02	50% POPC : 45% Cholesterol : 5% IKS02	102.1	0.042	-6.5 ± 1.8
AmBisome + IKS02	48% DSPC : 21% DSPG : 26% Cholesterol : 5% IKS02	104.8	0.079	-23.3 ± 2.7
EndoTAG-1 + IKS02	51.5% DOTAP : 43.5% DOPC : 5% IKS02	108.6	0.053	+43.2 ± 3.9
Myocet + DOPE-LR	54% POPC : 45% Cholesterol : 1% DOPE-LR	99.1	0.089	-5.2 ± 3.0
AmBisome + DOPE-LR	52% DSPC : 21% DSPG : 26% Cholesterol : 1% DOPE-LR	101.7	0.092	-28.9 ± 5.0
EndoTAG-1 + DOPE-LR	51.5% DOTAP : 47.5% DOPC : 1% DOPE-LR	104.5	0.063	+46.6 ± 5.9
Formulations in clinic/trials				
Formulation name	Lipid composition (mol%)	Size avg. (nm)	Surface charge	Encapsulated drug
Myocet	54% POPC : 45% Cholesterol : 1% DOPE-LR	150-200 nm	zwitterionic neutral	Doxorubicin
AmBisome	53% DSPC : 21% DSPG : 26% Cholesterol	78 nm	anionic	Amphotericin B
EndoTAG-1	51.5% DOTAP : 48.5% DOPC	200 nm	cationic	Paclitaxel

Table S1. Dynamic Light Scattering and zeta potential measurements for the formulations used in this study. All formulations were made through thin film hydration and extrusion described in the Biological Methods & Proteomics section of the Supplementary Information. Liposome composition and size of formulations used in clinic or clinical trials obtained from Ref. 1.

ISOQuant Configuration

parameter	value
isoquant.pluginQueue.name	design project and run ISOQuant analysis
process.peptide.deplete.PEP_FRAG_2	false
process.peptide.deplete.CURATED_0	false
process.peptide.statistics.doSequenceSearch	false
process.emrt.minIntensity	1000
process.emrt.minMass	500
process.emrt.rt.alignment.match.maxDeltaMass.ppm	10
process.emrt.rt.alignment.match.maxDeltaDriftTime	2
process.emrt.rt.alignment.normalizeReferenceTime	true
process.emrt.rt.alignment.maxProcesses	24
process.emrt.rt.alignment.referenceRun.selectionMethod	AUTO
process.emrt.clustering.preclustering.orderSequence	MTMTMT
process.emrt.clustering.preclustering.maxDistance.mass.ppm	6.06E-6
process.emrt.clustering.preclustering.maxDistance.time.min	0.202
process.emrt.clustering.preclustering.maxDistance.drift	2.02
process.emrt.clustering.distance.unit.mass.ppm	6.0E-6
process.emrt.clustering.distance.unit.time.min	0.2
process.emrt.clustering.distance.unit.drift.bin	2
process.emrt.clustering.dbscan.minNeighborCount	1
process.identification.peptide.minReplicationRate	2
process.identification.peptide.minScore	6
process.identification.peptide.minOverallMaxScore	0
process.identification.peptide.minSequenceLength	6
process.identification.peptide.acceptType.PEP_FRAG_1	true
process.identification.peptide.acceptType.IN_SOURCE	false
process.identification.peptide.acceptType.MISSING_CLEAVAGE	false
process.identification.peptide.acceptType.NEUTRAL_LOSS_H20	false
process.identification.peptide.acceptType.NEUTRAL_LOSS_NH3	false
process.identification.peptide.acceptType.PEP_FRAG_2	false
process.identification.peptide.acceptType.DDA	true
process.identification.peptide.acceptType.VAR_MOD	false
process.identification.peptide.acceptType.PTM	false
process.annotation.peptide.maxSequencesPerEMRTCuster	1
process.annotation.protein.resolveHomology	true
process.annotation.peptide.maxFDR	0.01
process.annotation.useSharedPeptides	unique
process.normalization.lowess.bandwidth	0.3
process.normalization.orderSequence	XPIR
process.normalization.minIntensity	3000
process.quantification.peptide.minMaxScorePerCluster	0
process.quantification.peptide.acceptType.IN_SOURCE	false
process.quantification.peptide.acceptType.MISSING_CLEAVAGE	false
process.quantification.peptide.acceptType.NEUTRAL_LOSS_H20	false
process.quantification.peptide.acceptType.NEUTRAL_LOSS_NH3	false
process.quantification.peptide.acceptType.PEP_FRAG_1	true
process.quantification.peptide.acceptType.PEP_FRAG_2	false
process.quantification.peptide.acceptType.VAR_MOD	false
process.quantification.peptide.acceptType.PTM	false
process.quantification.peptide.acceptType.DDA	true
process.quantification.topx.degree	3
process.quantification.topx.allowDifferentPeptides	false
process.quantification.minPeptidesPerProtein	3
process.quantification.absolute.standard.entry	ENO1_YEAST
process.quantification.absolute.standard.fmol	50
process.quantification.topx.allowDifferentPeptides	false
process.quantification.absolute.standard.entry	ENO1_YEAST
process.quantification.absolute.standard.fmol	50
process.quantification.maxProteinFDR	0.01

Table S2. ISOQuant label-free quantification (LFQ) configuration based on the TOP3 approach.

Human serum					
Abundance	Protein name	Protein entry	IEP	MW (kDa)	average ppm
1	Serum albumin	ALBU	5.89	71.4	26.08
2	Complement C3	CO3	5.99	188.7	65.56
3	Serotransferrin	TRFE	6.78	79.3	29.71
4	Alpha-2-macroglobulin	A2MG	6.04	164.7	58.25
5	Immunoglobulin heavy constant gamma 1	IGHG1	8.20	36.6	16.61
6	Alpha-1-antitrypsin	A1AT	5.25	46.9	19.39
7	Immunoglobulin heavy constant mu	IGHM	6.37	50.1	21.16
8	Apolipoprotein A-I	APOA1	5.44	30.8	14.74
9	Immunoglobulin heavy constant gamma 2	IGHG2	7.45	36.5	17.66
10	Vitamin D-binding protein	VTDB	5.16	54.5	23.22
11	Immunoglobulin heavy constant alpha 1	IGHA1	6.09	38.5	18.53
12	Immunoglobulin kappa constant	IGKC	6.13	11.9	10.02
13	Complement factor H	CFAH	6.21	143.8	54.33
14	Inter-alpha-trypsin inhibitor heavy chain H2	ITI2H	6.43	106.9	42.45
15	Apolipoprotein A-IV	APOA4	5.12	45.4	21.84
16	Complement factor B	CFAB	6.69	86.9	36.53
17	Haptoglobin	HPT	6.15	45.9	23.01
18	Immunoglobulin heavy constant gamma 3	IGHG3	7.79	42.3	22.70
19	Plasminogen	PLMN	6.93	93.3	39.75
20	C4b-binding protein alpha chain	C4BPA	7.02	69.1	32.04
21	Complement C4-B	CO4B	6.90	194.3	74.06
22	Plasma protease C1 inhibitor	IC1	6.11	55.4	27.83
23	Antithrombin-III	ANT3	6.33	53.1	27.46
24	Beta-2-glycoprotein 1	APOH	7.87	39.6	23.83
25	Hemopexin	HEMO	6.60	52.4	28.01
26	Enolase 1	ENO1	6.19	46.9	26.35
27	Immunoglobulin heavy constant gamma 4	IGHG4	7.13	36.5	23.53
28	Inter-alpha-trypsin inhibitor heavy chain H4	ITI4H	6.56	103.6	46.05
29	Complement C5	CO5	6.11	190.0	75.04
30	Gelsolin	GELS	5.87	86.1	40.66
31	Alpha-1-antichymotrypsin	AACT	5.19	47.8	28.00
32	Transthyretin	TTHY	5.42	16.0	17.81
33	Apolipoprotein A-II	APOA2	6.64	11.3	16.98
34	Inter-alpha-trypsin inhibitor heavy chain H1	ITI1H	6.35	101.8	47.40
35	Angiotensinogen	ANGT	5.88	53.4	31.44
36	Complement C1s subcomponent	C1S	4.66	78.2	39.63
37	Prothrombin	THRB	5.54	71.5	38.02
38	Ceruloplasmin	CERU	5.35	123.1	55.47
39	Apolipoprotein E	APOE	5.49	36.3	26.92
40	Heparin cofactor 2	HEP2	6.47	57.2	34.57
41	Alpha-2-HS-glycoprotein	FETUA	5.35	40.1	28.83
42	Hemoglobin subunit alpha	HBA	9.20	15.3	22.17
43	Apolipoprotein C-III	APOC3	5.06	10.9	19.64
44	Hemoglobin subunit beta	HBB	6.91	16.1	22.34
45	Complement C1r subcomponent	C1R	5.80	81.7	44.15
46	Complement C1q subcomponent subunit B	C1QB	8.87	26.9	27.27
47	N-acetylmuramoyl-L-alanine amidase	PGRP2	7.29	62.8	39.03
48	Alpha-2-antiplasmin	A2AP	5.87	54.9	36.26
49	Complement C1q subcomponent subunit C	C1QC	8.54	26.0	27.85
50	Complement C4-A	CO4A	6.68	194.4	83.69

Table S3. Abundance of proteins in human serum determined with LFQ based on the TOP3 approach, analysed with the ISOQuant software.

51	Histidine-rich glycoprotein	HRG	7.13	60.5	39.56
52	Clusterin	CLUS	5.87	53.1	36.98
53	Alpha-1B-glycoprotein	A1BG	5.50	54.8	37.77
54	Leucine-rich alpha-2-glycoprotein	A2GL	6.53	38.4	32.98
55	Serum amyloid P-component	SAMP	6.13	25.5	28.88
56	Kininogen-1	KNG1	6.38	73.0	45.14
57	Immunoglobulin heavy constant alpha 2	IGHA2	5.85	37.4	33.41
58	Haptoglobin-related protein	HPTR	6.71	39.5	34.75
59	Coagulation factor XII	FA12	7.55	70.1	45.54
60	Apolipoprotein C-I	APOC1	9.43	9.3	26.25
61	Corticosteroid-binding globulin	CBG	5.61	45.3	37.31
62	Apolipoprotein C-II	APOC2	4.44	11.3	25.91
63	Protein AMBP	AMBP	5.90	39.9	36.27
64	CD5 antigen-like	CD5L	5.15	39.6	36.26
65	Serum paraoxonase/arylesterase 1	PON1	4.93	39.9	36.61
66	Complement component C9	CO9	5.28	64.7	45.31
67	Apolipoprotein L1	APOL1	5.49	44.0	38.84
68	Vitronectin	VTNC	5.45	55.1	42.85
69	Vitamin K-dependent protein S	PROS	5.35	77.2	50.51
70	Afamin	AFAM	5.55	71.0	48.85
71	Apolipoprotein D	APOD	4.87	21.6	32.48
72	Immunoglobulin J chain	IGJ	4.91	18.6	31.82
73	Pigment epithelium-derived factor	PEDF	5.97	46.5	41.82
74	Carboxypeptidase B2	CBPB2	7.54	49.0	43.51
75	Kallistatin	KAIN	7.58	48.7	43.76
76	Plasma kallikrein	KLKB1	8.10	73.5	52.53
77	Properdin	PROP	7.75	53.8	46.18
78	Complement factor I	CFAI	7.31	68.1	51.15
79	Insulin-like growth factor-binding protein complex acid labile subunit	ALS	6.37	66.8	50.72
80	Carboxypeptidase N subunit 2	CPN2	5.59	61.4	49.00
81	Retinol-binding protein 4	RET4	5.68	23.4	36.68
82	Thyroxine-binding globulin	THBG	5.88	46.7	44.85
83	Apolipoprotein M	APOM	5.63	21.6	36.74
84	Serum amyloid A-4 protein	SAA4	9.41	14.9	36.09
85	Alpha-1-acid glycoprotein 1	A1AG1	4.74	23.7	37.83
86	Alpha-1-acid glycoprotein 2	A1AG2	4.85	23.9	38.25
87	Lumican	LUM	6.19	38.8	43.99
88	Immunoglobulin heavy constant delta	IGHD	8.10	42.8	46.30
89	Zinc-alpha-2-glycoprotein	ZA2G	5.66	34.5	43.05
90	Immunoglobulin lambda variable 1-51	LV151	6.86	12.5	36.45
91	Apolipoprotein C-IV	APOC4	9.13	14.9	38.34
92	Tetranectin	TETN	5.38	22.9	40.11
93	Hemoglobin subunit delta	HBD	8.23	16.2	39.13

Table S3. Continued.

Abundance	Protein name	Protein entry	IEP	MW (kDa)	average ppm
1	Serum albumin	ALBU	5,89	71	166624
2	Complement C3	CO3	5,99	189	125283
3	Immunoglobulin heavy constant mu	IGHM	6,37	50	42156
4	Apolipoprotein E	APOE	5,49	36	38054
5	Serotransferrin	TRFE	6,78	79	20767
6	Alpha-2-macroglobulin	A2MG	6,04	165	18900
7	Immunoglobulin heavy constant alpha 1	IGHA1	6,09	39	11451
8	Apolipoprotein A-IV	APOA4	5,12	45	10705
9	Apolipoprotein A-I	APOA1	5,44	31	9582
10	Clusterin	CLUS	5,87	53	6738
11	Haptoglobin	HPT	6,15	46	6114
12	Apolipoprotein D	APOD	4,87	22	2933

Table S4. Protein abundance for the AmBisome protein corona from the centrifugation method determined with LFQ based on the TOP3 approach, analysed with the ISOQuant software.

Myocet					
Abundance	Protein name	Protein entry	IEP	MW (kDa)	average ppm
1	Serum albumin	ALBU	5.89	71	132524
2	Complement C3	CO3	5.99	189	61074
3	Pyruvate carboxylase_ mitochondrial	PYC	6.41	130	51995
4	Vitronectin	VTNC	5.45	55	51013
5	Apolipoprotein E	APOE	5.49	36	47754
6	Propionyl-CoA carboxylase alpha chain_ mitochondrial	PCCA	7.27	81	45110
7	Immunoglobulin heavy constant mu	IGHM	6.37	50	43059
8	Inter-alpha-trypsin inhibitor heavy chain H1	ITI1H	6.35	102	31785
9	Inter-alpha-trypsin inhibitor heavy chain H2	ITI2H	6.43	107	29841
10	Prothrombin	THRB	5.54	72	28366
11	Alpha-2-macroglobulin	A2MG	6.04	165	17305
12	Serotransferrin	TRFE	6.78	79	16843
13	Apolipoprotein A-IV	APOA4	5.12	45	14697
14	Clusterin	CLUS	5.87	53	11392
15	Immunoglobulin heavy constant alpha 1	IGHA1	6.09	39	10089
16	Alpha-1-antitrypsin	A1AT	5.25	47	9162
17	Haptoglobin	HPT	6.15	46	7963
18	Serum paraoxonase/arylesterase 1	PON1	4.93	40	7590
19	Apolipoprotein A-I	APOA1	5.44	31	7056
20	Hyaluronan-binding protein 2	HABP2	6.11	65	5028
21	Apolipoprotein C-II	APOC2	4.44	11	4953
22	Heparin cofactor 2	HEP2	6.47	57	3657
23	Apolipoprotein D	APOD	4.87	22	1762
24	Dermcidin	DCD	6.14	11	1472

Table S5. Protein abundance for the Myocet protein corona from the centrifugation method determined with LFQ based on the TOP3 approach, analysed with the ISOQuant software.

No liposomes					
Abundance	Protein name	Protein entry	IEP	MW (kDa)	average ppm
1	Serum albumin	ALBU	5.89	71	111535
2	Complement C3	CO3	5.99	189	104869
3	Apolipoprotein E	APOE	5.49	36	35444
4	Serotransferrin	TRFE	6.78	79	28106
5	Alpha-2-macroglobulin	A2MG	6.04	165	21894
6	Immunoglobulin heavy constant alpha 1	IGHA1	6.09	39	21604
7	Alpha-1-antitrypsin	A1AT	5.25	47	20143
8	Immunoglobulin heavy constant mu	IGHM	6.37	50	19366
9	Apolipoprotein A-I	APOA1	5.44	31	18041
10	Immunoglobulin heavy constant gamma 1	IGHG1	8.2	37	17181
11	Apolipoprotein A-IV	APOA4	5.12	45	14567
12	Haptoglobin	HPT	6.15	46	12884
13	Clusterin	CLUS	5.87	53	12679
14	Complement C4-B	CO4B	6.9	194	8851
15	Complement C4-A	CO4A	6.68	194	8448
16	Vitronectin	VTNC	5.45	55	7579
17	Complement component C9	CO9	5.28	65	6327
18	Lactotransferrin	TRFL	8.02	80	5262
19	Apolipoprotein C-III	APOC3	5.06	11	5039
20	Lysozyme C	LYSC	9.34	17	4995
21	Gelsolin	GELS	5.87	86	4868
22	Apolipoprotein D	APOD	4.87	22	4548
23	Apolipoprotein L1	APOL1	5.49	44	4278
24	Alpha-1-antichymotrypsin	AACT	5.19	48	4244
25	Inter-alpha-trypsin inhibitor heavy chain H1	ITIH1	6.35	102	3949
26	Prothrombin	THRB	5.54	72	3850
27	Inter-alpha-trypsin inhibitor heavy chain H4	ITIH4	6.56	104	3623
28	Immunoglobulin kappa constant	IGKC	6.13	12	3404
29	Complement factor B	CFAB	6.69	87	3360
30	Serum paraoxonase/arylesterase 1	PON1	4.93	40	3319
31	Zinc-alpha-2-glycoprotein	ZA2G	5.66	34	2927
32	Dermcidin	DCD	6.14	11	2892
33	Apolipoprotein C-II	APOC2	4.44	11	2849
34	Kininogen-1	KNG1	6.38	73	2766
35	Polymeric immunoglobulin receptor	PIGR	5.44	84	2617
36	Desmoglein-1	DSG1	4.72	115	2596
37	Serum amyloid A-4 protein	SAA4	9.41	15	2372
38	Beta-2-glycoprotein 1	APOH	7.87	40	2063
39	Immunoglobulin heavy constant gamma 3	IGHG3	7.79	42	1923
40	Immunoglobulin J chain	IGJ	4.91	19	1624
41	Prolactin-inducible protein	PIP	8.1	17	1374
42	Cystatin-A	CYTA	5.22	11	1330
43	Annexin A1	ANXA1	6.67	39	1125
44	Zymogen granule protein 16 homolog B	ZG16B	7.56	23	1070
45	Hemoglobin subunit beta	HBB	6.91	16	1020
46	Apolipoprotein A-II	APOA2	6.64	11	993
47	Protein S100-A8	S10A8	6.65	11	726
48	Alpha-1-acid glycoprotein 1	A1AG1	4.74	24	657
49	Apolipoprotein C-IV	APOC4	9.13	15	653
50	Apolipoprotein C-I	APOC1	9.43	9	369

Table S6. Background protein abundance of the centrifugation method, determined with LFQ based on the TOP3 approach, analysed with the ISOQuant software.

EndoTag					
Abundance	Protein name	Protein entry	IEP	MW (kDa)	average ppm
1	Complement C3	CO3	5.99	189	107751
2	Inter-alpha-trypsin inhibitor heavy chain H2	ITI2	6.43	107	56604
3	Inter-alpha-trypsin inhibitor heavy chain H1	ITI1	6.35	102	52182
4	Kininogen-1	KNG1	6.38	73	41911
5	Inter-alpha-trypsin inhibitor heavy chain H3	ITI3	5.39	100	36208
6	Serum albumin	ALBU	5.89	71	36107
7	Prothrombin	THRB	5.54	72	36037
8	Clusterin	CLUS	5.87	53	30526
9	Complement C4-B	CO4B	6.9	194	30066
10	Serum paraoxonase/arylesterase 1	PON1	4.93	40	24734
11	Alpha-2-macroglobulin	A2MG	6.04	165	23372
12	Ceruloplasmin	CERU	5.35	123	20035
13	Alpha-1-antitrypsin	A1AT	5.25	47	19392
14	Antithrombin-III	ANT3	6.33	53	19378
15	Gelsolin	GELS	5.87	86	16063
16	Hyaluronan-binding protein 2	HABP2	6.11	65	14756
17	Apolipoprotein E	APOE	5.49	36	14519
18	Vitronectin	VTNC	5.45	55	14243
19	Immunoglobulin heavy constant mu	IGHM	6.37	50	13398
20	Complement C1s subcomponent	C1S	4.66	78	12534
21	Complement C4-A	CO4A	6.68	194	12532
22	Plasma protease C1 inhibitor	IC1	6.11	55	12190
23	Immunoglobulin heavy constant alpha 1	IGHA1	6.09	39	12126
24	Inter-alpha-trypsin inhibitor heavy chain H4	ITI4	6.56	55	11681
25	Heparin cofactor 2	HEP2	6.47	57	11613
26	Immunoglobulin heavy constant gamma 1	IGHG1	8.2	37	11328
27	Apolipoprotein A-I	APOA1	5.44	31	10414
28	Complement C1r subcomponent	C1R	5.8	82	7903
29	Complement C5	CO5	6.11	190	7690
30	Histidine-rich glycoprotein	HRG	7.13	61	7685
31	Protein AMBP	AMBP	5.9	40	7498
32	Apolipoprotein A-IV	APOA4	5.12	45	7359
33	Apolipoprotein F	APOF	5.31	36	6835
34	Vitamin K-dependent protein Z	PROZ	5.59	46	6812
35	Lumican	LUM	6.19	39	6654
36	C-reactive protein	CRP	5.32	25	6423
37	Vitamin K-dependent protein C	PROC	5.85	53	6359
38	Coagulation factor IX	FA9	5.19	53	6183
39	Complement component C9	CO9	5.28	65	5813
40	Beta-Ala-His dipeptidase	CNDP1	4.98	57	5729
41	Vitamin K-dependent protein S	PROS	5.35	77	5542
42	Alpha-2-antiplasmin	A2AP	5.87	55	5530
43	Apolipoprotein M	APOM	5.63	22	5496
44	Serotransferrin	TRFE	6.78	79	4806
45	Haptoglobin	HPT	6.15	46	4769
46	Thrombospondin-1	TSP1	4.53	133	4165
47	Coagulation factor X	FA10	5.59	56	3970
48	Alpha-1-antichymotrypsin	AACT	5.19	48	3725
49	Immunoglobulin kappa constant	IGKC	6.13	12	3478
50	Phosphatidylcholine-sterol acyltransferase	LCAT	5.69	50	3298

Table S7. Protein abundancy for the EndoTAG-1 protein corona from the centrifugation method determined with LFQ based on the TOP3 approach, analysed with the ISOQuant software.

51	Complement factor H	CFAH	6.21	144	3160
52	Ficolin-3	FCN3	6.25	33	3065
53	Apolipoprotein D	APOD	4.87	22	2992
54	Angiotensinogen	ANGT	5.88	53	2944
55	Cartilage oligomeric matrix protein	COMP	4.16	85	2936
56	Protein Z-dependent protease inhibitor	ZPI	8.6	51	2681
57	Apolipoprotein A-II	APOA2	6.64	11	2512
58	Galectin-3-binding protein	LG3BP	4.95	66	2411
59	Lipopolysaccharide-binding protein	LBP	6.27	54	2373
60	Endoplasmic	ENPL	4.56	93	2312
61	C4b-binding protein alpha chain	C4BPA	7.02	69	2268
62	Secreted phosphoprotein 24	SPP24	8.39	25	2140
63	Apolipoprotein C-II	APOC2	4.44	11	2136
64	Thrombospondin-4	TSP4	4.25	109	2072
65	Haptoglobin-related protein	HPTR	6.71	40	1926
66	Plasma serine protease inhibitor	IPSP	9.75	46	1885
67	Apolipoprotein C-III	APOC3	5.06	11	1831
68	Platelet glycoprotein Ib alpha chain	GP1BA	5.87	72	1663
69	Selenoprotein P	SEPP1	7.72	43	1613
70	Mannan-binding lectin serine protease 1	MASP1	5.16	81	1608
71	CD5 antigen-like	CDSL	5.15	40	1454
72	Apolipoprotein L1	APOL1	5.49	44	1426
73	Complement C1q subcomponent subunit C	C1QC	8.54	26	1420
74	SPARC-like protein 1	SPRL1	4.53	76	1310
75	Hemopexin	HEMO	6.6	52	1299
76	Insulin-like growth factor-binding protein complex acid labile subunit	ALS	6.37	67	1292
77	Immunoglobulin heavy constant gamma 3	IGHG3	7.79	42	1283
78	Serum paraoxonase/lactonase 3	PON3	5.11	40	1244
79	Transthyretin	TTHY	5.42	16	1191
80	Alpha-1B-glycoprotein	A1BG	5.5	55	1184
81	Phosphatidylinositol-glycan-specific phospholipase D	PHLD	5.92	93	1124
82	Immunoglobulin heavy constant alpha 2	IGHA2	5.85	37	1085
83	Immunoglobulin heavy constant gamma 2	IGHG2	7.45	37	1085
84	Vitamin D-binding protein	VTDB	5.16	55	1066
85	Alpha-2-HS-glycoprotein	FETUA	5.35	40	1002
86	Complement C1q subcomponent subunit B	C1QB	8.87	27	996
87	Fermitin family homolog 3	URP2	6.57	77	955
88	Complement component C6	CO6	6.37	108	954
89	Complement factor B	CFAB	6.69	87	864
90	Carboxypeptidase N subunit 2	CPN2	5.59	61	854
91	Prenylcysteine oxidase 1	PCYOX	5.78	57	841
92	C4b-binding protein beta chain	C4BPB	4.87	29	772
93	14-3-3 protein zeta/delta	1433Z	4.53	28	561
94	Complement C1q subcomponent subunit A	C1QA	9.45	26	543
95	Pregnancy zone protein	PZP	5.96	165	530
96	Serum amyloid P-component	SAMP	6.13	26	527
97	Lysozyme C	LYSC	9.34	17	517
98	Kallistatin	KAIN	7.58	49	514
99	Immunoglobulin heavy constant gamma 4	IGHG4	7.13	36	455
100	Extracellular superoxide dismutase [Cu-Zn]	SODE	6.17	26	442
101	Immunoglobulin J chain	IGJ	4.91	19	402
102	N-acetylmuramoyl-L-alanine amidase	PGRP2	7.29	63	359
103	Beta-2-glycoprotein 1	APOH	7.87	40	342
104	Retinol-binding protein 4	RET4	5.68	23	200
105	Zinc-alpha-2-glycoprotein	ZA2G	5.66	34	200
106	Hemoglobin subunit beta	HBB	6.91	16	174
107	Prolactin-inducible protein	PIP	8.1	17	168
108	Alpha-1-acid glycoprotein 2	A1AG2	4.85	24	159
109	Dermcidin	DCD	6.14	11	130
110	Apolipoprotein C-IV	APOC4	9.13	15	110
111	Protein S100-A8	S10A8	6.65	11	90
112	Apolipoprotein C-I	APOC1	9.43	9	57

Table S7. Continued.

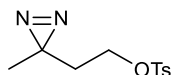
2. Materials and Methods

Chemical synthesis

General

All solvents and reagents were obtained from common commercial sources (Sigma Aldrich, Acros Organics, Alfa Aesar, Fluka, Merck) and used as received without further purification, unless stated otherwise. All reactions were performed under a nitrogen atmosphere, unless stated otherwise. Column chromatography was performed using silica gel (40–63 μm , 60 Å, Screening Devices, The Netherlands) or high purity silica gel (40–63 μm , 60 Å, Sigma-Aldrich). TLC analysis was performed on Merck silica gel 60/Kieselguhr F₂₅₄, 0.25 mm TLC plates. Compounds were visualized by UV adsorption or KMnO₄ stain (K₂CO₃ (15 g), KMnO₄ (2 g), and H₂O (200 mL)). ¹H, ¹³C and ³¹P NMR spectra were recorded on a Bruker AV 400 MHz or 850 MHz spectrometer. Chemical shifts are reported in ppm (δ), relative to the deuterated solvent as internal standard. Data are reported as follows: chemical shifts (δ), multiplicity (s = singlet, d = doublet, dd = doublet of doublet, t = triplet, q = quartet, br s = broad singlet, m = multiplet), coupling constants (J) reported in Hz. High resolution mass spectra were recorded by direct injection (2 μL of a 1 mM solution in methanol) using a mass spectrometer (Thermo Finnigan LTQ Orbitrap) with an electrospray ion source run in positive mode (source voltage 3.5 kV, sheath gas flow 10, capillary temperature 250°C), and with a resolution $R = 60,000$ at m/z 400 (mass range $m/z = 150$ –2,000) and dioctylphthalate ($m/z = 391.28428$) as a “lock mass”. The high-resolution mass spectrometer was calibrated prior to measurements with a calibration mixture (Thermo Finnigan).

methyl-3H-diazirin-3-yl)ethyl 4-methylbenzenesulfonate (1)²

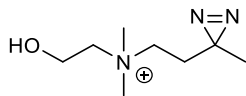


To 7N methanolic ammonia (11.2 mL, 79 mmol, 7 eq.) was added 4-hydroxybutan-2-one (0.98 mL, 11.35 mmol, 1 eq.) at 0 °C under nitrogen atmosphere. After stirring at 0 °C for 2.5 hours, the solution turned dark yellow. To the solution was added hydroxylamine-O-sulfonic acid (1.48 g, 13.05 mmol, 1.1 eq.) in methanol (9.7 mL) dropwise. The solution turned light yellow and was stirred overnight at room temperature until a white suspension was formed. The solid was filtered off and the ammonia was evaporated by gently blowing nitrogen through the solution. The solution was cooled down to 0 °C and to the solution

was added triethylamine (1.6 mL, 11.35 mmol, 1 eq.), then was added in portions molecular iodine (± 2 g) until the brown colour persisted. After 2 hours, the solution was quenched by the addition of brine (40 mL) and extracted with diethyl ether (3x). The organic layers were combined, washed with sodium thiosulfate (1x) and brine (1x). The organic layer was dried over anhydrous sodium sulfate and evaporated under reduced pressure. To the crude was added pyridine (8 mL) and *p*-toluenesulfonylchloride (2.30 g, 12 mmol, 1.1 eq.). After stirring overnight at room temperature, the solution was poured onto ice (120 g). The solution was quenched with concentrated hydrogen chloride (10 mL), which was added dropwise. The mixture was extracted with diethyl ether (3x). The organic layers were combined and washed with saturated sodium bicarbonate (1x) and brine (1x). The collected organic layers were dried over anhydrous sodium sulfate and concentrated under reduced pressure. Flash column chromatography (silica gel, 8% ethyl acetate in petroleum ether) yielded **1** (640 mg, 2.50 mmol, 20%).

TLC: R_f = 0.4 (dichloromethane/methanol, 80:20 v/v). $^1\text{H NMR}$ (400 MHz, CDCl_3) δ 7.81 (d, J = 8.3 Hz, 2H), 7.36 (d, J = 8.0 Hz, 2H), 3.94 (t, J = 6.4 Hz, 2H), 2.45 (s, 3H), 1.66 (t, J = 6.4 Hz, 2H), 0.99 (s, 3H). $^{13}\text{C NMR}$ (100 MHz, CDCl_3) δ 145.17, 130.04, 128.08, 125.37, 65.23, 34.27, 23.50, 21.78, 19.88.

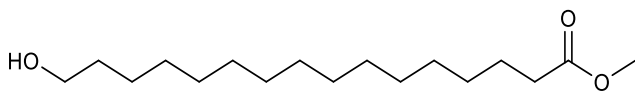
2-hydroxy-N,N-dimethyl-N-(2-(3-methyl-3H-diazirin-3-yl)ethyl)ethan-1-aminium (**2**)²



To a solution of **1** (200 mg, 0.78 mmol, 1.1 eq.) in acetonitrile (700 μL) was added 2-dimethylaminoethanol (72 μL , 0.71 mmol, 1 eq.). After stirring overnight at 80 $^\circ\text{C}$, additional **13** (10 mg, 0.039 mmol, 0.55 eq.) was added. After stirring overnight at 80 $^\circ\text{C}$, the mixture was concentrated under reduced pressure to give the yellow/brown solid **2** (134 mg, 0.78 mmol, quant).

$^1\text{H NMR}$ (400 MHz, MeOD) δ 7.71 (d, J = 8.2 Hz, 2H), 7.25 (d, J = 8.0 Hz, 2H), 4.02 – 3.89 (m, 2H), 3.50 – 3.44 (m, 2H), 3.43 – 3.40 (m, 2H), 3.13 – 3.09 (m, 4H), 2.38 (s, 3H), 1.88 – 1.80 (m, 2H), 1.07 (s, 2H). $^{13}\text{C NMR}$ (100 MHz, MeOD) δ 143.62, 141.73, 129.87, 126.93, 66.43, 61.33, 56.81, 52.33, 52.29, 52.25, 29.28, 21.31, 19.35, 0.81.

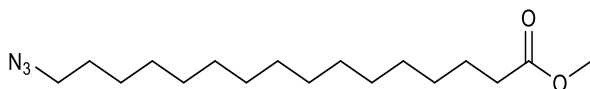
Methyl 16-hydroxyhexadecanoate (**3**)



To a solution of 16-hydroxyhexadecanoic acid (1.70 g, 6.6 mmol, 1 eq.) in methanol (100 mL) was added acetyl chloride (3.24 mL, 44.7 mmol, 8 eq.) at 0 °C. After stirring overnight, additional acetyl chloride (3 mL, 41.4 mmol) was added. Monitoring by TLC showed complete conversion after 2 hours. The mixture was then concentrated under reduced pressure and dissolved in dichloromethane. The solution was washed with a saturated sodium bicarbonate solution (2x), water (2x) and brine (1x). Every aqueous phase was extracted with dichloromethane (1x). The organic layers were combined, dried over anhydrous sodium sulfate and evaporated under reduced pressure, yielding **3** as a white solid (1.73 g, 6.06 mmol, 92%).

R_f = 0.8 (Pentanes/Ethyl acetate, 75:25 v/v). $^1\text{H NMR}$ (400 MHz, CDCl_3) δ 3.66 (s, 3H), 3.63 (t, J = 6.6 Hz, 2H), 2.30 (t, J = 7.6 Hz, 2H), 1.66 – 1.50 (m, 4H), 1.38 – 1.19 (m, 22H). $^{13}\text{C NMR}$ (100 MHz, CDCl_3) δ 63.24, 51.60, 34.26, 32.94, 29.77, 29.76, 29.74, 29.72, 29.57, 29.39, 29.29, 25.87, 25.17, 25.10

Methyl 16-azidohexadecanoate (**4**)³



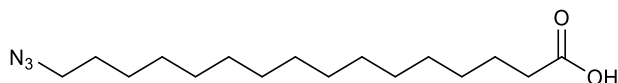
To a solution of **3** (1.70 g, 6.06 mmol) and triethylamine (5.07 mL, 36.4 mmol, 6 eq.) in methanol (100 mL) was added methanesulfonyl chloride (1.88 mL, 24.2 mmol, 4 eq.) dropwise at 0 °C. After addition, the mixture was allowed to warm to room temperature and monitoring by TLC showed complete conversion of the starting materials after 3 hours. The mixture was concentrated under reduced pressure, dissolved in dichloromethane and the solution was washed with a saturated sodium bicarbonate solution (1x), water (1x) and brine (1x). The organic layer was dried over anhydrous sodium sulfate and evaporated under reduced pressure, yielding the mesylate intermediate which was taken to the next step without further purification.

To a solution of mesylate intermediate in *N,N*-dimethylformamide (40 mL) was added sodium azide (2.15 g, 33 mmol) and the solution was stirred at 70 °C for 2 hours. The mixture was concentrated under reduced pressure, dissolved in DCM and washed with water (3x), a saturated sodium bicarbonate solution (1x) and brine (1x). The organic layer

was dried over anhydrous sodium sulfate and evaporated under reduced pressure. Flash column chromatography (silica gel, 5-10% ethyl acetate in pentane) yielded **4** as a white solid (1.71 g, 5.51 mmol, 91%)

$R_f = 0.8$ (Pentanes/Ethyl acetate, 75:15 v/v). $^1\text{H NMR}$ (400 MHz, CDCl_3) δ 3.66 (s, 3H), 3.25 (t, $J = 8$ Hz, 2H), 2.29 (t, $J = 8$ Hz, 2H), 1.66 - 1.59 (m, 4H), 1.42 - 1.25 (m, 22H). $^{13}\text{C NMR}$ (100 MHz, CDCl_3) δ 174.43, 51.61, 51.56, 34.24, 29.75, 29.71, 29.66, 29.61, 29.57, 29.38, 29.38, 28.96

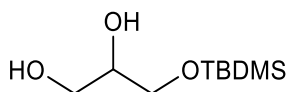
16-Azidohexadecanoic acid (**5**)³



To a solution of **4** (1.70 g, 5.49 mmol) in tetrahydrofuran and dioxane (1:1, 15 mL) was added a 4M NaOH solution (15 mL) and the reaction was stirred at room temperature overnight. The mixture was diluted with ethyl acetate (200 mL) and washed with a 1M HCl solution (2x), water (1x) and brine (1x). The organic layer was dried over anhydrous sodium sulfate and concentrated under reduced pressure yielding **5** as a white solid (1.62 g, 5.21 mmol, 95%)

$R_f = 0.2$ (Pentanes/Ethyl acetate, 75:25 v/v). $^1\text{H NMR}$ (400 MHz, CDCl_3) δ 3.25 (t, $J = 8$ Hz, 2H), 2.34 (t, $J = 8$ Hz, 2H), 1.66 - 1.59 (m, 4H), 1.35 - 1.25 (m, 22H). $^{13}\text{C NMR}$ (100 MHz, CDCl_3) δ 180.53, 51.60, 29.74, 29.70, 29.66, 29.60, 29.55, 29.36, 29.28, 29.17, 28.95, 26.84, 24.78

3-((*tert*-Butyldimethylsilyl)oxy)propane-1,2-diol (**6**)

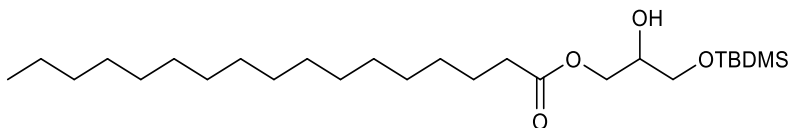


To a solution of *tert*-Butyldimethylsilyl chloride (1.0 gram, 6.6 mmol, 1 eq.) in dichloromethane (25 mL) was added dropwise a solution of glycerol (17.8 gram, 198.6 mmol, 30 eq.) and imidazole (1.35 gram, 19.8 mmol, 3 eq.) in dichloromethane (30 mL) and DMF (12 mL) at -18°C . After stirring the solution for one hour at -18°C , water (50 mL) was added. The resulting mixture was extracted with dichloromethane (3x). The organic layers were combined and washed with water (1x) and brine (1x), dried over anhydrous sodium sulfate and evaporated under reduced pressure. Flash column chromatography

(silica gel, 40% ethyl acetate in pentane) yielded **6** as a transparent oil (478 mg, 2.27 mmol, 34%).

$R_f = 0.54$ (Pentane/Ethyl acetate, 50:50 v/v). $^1\text{H NMR}$ (400 MHz, CDCl_3) δ 3.81 – 3.55 (m, 5H), 0.90 (s, 9H), 0.08 (s, 6H). $^{13}\text{C NMR}$ (100 MHz, CDCl_3) δ 71.71, 64.89, 64.35, 64.19, 25.98, 18.39, -5.34.

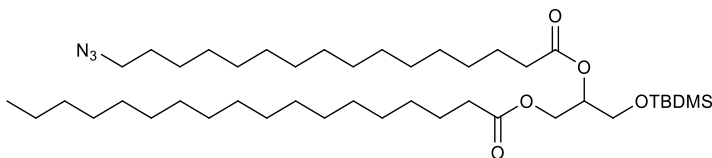
3-((*tert*-Butyldimethylsilyl)oxy)-2-hydroxypropyl propionate (**7**)



To a solution of stearic acid (295 mg, 1.04 mmol, 0.7 eq.) in dichloromethane (8 mL) were added *N,N'*-dicyclohexylcarbodiimide (257 mg, 1.04 mmol, 0.7 eq.) and 4-dimethylaminopyridine (90 mg, 0.74 mmol, 0.5 eq.). After stirring for 30 minutes at room temperature, the solution was cooled down to 0 °C. To the cooled solution was added **5** (310 mg, 1.48 mmol, 1 eq.). The solution was stirred at 0 °C for 30 min, allowed to warm up to room temperature and stirred overnight. The formed suspension was filtered and the filtrate was washed with saturated sodium bicarbonate solution (2x), water (2x) and brine (1x). The separate aqueous layers were extracted with dichloromethane (1x). The combined organic layers were dried over anhydrous sodium sulfate and evaporated under reduced pressure. Flash column chromatography (silica gel, 6% ethyl acetate in pentane), yielded **6** as a mixture of regioisomers ($2^\circ:1^\circ = 7:43$, determined by $^1\text{H-NMR}$) (374 mg, 0.790 mmol, 76%).

$R_f = 0.65$ & 0.7 (Pentane/Ethyl acetate, 80:20 v/v). $^1\text{H NMR}$ (400 MHz, CDCl_3) δ 4.19 – 4.05 (m, 1H), 3.92 – 3.84 (m, 1H), 3.84 – 3.72 (m, 1H), 3.67 (dd, $J = 10.1, 4.6$ Hz, 1H), 3.60 (dd, $J = 10.1, 5.6$ Hz, 1H), 2.33 (t, $J = 7.6$ Hz, 2H), 1.70 – 1.55 (m, 2H), 1.25 (s, 28H), 0.94 – 0.77 (m, 12H), 0.07 (d, $J = 2.6$ Hz, 6H). $^{13}\text{C NMR}$ (100 MHz, CDCl_3) δ 174.13, 74.38, 65.12, 63.81, 63.02, 62.70, 34.55, 34.34, 32.07, 29.84, 29.82, 29.80, 29.75, 29.61, 29.51, 29.42, 29.29, 25.97, 25.09, 22.84, 14.27, -5.33.

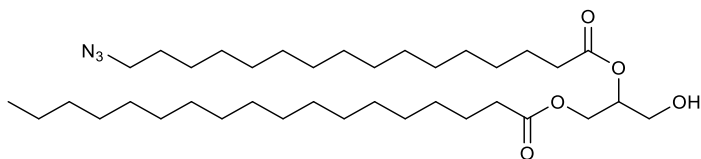
2-((16-Azidohexadecanoyl)oxy)-3-((*tert*-butyldimethylsilyl)oxy)propyl stearate (**8**)



To a solution of **5** (221 mg, 0.746 mmol, 1.05 eq.) in dichloromethane (8 mL), were added *N,N'*-dicyclohexylcarbodiimide (185 mg, 0.746 mmol, 1.05 eq.) and 4-dimethylaminopyridine (65 mg, 0.530 mmol, 0.75 eq.). After stirring for 30 minutes at room temperature, **7** was added (336 mg, 0.751 mmol, 1 eq.) and the solution was stirred overnight. The formed suspension was filtered and the organic phase was washed with saturated sodium bicarbonate solution (2x), water (2x) and brine (1x). The combined organic layers were dried over anhydrous sodium sulfate and evaporated under reduced pressure. Flash column chromatography (silica gel, 1.5% ethyl acetate in pentane) yielded **12** (340 mg, 0.452 mmol, 64%) as a mixture of regioisomers.

R_f = 0.3 (Pentane/Ethyl acetate, 95:5 v/v). $^1\text{H NMR}$ (400 MHz, CDCl_3) δ 5.17 – 4.95 (m, 1H), 4.33 (dd, J = 11.8, 3.7 Hz, 1H), 4.15 (dd, J = 11.8, 6.3 Hz, 1H), 3.79 – 3.54 (m, 2H), 3.25 (t, J = 7.0 Hz, 2H), 2.29 (dd, J = 7.9, 7.1, 2.1 Hz, 4H), 1.68 – 1.51 (m, 6H), 1.25 (s, 50H), 0.96 – 0.76 (m, 12H), 0.07 (s, 6H). $^{13}\text{C NMR}$ (100 MHz, CDCl_3) δ 173.61, 173.26, 71.80, 62.58, 61.58, 51.62, 34.49, 34.30, 32.07, 29.84, 29.81, 29.79, 29.77, 29.69, 29.63, 29.51, 29.44, 29.30, 29.27, 29.25, 28.98, 26.86, 25.08, 25.05, 22.83, 14.26, -5.36 (d, J = 4.2 Hz).

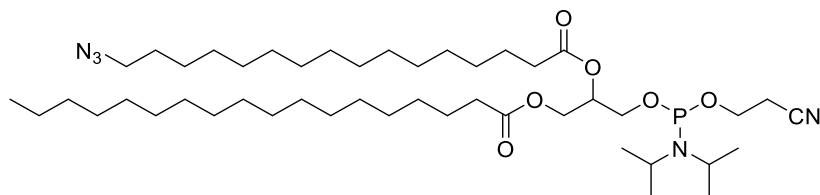
2-((16-Azidohexadecanoyl)oxy)-3-hydroxypropyl stearate (**9**)



To a solution of **8** (340 mg, 0.452 mmol, 1 eq.) in acetonitrile:tetrahydrofuran (1:1, 8 mL) was added triethylamine trihydrofluoride (0.74 mL, 4.52 mmol, 10 eq.). After stirring overnight at room temperature, the solution was quenched on ice with a saturated sodium bicarbonate solution. After extraction with dichloromethane (4x), the organic layers were combined, dried over anhydrous sodium sulfate and concentrated under reduced pressure. Flash column chromatography (silica gel, 20% ethyl acetate in pentane) yielded **9** (289 mg, 0.452 mmol, quant) as a mixture of regioisomers.

R_f = 0.8 (Pentane/Ethyl acetate, 80:20 v/v). $^1\text{H NMR}$ (400 MHz, CDCl_3) δ 5.08 (p, J = 5.0 Hz, 1H), 4.32 (dd, J = 11.9, 4.5 Hz, 1H), 4.24 (dd, J = 11.9, 5.6 Hz, 1H), 4.21 – 4.13 (m, 1H), 3.75 – 3.71 (m, 1H), 3.25 (t, J = 7.0 Hz, 2H), 2.38 – 2.29 (m, 4H), 1.66 – 1.55 (m, 8H), 1.35 – 1.21 (m, 48H), 0.88 (t, J = 6.4 Hz, 3H). $^{13}\text{C NMR}$ (101 MHz, CDCl_3) δ 72.24, 62.11, 61.71, 51.64, 34.44, 34.26, 32.08, 29.85, 29.81, 29.79, 29.77, 29.69, 29.63, 29.52, 29.42, 29.40, 29.31, 29.27, 29.24, 28.99, 26.87, 25.09, 25.04, 22.85, 14.28.

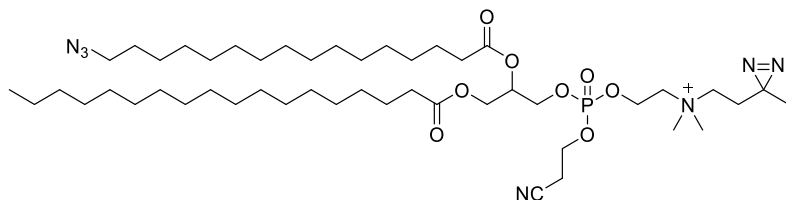
2-(((16-azidohexadecanoyl)oxy)-3-(((2-cyanoethoxy)(diisopropylamino)phosphanyl)oxy)propyl stearate (10)



A solution of **13** (200 mg, 0.313 mmol, 1 eq.) and diisopropylethylamine (329 μ l, 1.88 mmol, 6 eq.) in dry dichloromethane (5 mL) was dried over freshly oven-dried 3Å molecular sieves and stored under nitrogen atmosphere. The mixture was transferred to a dry flask under nitrogen atmosphere and to the solution was added 2-cyanoethyl N,N-diisopropylchlorophosphoramidite (250 mg, 1.056 mmol, 3 eq.). After stirring for 1.5 hours the solution was concentrated under reduced pressure until 600 mbar. Flash column chromatography, (high purity silica gel pre-treated with 5% triethylamine in pentane, 3% ethyl acetate and 3% Et₃N in pentane) yielded **16** (194 mg, 0.231 mmol, 74%). The product was stored in 20% triethylamine in dichloromethane (2 mL) under nitrogen atmosphere overnight. For the next reaction, the product was concentrated under reduced pressure until 60 mbar for maximum 10 minutes.

R_f = 0.6 (Pentane/Ethyl acetate/Et₃N, 90:7:3 v/v/v). ¹H NMR (400 MHz, CDCl₃) δ 4.29 – 4.06 (m, 2H), 3.92 – 3.72 (m, 2H), 3.67 – 3.54 (m, 1H), 3.25 (t, J = 7.0 Hz, 1H), 2.63 (td, J = 6.5, 2.3 Hz, 2H), 2.54 (q, J = 7.2 Hz, 4H), 2.30 (tt, J = 7.0, 3.5 Hz, 4H), 1.68 – 1.54 (m, 6H), 1.32 – 1.18 (m, 50H), 1.17 (q, J = 2.9 Hz, 12H), 0.87 (t, J = 6.8 Hz, 3H). ¹³C NMR (100 MHz, CDCl₃) δ 173.61, 69.68, 69.52, 64.03, 58.64, 58.46, 51.63, 46.38, 43.43, 43.31, 34.30 (d, J = 4.3 Hz), 32.07, 29.82 (d, J = 4.6 Hz), 29.66 (d, J = 5.9 Hz), 29.51, 29.45, 29.30, 28.98, 26.86, 25.03, 24.75, 24.65, 24.57, 22.83, 14.27, 11.69. ³¹P NMR (162 MHz, CDCl₃) δ 150.08, 149.50.

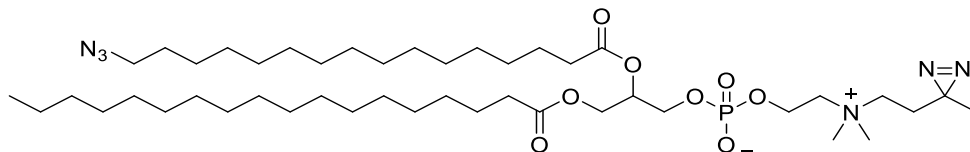
2-(((2-(((16-azidohexadecanoyl)oxy)-3-(stearoyloxy)propoxy)(2-cyanoethoxy)phosphoryl)oxy)-n,n-dimethyl-n-(2-(3-methyl-3h-diazirin-3-yl)ethyl)ethan-1-aminium (11)



A solution of **10** (194 mg, 0.231 mmol, 1 eq.) in dry dichloromethane (5 mL) was dried over freshly oven-dried 3 Å molecular sieves under nitrogen atmosphere. To the solution were added **2** (79 mg, 0.231 mmol, 1 eq.) and tetrazole (1.03 mL, 0.462 mmol, 2 eq.). After stirring for 45 minutes, additional tetrazole (0.51 mL, 0.231 mmol, 1eq.) and **15** (20 mg, 0.058 mmol, 0.25 eq.) were added. After 1 hour, ³¹P-NMR indicated complete conversion of the starting material (main peak shifted from 150 ppm to 140 ppm) to the solution was added *tert*-Butyl hydroperoxide (66 µL, 0.347 mmol, 1.5 eq.). After 45 minutes, ³¹P-NMR showed oxidation was complete (peak shifted from 140 ppm to -3 ppm), the solution was diluted with dichloromethane and washed with saturated sodium bicarbonate (1x) and brine (1x). The collected organic layers were dried over anhydrous sodium sulfate and concentrated under reduced pressure. Flash column chromatography (high purity silica gel, 10% methanol in dichloromethane) yielded **11** (20.5 mg, 5.54 µmol, 10%).

R_f = 0.3 (dichloromethane/methanol, 80:20 v/v). ¹H NMR (400 MHz, CDCl₃) δ 4.88 – 4.63 (m, 2H), 4.50 – 4.31 (m, 3H), 4.27 – 4.12 (m, 4H), 3.65 (d, *J* = 5.4 Hz, 2H), 3.40 (s, 6H), 3.25 (t, *J* = 7.0 Hz, 2H), 3.11 (qd, *J* = 7.3, 4.8 Hz, 4H), 2.90 (s, 2H), 2.43 – 2.26 (m, 4H), 1.90 (s, 2H), 1.65 – 1.52 (m, 6H), 1.25 (s, 50H), 1.17 (s, 3H), 0.87 (t, *J* = 6.7 Hz, 3H). ³¹P NMR (162 MHz, CDCl₃) δ -2.68, -3.33. ESI-HRMS (*m/z*) C₄₈H₉₁N₇O₈P⁺: [M]⁺ calculated: 925.27, found: 923.98.

2-((16-azidohexadecanoyl)oxy)-3-(stearoyloxy)propyl(2-(dimethyl(2-(3-methyl-3h-diazirin-3-yl)ethyl)ammonio)ethyl) phosphate (ikso2)



To a solution of **17** (10.26 mg, 11.08 µmol) in dry dichloromethane (3 mL) was added a mixture of *tert*-butylamine and dichloromethane (1:1, 100 µL) and the mixture was stirred at room temperature for 3 hours. The solution was concentrated under reduced pressure. The product was purified with column chromatography (high purity silica gel, 17% methanol in dichloromethane) and yielded **IKSo2** as a white solid (5.66 mg, 5.32 µmol, 48%).

R_f = 0.3 (dichloromethane/methanol, 70:30 v/v). ¹H NMR (850 MHz, CDCl₃) δ 4.55 (s, 1H), 4.40 (s, 3H), 4.27 (dd, *J* = 11.7, 5.3 Hz, 2H), 4.24 (dd, *J* = 11.5, 4.6 Hz, 2H), 4.01 (s, 1H), 3.86 (s, 2H), 3.58 (t, *J* = 8.4 Hz, 2H), 3.30 (s, 6H), 3.25 (t, *J* = 7.0 Hz, 2H), 2.31 (t, *J* = 7.7 Hz, 6H), 1.87

(q, J = 8.8 Hz, 2H), 1.59 (h, J = 7.1 Hz, 6H), 1.33 – 1.18 (m, 48H), 1.15 (s, 3H), 0.88 (t, J = 7.1 Hz, 3H). ³¹P NMR (162 MHz, CDCl₃) δ -1.82. ESI-HRMS (*m/z*) C₄₅H₈₇N₆O₈P: [M]⁺ calculated: 871.1780, found: 871.63958.

Biological methods and proteomics

General

All solvents and reagents were obtained from common commercial sources (Sigma Aldrich, Acros Organics, Alfa Aesar, Fluka, Merck) and used without further purification, unless stated otherwise. Dynamic light scattering and zeta potential measurements were performed on a Malvern Zetasizer Nano ZS. For light irradiation, a CaproBox™ (Caprotec Bioanalytics GmbH) was used with a wavelength of 350 nm and applying a 300 nm light filter. Human serum was purchased from Sigma-Aldrich (Non Heat Inactivated, Human Male AB plasma, USA origin, sterile-filtered, product code: H4522) with a protein concentration of 60.2 µg/µl determined by a Pierce BCA Protein Assay Kit (Thermo Scientific). The serum was aliquoted, snap-frozen with liquid nitrogen and stored for a maximum of 6 months at -80 °C. Albumin from human serum (SRP6182), Human transferrin (T3309) and recombinant human apolipoprotein E3 (SRP4696) were purchased from Sigma-Aldrich. Human prothrombin (RP-43087) was purchased from Thermo-Fisher Scientific. Recombinant human Apolipoprotein A1 (ab50239) was purchased from Abcam B.V. (Amsterdam, The Netherlands).

Evaporation of solvents with a vacuum centrifuge was performed using an Eppendorf speedvac (Eppendorf Concentrator Plus 5301). Sequencing grade modified trypsin was purchased from Promega (product code = V5111). Acetonitrile (LC-MS grade) and methanol (LC-MS grade) were purchased from Biosolve. Formic acid (LC-MS grade) was purchased from Actu-All Chemicals. BioSpin columns were purchased from Bo-Rad. The Empore C18 47-mm extraction disks (model 2215) were purchased from 3M™ Purification. Enolase digest standard was purchased from Waters MassPREP™.

Liposome preparation

Lipids were combined from stock solutions (10 mM in CHCl₃:MeOH 1:1 v/v) at the desired molar ratios. The solvents were evaporated under a nitrogen flow and traces of solvents were removed *in vacuo* for at least 30 minutes. Lipid films were hydrated with the desired volume of 20 mM HEPES (pH 7.4), vortexed and warmed to 65 °C for 5 minutes. The mixture was extruded thirteen times through two stacked 100 nm polycarbonate membranes (Nucleopore Track-Etch, Whatman) using an Avanti Mini Extruder (Avanti

Polar Lipids). Size and surface charge were measured by Dynamic Light Scattering (DLS) and Zeta Potential measurement and liposomes were stored in the dark at 4 °C for no longer than two weeks.

Photoaffinity method

Incubation, crosslinking and click chemistry

Liposomes containing the photoaffinity probe (25 μ L, 5 mM) were added to pre-warmed human serum (37 °C, 25 μ L, 60.26 mg/ml protein) and incubated in the dark at 37 °C for 1 hour. For every liposome formulation, twelve replicates were prepared. Half of the replicates were irradiated with 350 nm light for 15 minutes, while cooling. The other replicates were kept at room temperature in the dark for 15 minutes. Afterwards, the liposomes were solubilized by addition of 10 μ L 0.2% Triton X-100 in ultrapure water and incubation for 30 minutes. The samples were diluted by adding 140 μ L of 0.1% SDS in ultrapure water. Aliquots of 100 μ L were taken and protein precipitation was performed according to Wessel and Flügge.⁴ Briefly, ultrapure water (400 μ L), methanol (650 μ L), chloroform (200 μ L) and ultrapure water (150 μ L) were added sequentially, followed by vigorous vortexing and centrifugation (3000 g, 10 min, rt). The liquid layers were removed, the pellet resuspended with methanol (600 μ L) and centrifuged (14,000 g, 5 min, rt). The supernatant was discarded and the pellet was dissolved in HEPES buffer containing 0.5% SDS (200 μ L, 100 mM, pH 8.0).

A BCA assay was performed to determine the protein concentration and the samples were diluted to a volume of 450 μ L with HEPES buffer with 0.5% SDS (100 mM, pH 8.0) with a protein concentration of 0.5-1.0 mg/mL. For each protein sample, click reagent mixture (50 μ L) was added from a 10x concentrated stock to give a final concentration of 100 μ M CuSO₄, 1000 μ M sodium ascorbate, 500 μ M THPTA, 5000 μ M aminoguanidine and 20 μ M Cy5-alkyne or Biotin-alkyne, followed by incubation at room temperature for 1 hour. Methanol (650 μ L), chloroform (150 μ L) and ultrapure water (150 μ L) were added sequentially, the mixture vortexed and centrifuged (3000 g, 10 min, rt). The liquid layers were removed, resuspended with methanol (600 μ L) and centrifuged (14,000 g, 5 min, rt). The pellet was air-dried at room temperature for 5-10 minutes and resuspended in freshly prepared denaturing buffer (250 μ L, 6 M urea, 25 mM NH₄HCO₃) and used for in-gel fluorescence imaging or enrichment. Alternatively, samples were snap-frozen with liquid nitrogen and stored for no longer than 2 weeks at -80 °C.

SDS-Page and in-gel fluorescence imaging

Protein concentration was determined by BCA assay prior to loading samples for in-gel fluorescence. To a volume corresponding to 10 µg of protein was added Laemmli buffer (4x stock) and the proteins were resolved on a 12.5% PA gel at 180 V. The subset of fluorescent proteins was imaged on a Typhoon FLA 9500 (GE Healthcare), followed by staining of all the proteins with Coomassie Brilliant Blue R-250 staining solution (Bio-Rad) and imaging on a ChemiDoc MP system (Bio-Rad).

Reduction and alkylation

To lipid-protein samples conjugated to biotin, 5 µL (1 M DTT; 20 mM final concentration) was added. Samples were vortexed, centrifuged and incubated at 56 °C while shaking (600 rpm) for 30 minutes. The samples were allowed to cool down to room temperature, after which 40 µl 0.5 M iodoacetamide (80 mM final concentration) was added and the samples incubated at room temperature in the dark for 30 minutes. Afterwards, 20 µL 1 M DTT (100 mM final concentration) was added and the samples were vortexed and incubated at 56 °C for 5 minutes. Reduced and alkylated proteins were used directly for avidin bead enrichment.

Enrichment and on-bead digestion

Avidin agarose beads (50% slurry, 100 µL per sample, Thermo Fisher Scientific) were washed three times with PBS (10 mL PBS per 400 µL slurry), centrifuging at 2500 g for 3 minutes. The beads were resuspended in PBS (1 mL PBS per 100 µL slurry) and divided over 15 mL tubes in 1 mL fractions. An additional 2 mL PBS was added to each tube, after which the denatured and alkylated protein samples were added and the samples were shaken gently in an overhead shaker at RT for at least 3 hours. Beads were pelleted (2,500 g, 5 min) and the supernatant discarded. The beads were washed twice with SDS in PBS (0.5% w/v, 10 mL), three times with PBS (10 mL) and twice with ultrapure water (10 mL). In between each washing step, the samples were vortexed, centrifuged (2,500 g, 5 min) and the supernatants were discarded. The washed beads were resuspended in 250 µL on-bead digestion buffer (100 mM TRIS pH 8.0, 100 mM NaCl, 1 mM CaCl₂ and 2% v/v acetonitrile (LC-MS grade)) and transferred to 1.5 mL low-binding Eppendorf tubes, after which 10 µL 0.1 µg/µL trypsin was added and the samples were incubated at 37 °C while shaking (950 rpm) overnight. To the samples was added 12.5 µL formic acid, after which they were loaded onto Bio-Spin columns (Bio-Rad) and the flow-through was collected by centrifugation

(2,500 g, 2 min) in low-binding Eppendorf tubes. The samples were desalted using the StageTips procedure described below.

Protein binding validation experiment

Human serum albumin (ALBU, 25 µg), transferrin (TRFE, 10 µg), apolipoprotein A1 (APOA1, 2 µg), apolipoprotein E3 (APOE, 2 µg) and prothrombin (THRB, 2 µg) were mixed in a total volume of 17.5 µL (PBS) for each replicate. To each replicate was added liposomes containing IKSO₂ (7.5 µL, 5 mM). For competition experiments, liposomes without IKSO₂ added were according to the competitive ratio (5 mM, 1:1 = 7.5 µL, 1:4 = 30 µL, 1:9 = 67.5 µL). The mixture was incubated at 37 °C for 1 hour followed by liposome solubilisation with 1% Triton X-100 (5 µL). Proteins were precipitated by addition of ultrapure water, up to a volume of 100 µL, methanol (100 µL) and chloroform (50 µL), followed by vigorous vortexing and centrifugation (3000 g, 10 min, rt). The liquid layers were removed, the pellet resuspended with methanol (200 µL) and centrifuged (14,000 g, 5 min, rt). The supernatant was discarded and the pellet was dissolved in HEPES buffer (45 µL, 100 mM, pH 8.0). For each protein sample, click reagent mixture (5 µL) was added from a 10x concentrated stock to give a final concentration of 100 µM CuSO₄, 1000 µM sodium ascorbate, 500 µM THPTA, 5000 µM aminoguanidine and 20 µM Cy5-alkyne or Biotin-alkyne, followed by incubation at room temperature for 1 hour. Protein precipitation was repeated as prior to the click reaction and the pellet was dissolved in PBS (50 µL) from which an aliquot was taken to perform a BCA assay. For in-gel fluorescence measurement, aliquots containing 10 µg protein were analysed by SDS-PAGE and in-gel fluorescence as described before. For MS/MS experiments, aliquots containing 20 µg protein were taken for reduction and alkylation and further steps as described before.

Centrifugation method

Centrifugation, washing and SDS-Page

The centrifugation method for protein corona determination was performed as previously described.⁵⁻⁷ Briefly, human serum (100 µL, 60.26 µg/µL protein) was thawed on ice and warmed to 37 °C prior to incubation with liposomes (100 µL, 1 mg/mL) at 37 °C in low-binding Eppendorf tubes for one hour. The samples were centrifuged (17,500 g, 15 min) and the supernatant was discarded. The pellets were washed by dissolving in PBS (100 µL, pH 7.4) and centrifugation (17,500 g, 15 min). This washing step was performed two more times, after which the pellets were dissolved in 1% SDS containing Laemmli buffer (20 µL), denatured at 95 °C for 5 minutes and resolved on a 12.5% poly acrylamide gel. The gel was

fixed and stained using Coomassie Brilliant Blue R-250 staining solution, imaged on a ChemiDoc MP system (Bio-Rad) followed by in-gel reduction, alkylation and digestion as described below.

In-gel reduction, alkylation and digestion

The SDS-PAGE gel lanes were cut in pieces of approximately 3 mm and transferred to 1.5 mL low-binding Eppendorf tubes. The gel pieces were washed with 25 mM NH_4HCO_3 /acetonitrile (95:5, v/v) (400 μL) for 30 minutes and twice with 50 mM NH_4HCO_3 /acetonitrile (50:50 v/v, 400 μL) for 30 minutes. The gel pieces were dehydrated by the addition of acetonitrile (300 μL , 10 min), after which the liquids were removed and the gel pieces were dried with a vacuum centrifuge. The gel pieces were hydrated with a 10 mM DTT in 100 mM NH_4HCO_3 solution (200 μL) and incubated at 56 °C for 1 hr. The excess liquid was removed, 55 mM IAA in 100 mM NH_4HCO_3 (200 μL) added and the solution incubated at room temperature in the dark for 45 minutes. The gel pieces were subsequently washed with 100 mM NH_4HCO_3 (200 μL) for 10 minutes and acetonitrile (200 μL) for 10 minutes. These washing steps were repeated two more times and the pieces were dried with a vacuum centrifuge.

The gel pieces were hydrated with digestion buffer (200 μL , 5 ng/ μL trypsin in 50 mM NH_4HCO_3 /acetonitrile 90:10 v/v) and incubated at 37 °C overnight. Formic acid in 50 mM NH_4HCO_3 (100 μL , 5:95 v/v) was added and the supernatants of the corresponding gel lanes were combined. To the gel pieces was added a solution of acetonitrile/50 mM NH_4HCO_3 /formic acid (50:45:5 v/v, 100 μL) followed by incubation at room temperature for 45 minutes. The gel pieces were sonicated for 5 minutes and the supernatants were combined with the previous supernatants of the corresponding gel lanes. This last extraction step was performed one more time. Finally, a solution of acetonitrile/50 mM NH_4HCO_3 /formic acid (90:5:5 v/v, 100 μL) was added and incubated at room temperature for 5 minutes. The supernatants were combined and dried using a vacuum centrifuge. The protein digests were dissolved in 100 μL StageTip solution A (0.5% (v/v) formic acid in ultrapure water) and desalted, using the StageTip procedure described below, before analysis by UPLC MS/MS.

In-solution reduction, alkylation and digestion

Six aliquots of human serum (20 μL , 60.26 mg/ml protein) were precipitated according to Wessel and Flügge⁴. Briefly, ultrapure water (480 μL), methanol (650 μL), chloroform (200 μL) and ultrapure water (150 μL) were added sequentially, followed by vigorous vortexing

and centrifugation (3000 g, 10 min, RT). The liquid layers were removed, the pellet resuspended with methanol (600 µL) and centrifuged (14,000 g, 5 min, RT). The supernatant was discarded and the pellet was dissolved in freshly prepared denaturing buffer (250 µL, 6M Urea and 25 mM NaHCO₃). A BCA assay was performed to determine the protein concentration and aliquots were taken corresponding to 100 µg of protein, followed by dilution to 100 µL with denaturing buffer. To the sample was added 5 µL 0.2 M DTT and the sample was incubated at 56 °C for 30 minutes, followed by the addition of 25 µL 0.2 M Iodoacetamide and incubation at room temperature for 30 minutes. An additional 20 µL 0.2 M DTT was added and the sample was incubated at 56 °C for 5 minutes. Aliquots of 22.5 µL (15 µg of protein) were transferred to low-binding Eppendorf tubes and diluted to 200 µL with digestion buffer (100 mM TRIS pH 8.0, 100 mM NaCl, 1 mM CaCl₂ and 2% v/v acetonitrile (LC-MS grade)), to reduce the urea concentration to ~0.6 M, after which 3 µL, 0.1 µg/µL trypsin (1:50 w/w trypsin:protein) was added and the samples were incubated at 37 °C while shaking (950 rpm) overnight. After digestion, 10 µL formic acid was added and the samples were desalted using the StageTip procedure described below.

StageTip desalting

The protein digest desalting procedure was conducted as previously described.⁸ Briefly, C₁₈ extraction disks (47 mm) were placed in 200 µL pipette tips. These StageTips were conditioned, loaded, washed and eluted, following the scheme below. The eluted fractions were collected into low-binding Eppendorf tubes, dried using a vacuum centrifuge and stored at -20 °C or immediately prepared for UPLC-MS/MS measurements.

STAGE	BUFFER
Conditioning 1	50 µL MeOH (LC-MS grade)
Conditioning 2	50 µL StageTip solution B: 0.5% (v/v) formic acid, 80% (v/v) acetonitrile and 19.5% ultrapure water
Conditioning 3	50 µL StageTip solution A: 0.5% (v/v) formic acid in ultrapure water
Loading	Sample
Washing	100 µL StageTip solution A
Elution	100 µL StageTip solution B

NanoUPLC-MS/MS analysis

LC-MS was performed as described previously.⁹ Peptide samples were dissolved in 50 μ L LC-MS sample solution (ultrapure water:acetonitrile:formic acid 97:3:0.1) containing 10 fmol/ μ L enolase digest as an internal standard for label-free quantification. DMSO was not added to the LC solvents. Instead, a lower source temperature (80 °C instead of 100 °C) was used. A trap–elute protocol was used, in which a digest is loaded on a trap column and eluted and separated on the analytical column. The samples were brought on this trap column at a flow rate of 10 μ L/min with 99.5% solvent A for 2 min, after which the column was switched to the analytical column. The peptide separation was achieved using a multistep concave gradient based on the gradients described elsewhere.¹⁰ After washing with 90% solvent B, the column was re-equilibrated to initial conditions.

The detailed protocol is specified below:

TIME (MIN)	GRADIENT COMPOSITION (%B)	FLOW RATE (NL/MIN)
0	1.0	300
2.4	1.0	300
4.2	5.0	300
10.2	7.6	300
15.6	10.3	300
21	13.1	300
25.8	16.1	300
30.6	19.2	300
35.4	22.4	300
40.2	25.7	300
45	29.1	300
49.8	32.6	300
54	36.2	300

58.2	40.0	300
58.8	90.0	300
60.3	90.0	300
61.2	90.0	300
61.5	1.0	300
70.8	1.0	300

The rear seals of the pump were flushed every 30 min with 10% (v/v) ACN. [Glu1]-fibrinopeptide B (GluFib) was used as a lock mass compound. The auxiliary pump of the LC system was used to deliver this peptide to the reference sprayer (0.2 µl/min). As MS acquisition method, UDMS[®] method was set up as described previously.¹⁰ Briefly, these settings include that the mass range was set from 50 to 2,000 Da, with a scan time of 0.6 s in positive resolution mode. To be able to use the low-energy MS mode, the collision energy was set to 4 V in the trap cell. Besides, the transfer cell collision energy was ramped using drift-time-specific collision energies for the elevated energy scan¹¹. The lock mass was sampled every 30 s.

MS acquisition method

The Synapt G2Si mass spectrometer (Waters) operating with Masslynx for acquisition and PLGS for peptide identification was used for analysis. The following settings in positive resolution mode were used: source temperature of 80°C, capillary voltage 3.0 kV, nano flow gas of 0.25 Bar, purge gas 250 L/h, trap gas flow 2.0 ml/min, cone gas 100 L/h, sampling cone 25V, source offset 25, lock mass acquiring was done with a mixture of Leu Enk (556.2771) and Glu Fib (785.84265), lock spray voltage 2.5 kV, Glufib fragmentation was used as calibrant. An UDMS[®] data-independent acquisition method was used for analysis. Briefly, the mass range is set from 50 to 2,000 Da with a scan time of 0.6 seconds in positive, resolution mode. The collision energy is set to 4 V in the trap cell for low-energy MS mode. For the elevated energy scan, the transfer cell collision energy is ramped to higher collision energies and data is recorded. The lock mass was sampled every 30 seconds and used for accurate determination of parent ions mass after peak picking. The PLGS search engine was used for peptide identification against the Uniprot human database to which the streptavidin, avidin, yeast enolase and trypsin sequences were manually added. The ISOQuant software¹⁰ was used for label free quantification of proteins using 50 fmol of yeast enolase digest as benchmark.

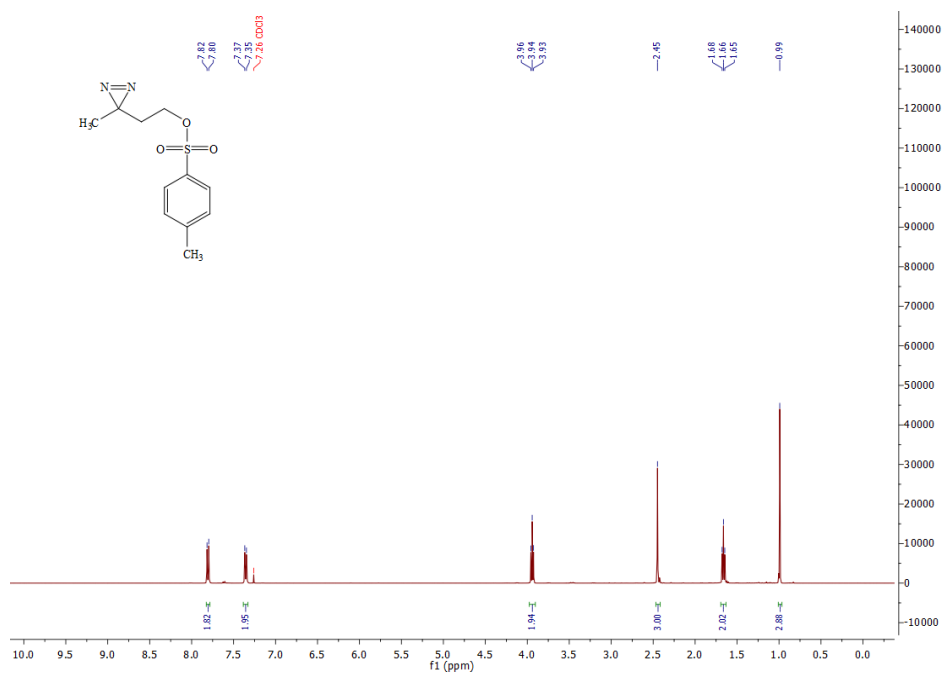
Proteomic analysis

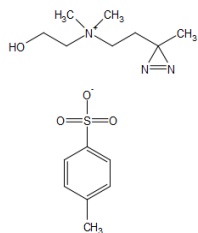
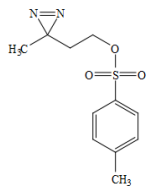
Configuration parameters for label-free quantification (LFQ) in the ISOQuant software are listed in Supplementary Table 2. For quantification, +UV and –UV replicates for all samples were compared in separate groups. The protein lists were filtered by excluding proteins that are considered as contamination (e.g. keratins), non-endogenous (e.g. trypsin, avidin) or non-reproducible (not present in six out of six +UV or centrifugation samples). For the volcano plots, the ratio of average ppm for each protein was calculated and is displayed as a logarithmic value ($^2\log$). Furthermore, the p-value was determined by multiple t-tests comparing the replicates of each group using the GraphPad Prism software. In addition, a Benjamini-Hochberg correction was applied to adjust the p-value for multiple comparisons. The final adjusted p-value is displayed as a logarithmic value ($^{10}\log$). Proteins that were exclusive for +UV samples or did not occur more than once in the –UV samples, making a t-test impossible, were labelled as ‘exclusive’ and are listed next to the volcano plot. Abundance plots were generated by plotting the ppm values of all six replicates. Similar statistical analysis was performed for validation experiments, with slight modifications: (1) the number of replicates here was four, but proteins still had to be present in four out of four replicates. (2) A Benjamini-Hochberg correction was no longer performed as the processing did not require a high amount of comparisons for the t-test. Instead, p-values were directly taken from t-tests and displayed as the logarithmic value ($^{10}\log$).

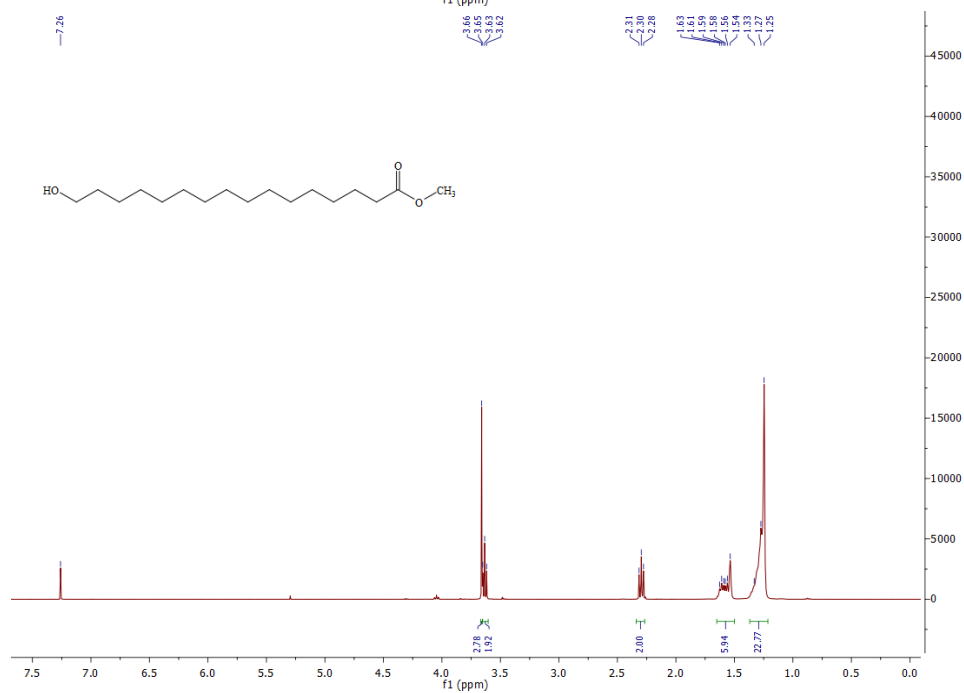
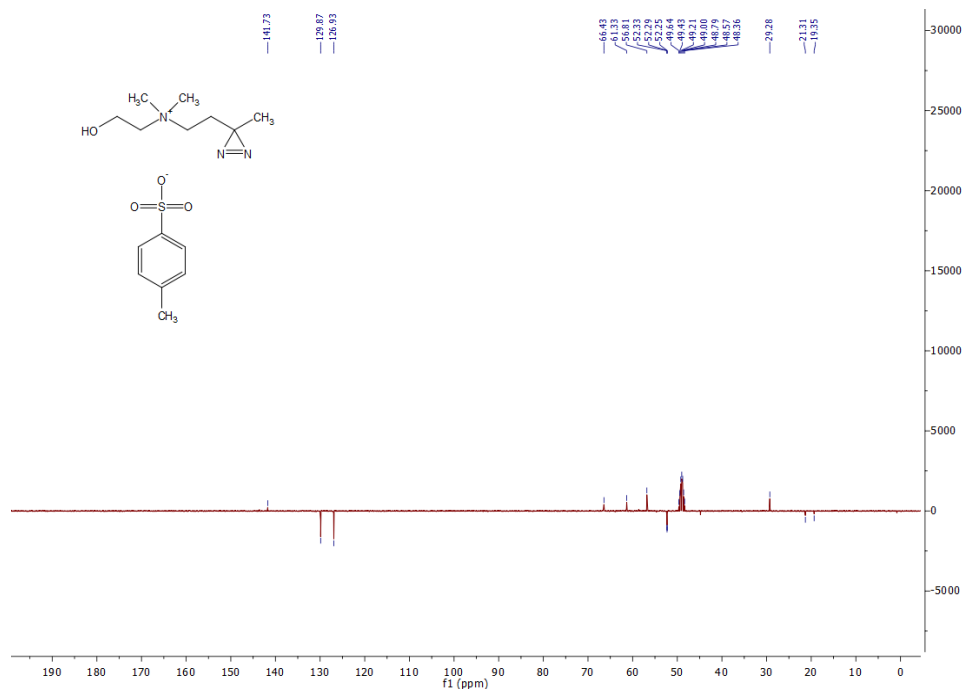
Absolute quantification was achieved from the same LFQ in ISOQuant, based on a comparison to the internal standard (ENLS digest, 50 fmol). The proteins that passed the criteria for the volcano plots were selected. The average absolute amount of these proteins in the +UV samples was corrected for the average in the –UV samples. For heat map construction, the sum of ppm values for all ‘accepted’ proteins within the sample was taken and the relative abundance of every protein was calculated as a ratio expressed in percentages of this value. For the photoaffinity method, the proteins within the enrichment and p-value boundaries of the volcano plot were considered as ‘accepted’. For the centrifugation method, all besides the initially filtered proteins were considered as ‘accepted’. Fully processed proteomic data for all samples is provided in two separate excel spreadsheets.

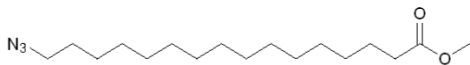
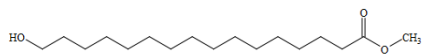
The mass spectrometry proteomics data have also been deposited to the ProteomeXchange Consortium via the PRIDE¹² partner repository with the dataset identifier PXD016229.

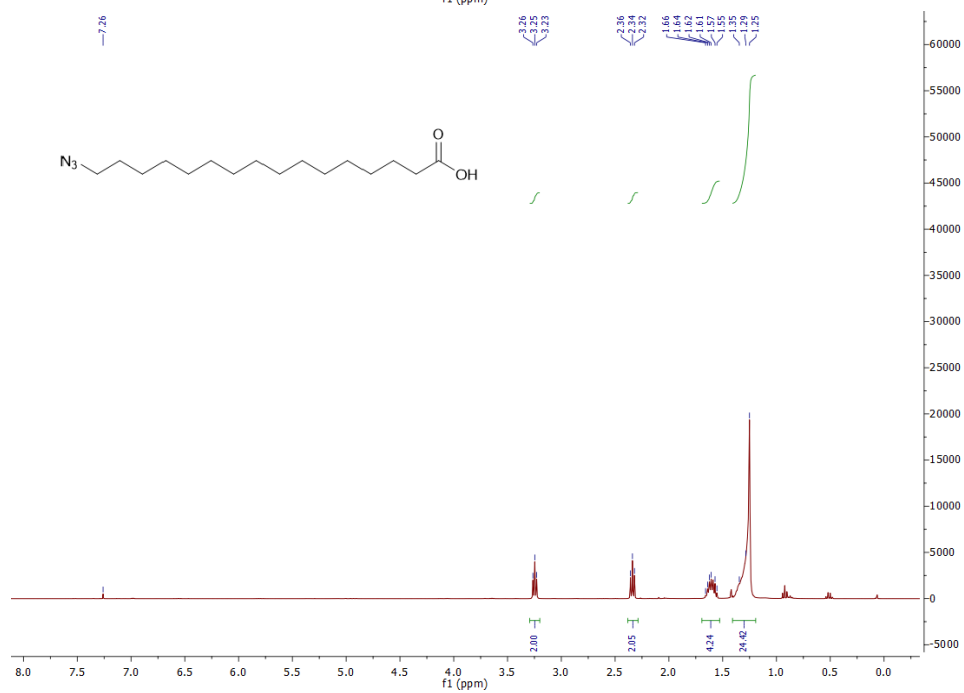
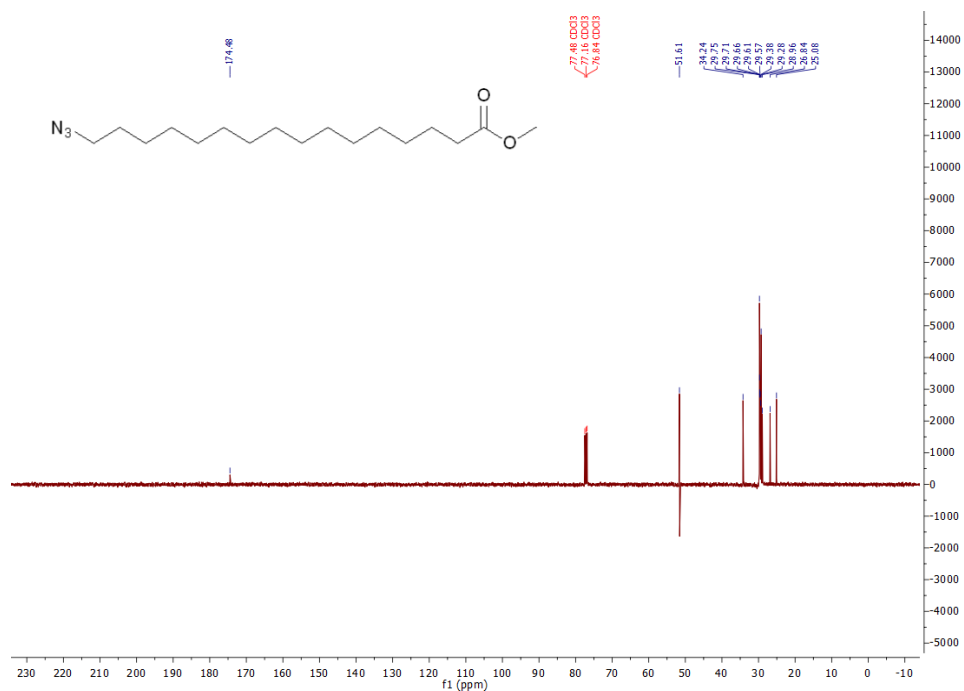
3. NMR and MS spectra

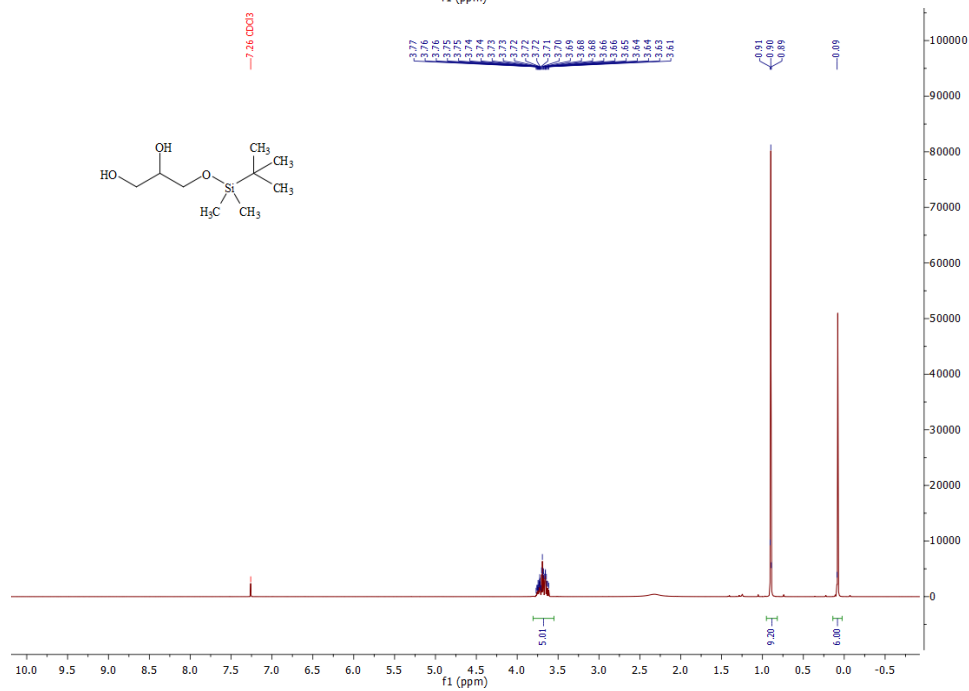
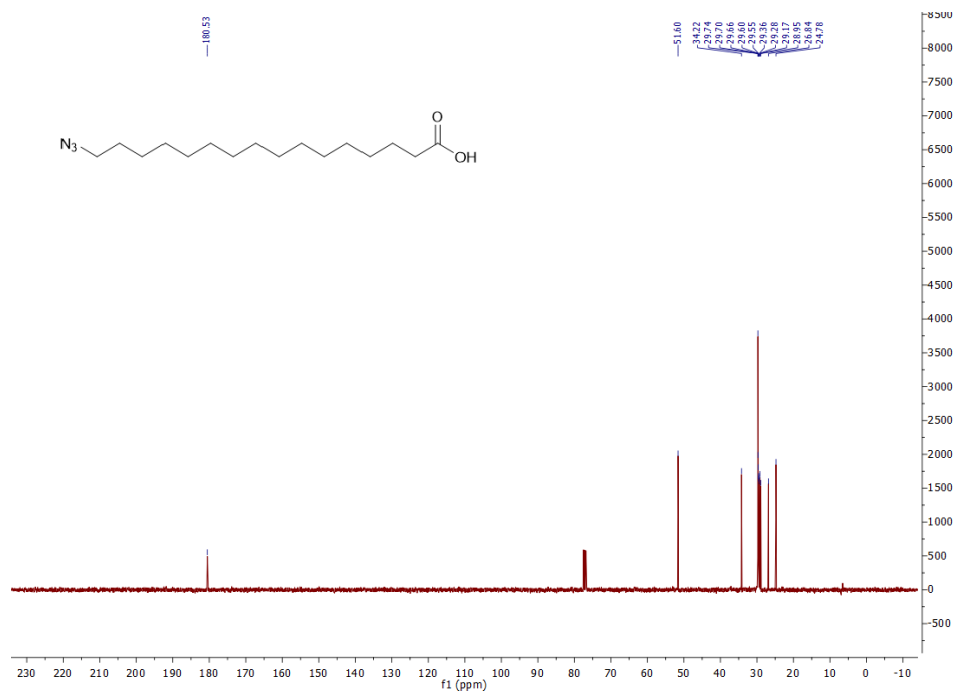


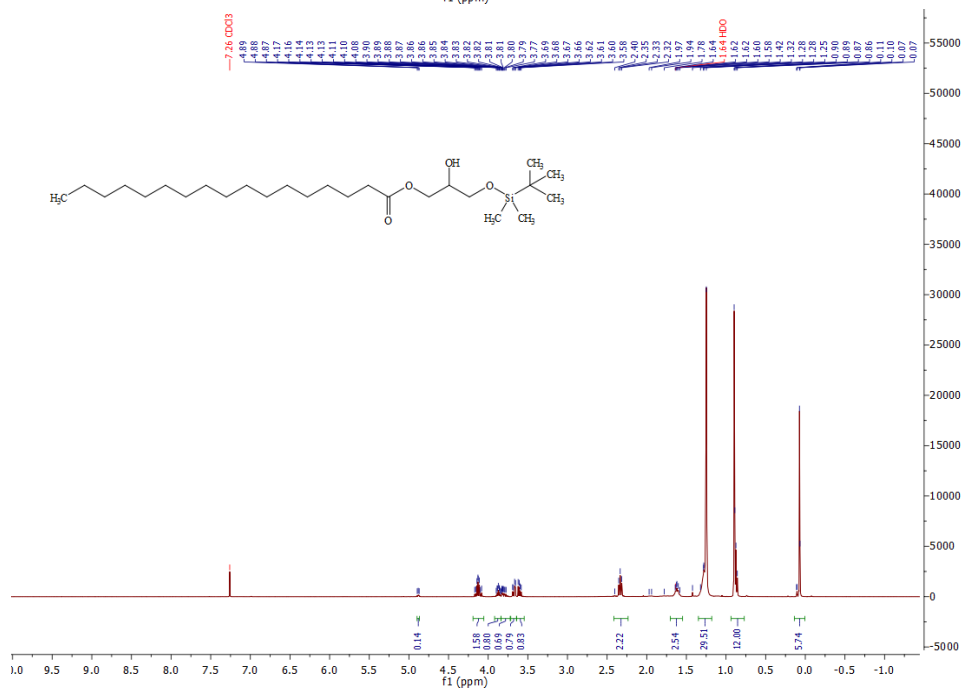
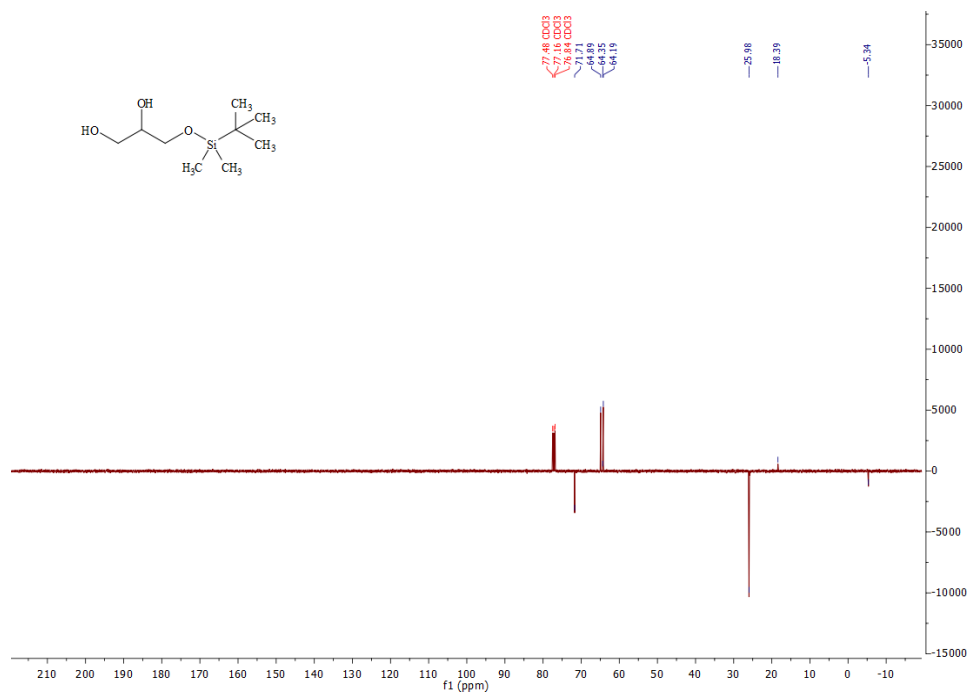


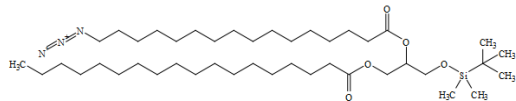
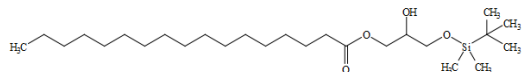


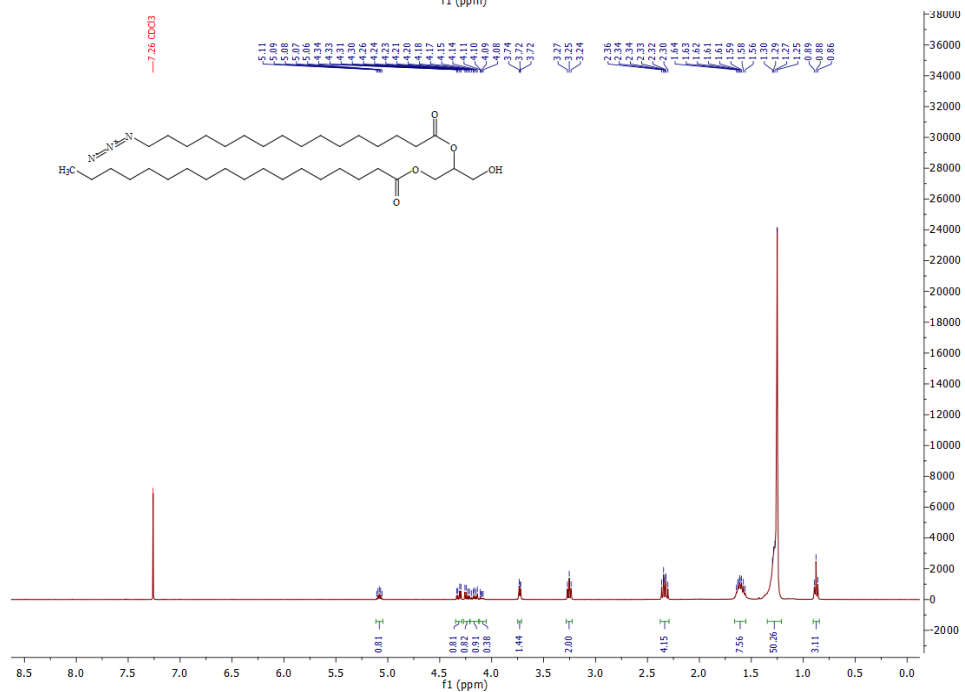
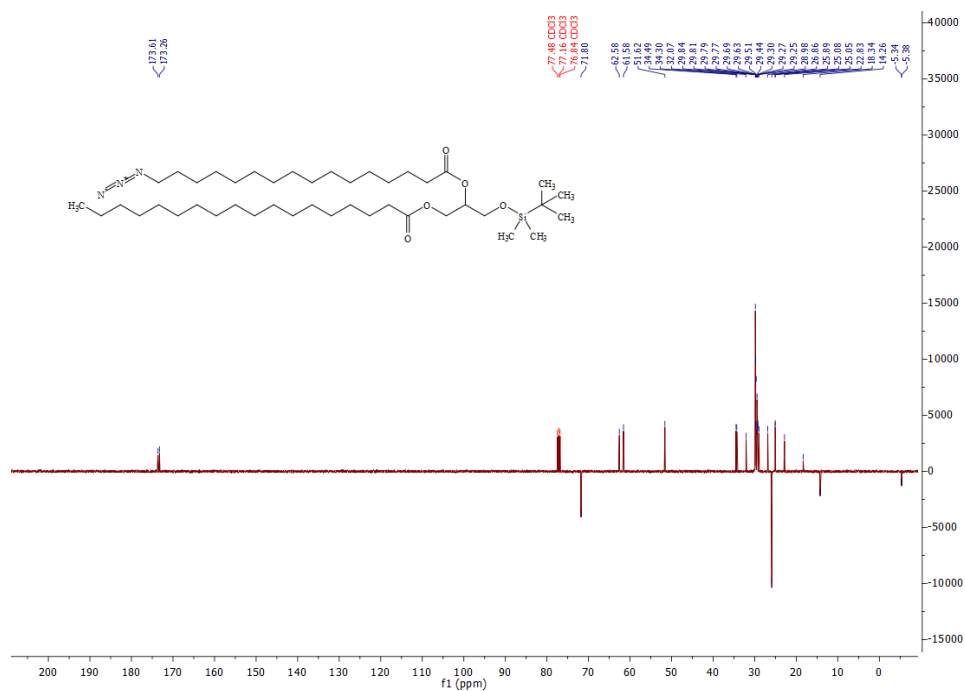


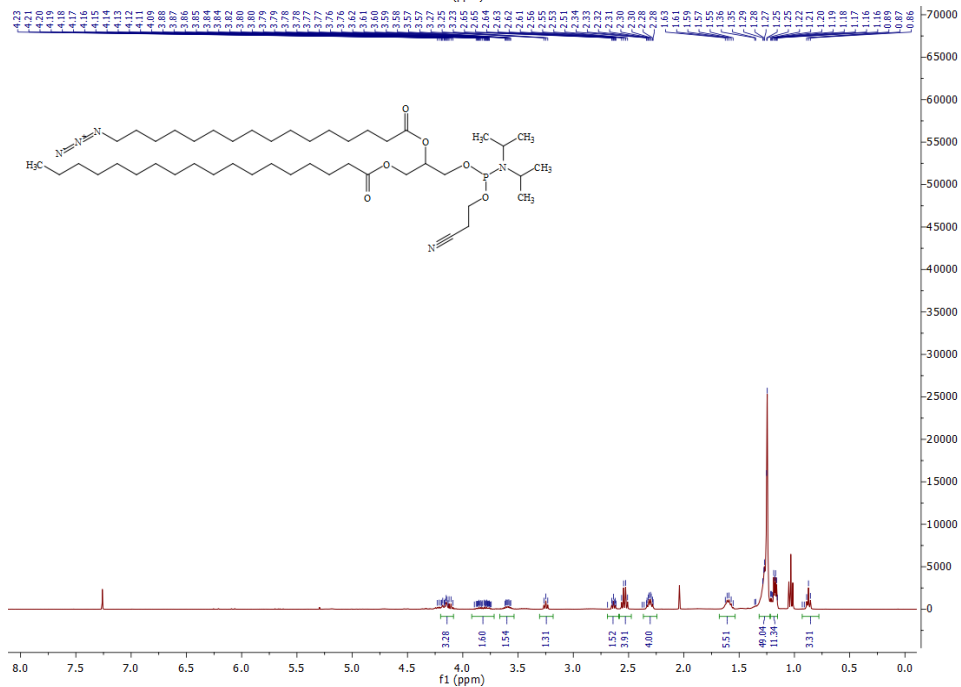


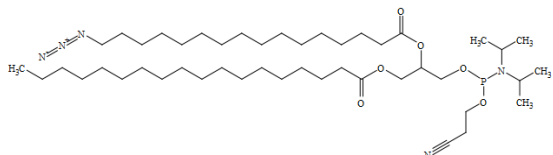
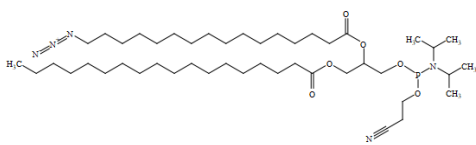


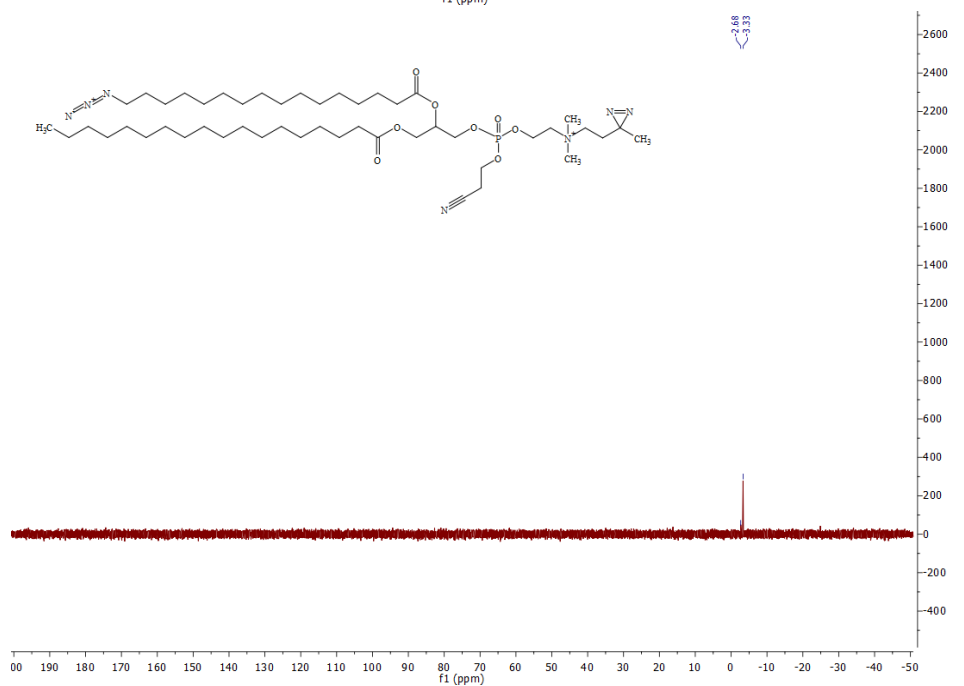


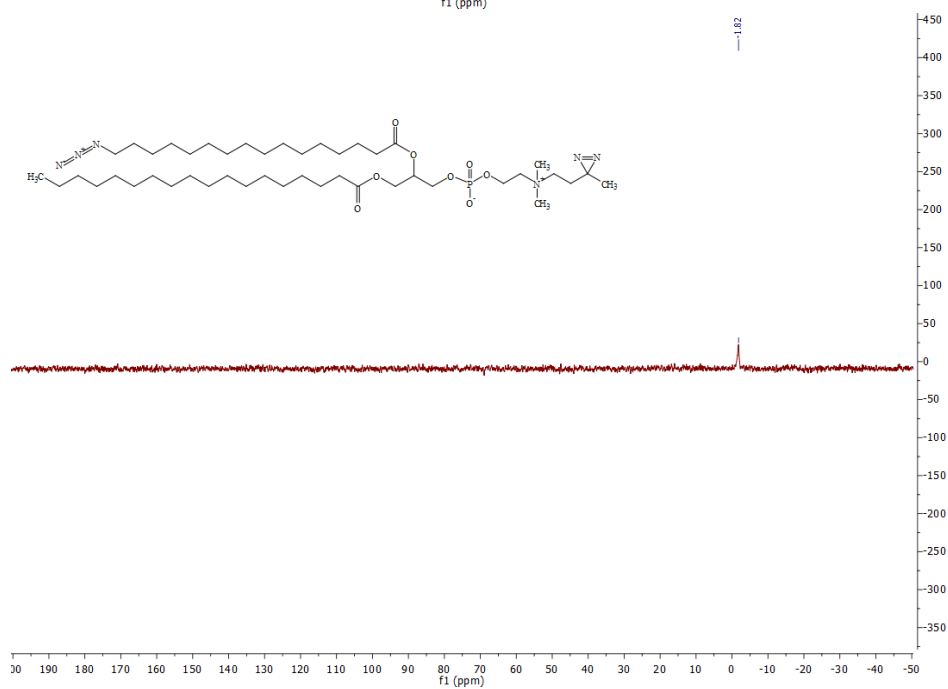


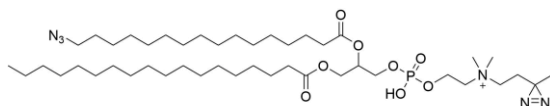




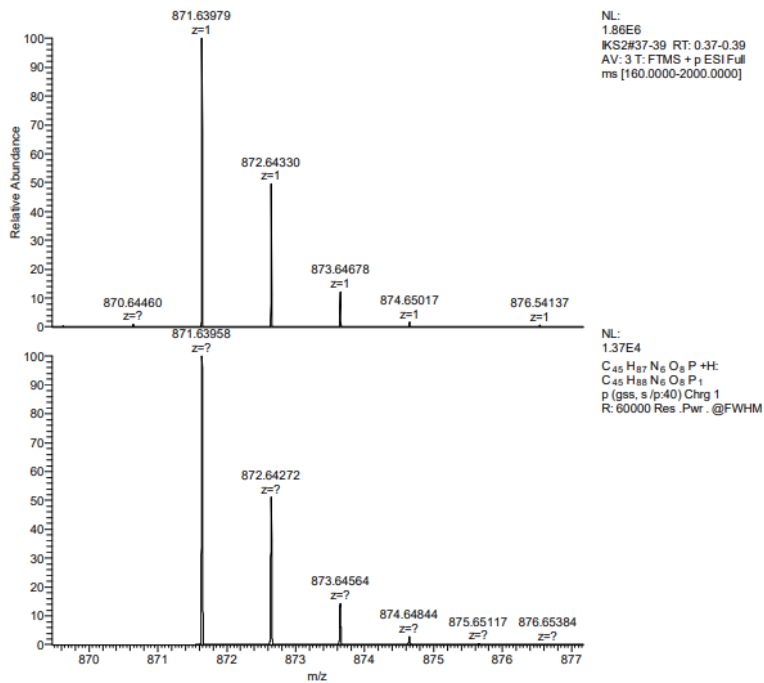








Exact Mass: 871.64



4. References

1. Bulbake, U., Doppalapudi, S., Kommineni, N. & Khan, W. Liposomal Formulations in Clinical Use: An Updated Review. *Pharmaceutics* 9, 12 (2017).
2. Shen, K. *et al.* Diazirines as Potential Molecular Imaging Tags: Probing the Requirements for Efficient and Long-Lived SABRE-Induced Hyperpolarization. *Angew. Chemie Int. Ed.* 56, 12112–12116 (2017).
3. Heal, W. P. *et al.* Bioorthogonal chemical tagging of protein cholesterylation in living cells. *Chem. Commun.* 47, 4081–4083 (2011).
4. Wessel, D. & Flügge, U. I. A method for the quantitative recovery of protein in dilute solution in the presence of detergents and lipids. *Anal. Biochem.* 138, 141–143 (1984).
5. Bigdeli, A. *et al.* Exploring Cellular Interactions of Liposomes Using Protein Corona Fingerprints and Physicochemical Properties. *ACS Nano* 10, 3723–3737 (2016).
6. Capriotti, A. L. *et al.* Analysis of plasma protein adsorption onto DC-Chol-DOPE cationic liposomes by HPLC-CHIP coupled to a Q-TOF mass spectrometer. *Anal. Bioanal. Chem.* 398, 2895–2903 (2010).
7. Barrán-Berdón, A. L. *et al.* Time evolution of nanoparticle-protein corona in human plasma: Relevance for targeted drug delivery. *Langmuir* 29, 6485–6494 (2013).
8. Rappsilber, J., Mann, M. & Ishihama, Y. Protocol for micro-purification, enrichment, pre-fractionation and storage of peptides for proteomics using StageTips. *Nat. Protoc.* 2, 1896–1906 (2007).
9. van Rooden, E. J. *et al.* Mapping in vivo target interaction profiles of covalent inhibitors using chemical proteomics with label-free quantification. *Nat. Protoc.* 13, 752–767 (2018).
10. Distler, U., Kuharev, J., Navarro, P. & Tenzer, S. Label-free quantification in ion mobility-enhanced data-independent acquisition proteomics. *Nat. Protoc.* 11, 795–812 (2016).
11. Distler, U. *et al.* Drift time-specific collision energies enable deep-coverage data-independent acquisition proteomics. *Nat. Methods* 11, 167–170 (2014).
12. Vizcaíno, J. A. *et al.* The Proteomics Identifications (PRIDE) database and associated tools: status in 2013. *Nucleic Acids Res.* 41, D1063–D1069 (2012).

Appendix 2

Supplementary Information to Chapter 3

1. Supplementary Figures and Tables

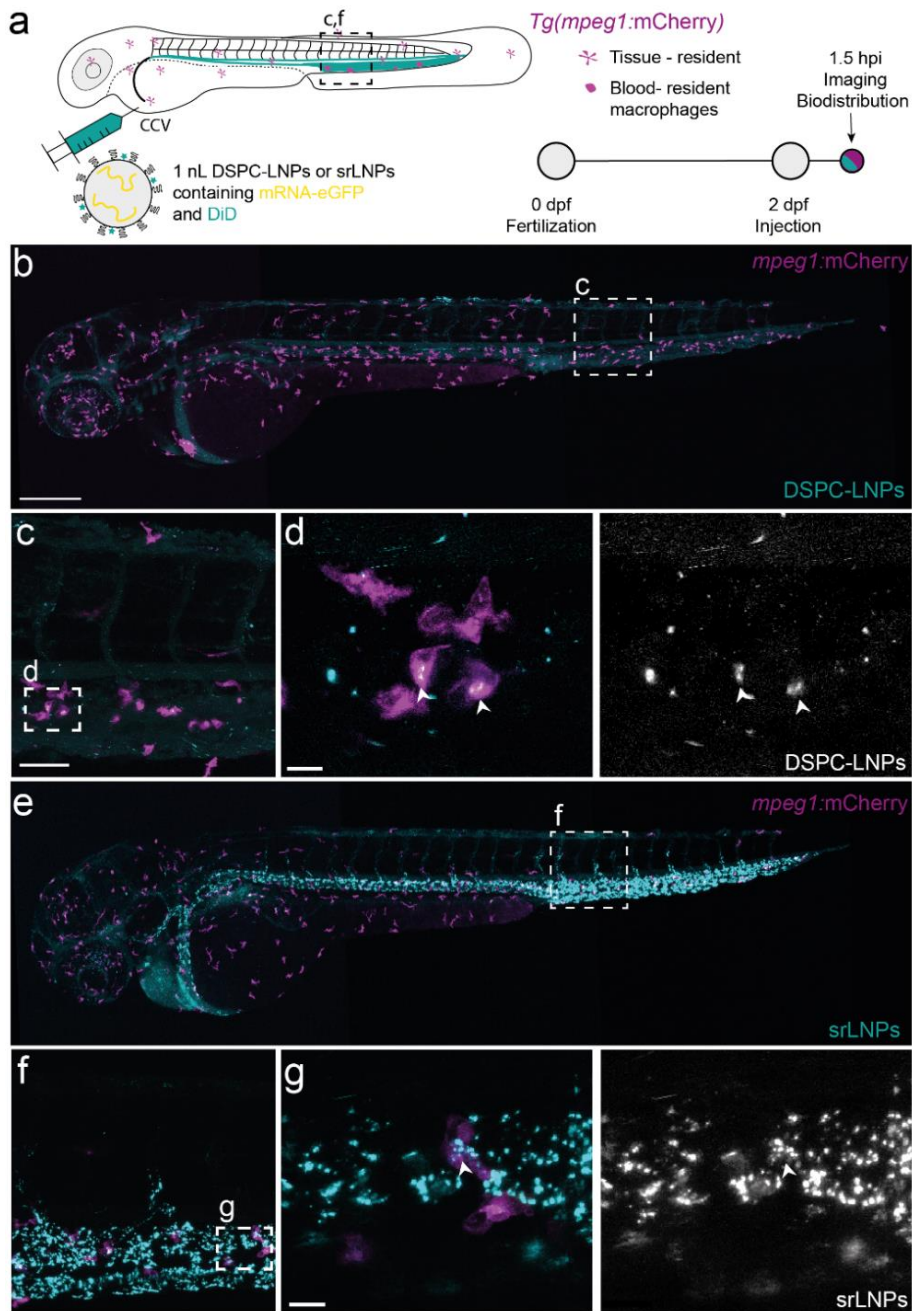


Figure S1. Biodistribution of DSPC-LNPs and srLNPs in *mpeg1:mCherry* transgenic zebrafish embryos at 1.5 hpi. (a) Schematic showing the site of LNP injection (*i.v*) within the embryonic zebrafish (2 dpf) and imaging timeframe. LNPs contained DiD (cy5, 0.1 mol%) as fluorescent lipid probe and unlabeled eGFP mRNA. Transgenic *mpeg1:mCherry* zebrafish embryos stably express mCherry (magenta) within all macrophages. *Injected dose:* ~10 mM lipid, ~0.2 mg/kg mRNA. *Injection volume:* 1 nL. CCV – common cardinal vein (a) Whole embryo view (10x magnification), (b) tissue level view (40x magnification), and (c) a zoom of a maximum projection of three confocal z-stacks, showing fluorescent co-localisation of DiD (LNP probe) and transgenic mCherry (white arrowheads), confirmed low-level DSPC-LNP uptake within blood resident macrophages. (d) Whole embryo view (10x magnification), (e) tissue level view (40x magnification) and (f) a zoom of a maximum projection of three confocal z-stacks, showing fluorescent co-localisation of DiD (LNP probe) and transgenic mCherry (white arrowheads), confirmed simultaneous uptake of srLNPs within both SECs and blood resident macrophages. Scale bars: 200 μ m (whole body), 50 μ m (tissue level), 10 μ m (zoom).



Figure S2. Biodistribution of srLNPs and DSPC-LNPs in double knock-out (*stab1^{-/-}/stab2^{-/-}*) mutant embryos at 1.5 hpi. (a) Schematic showing the site of LNP injection (*i.v.*) within double

knockout ($stab1^{ibl3}/stab2^{ibl2}$)¹ zebrafish embryos (2 dpf) and imaging timeframe. LNPs contained DOPE-LR (cyan, 0.2 mol%) as fluorescent lipid probe and Cy5-labelled eGFP mRNA (magenta) as fluorescent mRNA probe. *Injected dose*: ~10 mM lipid, ~0.2 mg/kg mRNA. *Injection volume*: ~1 nL. CV – cardinal vein; PCV – posterior cardinal vein; CCV – common cardinal vein. (b,c) Whole embryo (10x magnification) views of srLNP and DSPC-LNP biodistribution within $stab1^{-}/stab2^{-}$ mutant embryos (2 dpf) at 1.5 hpi. In both cases, LNPs were mostly freely circulating throughout the vasculature of the embryo at 1.5 hpi. Scale bar: 200 μ m.

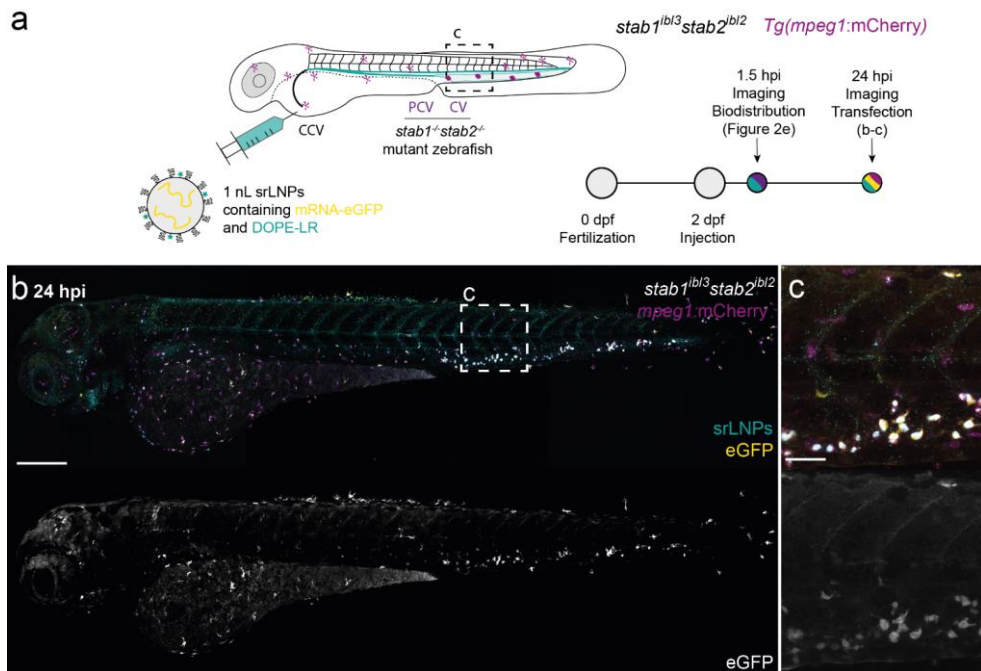


Figure S3. srLNP biodistribution and eGFP expression in double knock-out ($stab1^{-}/stab2^{-}$) mutant embryos at 24 hpi. (a) Schematic showing the site of LNP injection (*i.v.*) within transgenic *mpeg1:mCherry*, double knockout ($stab1^{ibl3}/stab2^{ibl2}$)¹ zebrafish embryos (2 dpf) and imaging timeframe. LNPs contained DiD (cy5, 0.1 mol%, cyan) as fluorescent lipid probe and unlabeled eGFP mRNA. *Injected dose*: ~10 mM lipid, ~0.2 mg/kg mRNA. *Injection volume*: ~1 nL. CCV – common cardinal vein, CV – cardinal vein; PCV – posterior cardinal vein. (b,c) Whole embryo (10x magnification) and tissue level (40x magnification) views of srLNP biodistribution and eGFP expression within $stab1^{-}/stab2^{-}$ mutant embryos at 24 hpi. Within these embryos, srLNP localisation and eGFP expression is observed within blood resident macrophages (magenta) but not SECs at 24 hpi. Scale bars: 200 μ m (whole embryo) and 50 μ m (tissue level).

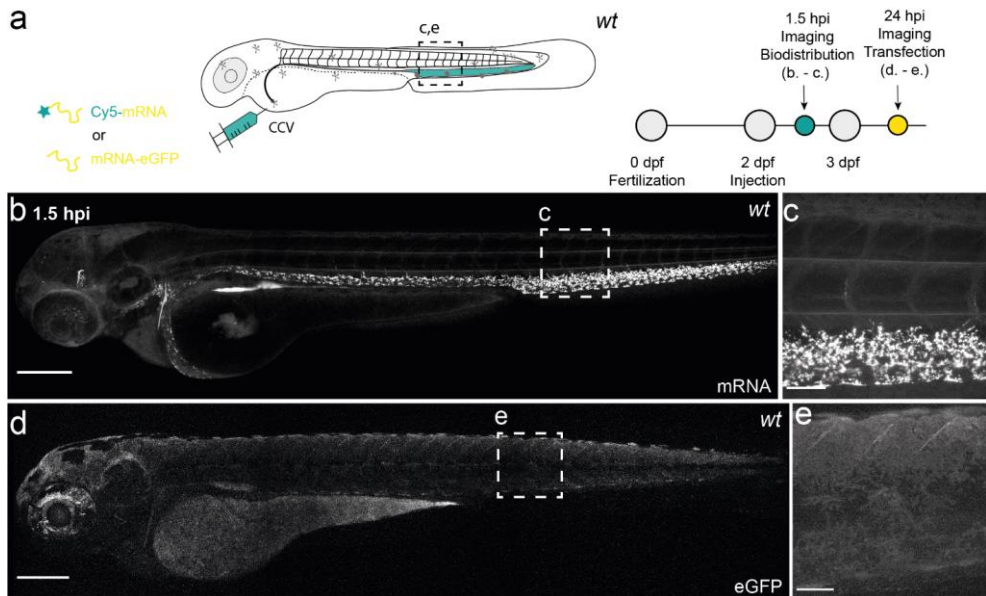


Figure S4. Biodistribution and expression of free eGFP mRNA in wildtype (AB/TL) embryonic zebrafish. (a) Schematic showing the site of free mRNA injection (*i.v.*; 0.2 mg/kg, 1 nL) within embryonic zebrafish (2 dpf) and imaging timeframe. CCV – common cardinal vein. (b,c) Whole embryo (10x magnification) and tissue level (40x magnification) views of free mRNA (Cy5-labelled) biodistribution at 1.5 hpi. Free mRNA primarily accumulated within SECs of the embryonic zebrafish at 1.5 hpi, likely mediated by Stabilin receptors.² Any phagocytotic uptake of free mRNA within blood resident macrophages cannot be clearly defined within the CHT of the wild-type embryo given the high fluorescence signal (Cy5) within overlapping SECs. (d,e) Whole embryo (10x magnification) and tissue level (40x magnification) views of eGFP expression (unlabeled mRNA) at 24 hpi. No significant eGFP expression is observed within SECs or blood resident macrophages of the embryonic fish. Scale bars: 200 μ m (whole embryo) and 50 μ m (tissue level).

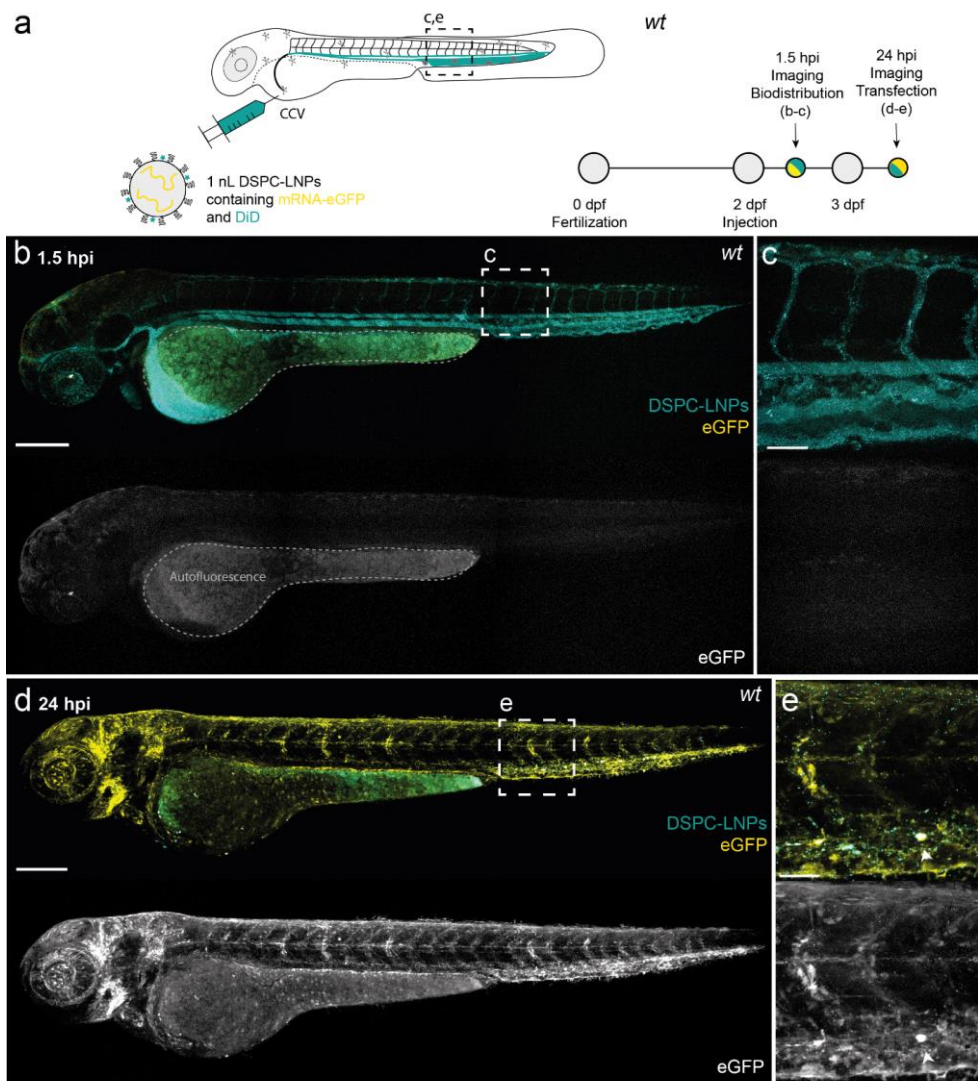


Figure S5. DSPC-LNP biodistribution and eGFP expression within wild-type (AB/TL) zebrafish embryos at 1.5 and 24 hpi. (a) Schematic showing the site of DSPC-LNP (*i.v.*) injection within embryonic zebrafish (2 dpf) and imaging timeframe. DSPC-LNPs contained DiD (Cy5, 0.1 mol%) as fluorescent lipid probe and unlabeled eGFP mRNA (capped) payload. *Injected dose*: ~10 mM lipid, ~0.2 mg/kg mRNA. *Injection volume*: ~1 nL. CCV – common cardinal vein. (b,c) Whole embryo (10x magnification) and tissue level (40x magnification) views of DSPC-LNP biodistribution and eGFP expression within the embryonic zebrafish at 1.5 hpi. DSPC-LNPs were mostly freely circulating, confined to and homogeneously distributed throughout the vasculature of the embryo at 1.5 hpi. Low

level embryo autofluorescence (GFP channel) within the yolk sac and pigment cells of the embryo is highlighted. (d,e) Whole embryo and tissue level views of DSPC-LNP biodistribution and eGFP expression within the embryonic zebrafish at 24 hpi. Widespread eGFP expression throughout the embryo indicates non-specific uptake of DSPC-LNPs in many different cell types. eGFP expression within macrophages (based on location and morphology) highlighted with white arrowheads. Scale bars: 200 μ m (whole embryo) and 50 μ m (tissue level).

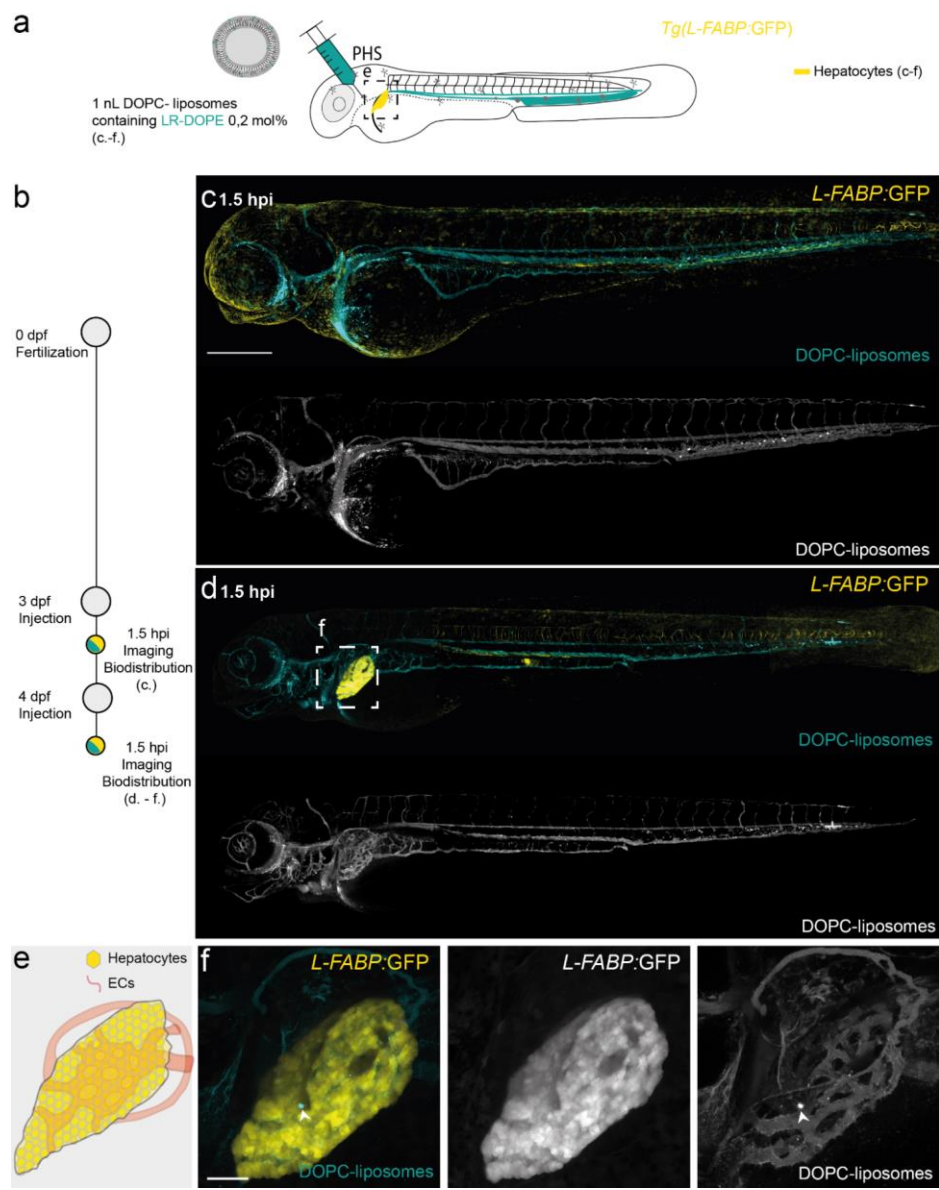


Figure S6. DOPC liposome biodistribution in *L-FABP:eGFP* transgenic zebrafish embryos (3 and 4 dpf) at 1.5 hpi. (a) Schematic showing the site of liposome injection (*i.v.*) within embryonic zebrafish (3 or 4 dpf). Liposomes contained 0.2 mol% DOPE-lissamine rhodamine as fluorescent lipid probe (cyan). *Injected dose*: ~5 mM lipid. *Injection volume*: 1 nL. Transgenic *L-FABP:eGFP* zebrafish embryos stably express eGFP (yellow) in hepatocytes. PHS – primary head sinus. (b) Injection and imaging timeframe. (c,d) Whole embryo (10x magnification) views of DOPC liposome biodistribution within the embryonic zebrafish (3 or 4 dpf) at 1.5 hpi. (e) Tissue level schematic of the embryonic liver at 4 dpf. (f) Tissue level (40x magnification) views of DOPC liposome biodistribution within the liver of a four-day old embryo. Liposomes freely circulate throughout the liver vasculature and do not associate with either ECs or hepatocytes of the embryonic liver. The single, intense fluorescent (DOPE-LR) punctum (white arrowhead) observed within the liver of the four-day old embryo is most likely due to macrophage uptake. Scale bars: 200 μ m (whole embryo) and 50 μ m (tissue level).

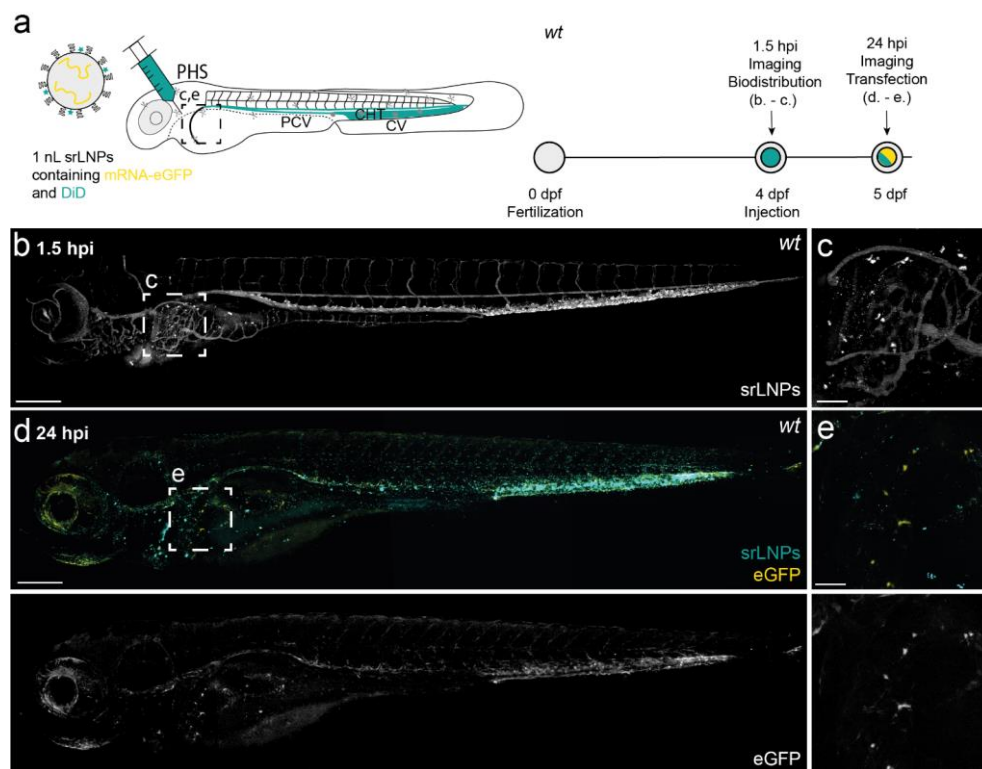
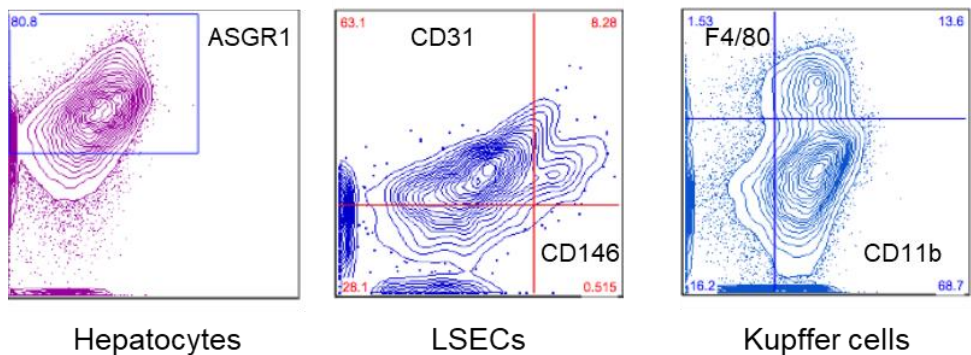
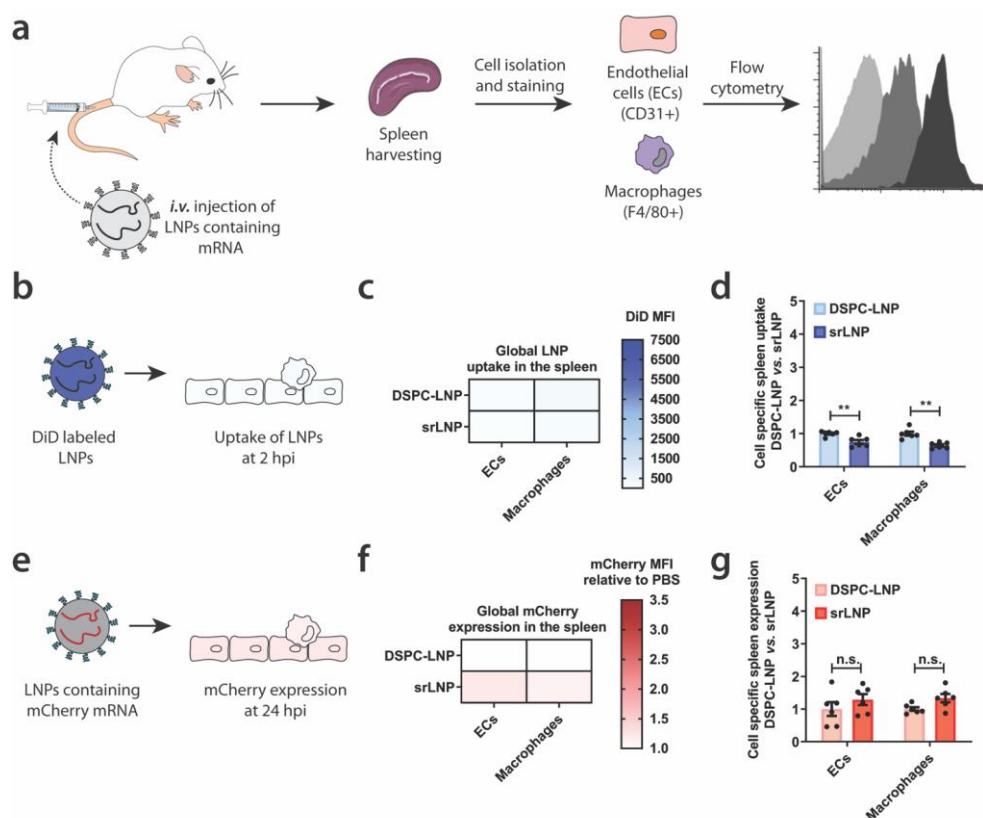


Figure S7. srLNP (30 mM) biodistribution and mRNA expression within wildtype (AB/TL) embryonic zebrafish. (a) Schematic showing the site of srLNP injection (*i.v.*) within embryonic zebrafish (4 dpf). srLNPs contained DiD (approx. 0.1 mol%) as fluorescent lipid probe and unlabeled, eGFP mRNA (capped) payload. *Injected dose*: ~10 mM lipid, ~0.2

mg/kg mRNA. *Injection volume*: 1 nL. PHS – primary head sinus. (b,c) Whole embryo (10x magnification) and tissue level (40x magnification, liver region) views of srLNP biodistribution (DiD, cyan) at 1.5 hpi. srLNPs were mainly associated with SECs within the PCV, CV and CHT of the four-day old embryo at 1.5 hpi. Due to the higher injected dosage, a significant fraction of srLNPs are also observed in circulation, possibly due to saturation of Stabilin receptors. Within the liver region, individual fluorescent punctae associated with srLNP accumulation are most likely due to macrophage uptake. (d,e) Whole embryo (10x magnification) and tissue level (40x magnification, liver region) views of srLNP biodistribution and eGFP expression within the embryonic zebrafish at 24 hpi. srLNPs remain predominantly localized within the PCV, CV and CHT at 24 hpi, with exogenous eGFP expression mainly restricted to this region of the five day-old embryo. Within the liver region, eGFP fluorescence is restricted to a handful of individual cells and does not evidently colocalize with srLNP-associated fluorescence (DiD). From these images, it is not clear whether eGFP fluorescence within the liver is due to macrophage uptake (possibly distal from the liver, and following macrophage migration), embryo autofluorescence or uptake within an alternative cell type. Scale bars: 200 μ m (whole embryo) and 50 μ m (tissue level).



Figures S8. Detection of major cell types in the liver microenvironment. Representative flow cytometry density plots illustrate the detection of specific hepatic cell types following liver perfusion and cell harvesting.



not significant, ** $p < 0.01$, *** $p < 0.001$. Exact P values for d: ECs $P = 0.0039$, Macrophages $P = 0.0011$. Exact P values for g: ECs $P = 0.308$, Macrophages $P = 0.074$.

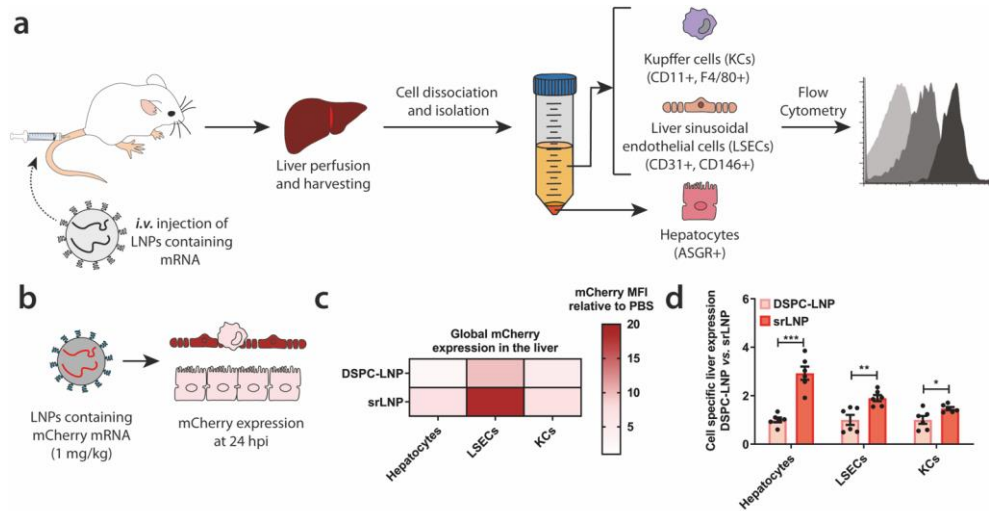


Figure S10. Functional mCherry mRNA delivery to hepatic RES cell types at an injected mRNA dose of 1 mg/kg. (a) Schematic illustrating the procedure to isolate different hepatic cell types and determine LNP-mRNA targeting and functional mRNA delivery. Following intravenous LNP injection (*i.v.*) the liver was perfused with collagenase IV, hepatic cells were isolated and stained with specific antibodies, and flow cytometry was used to analyze LNP uptake and gene expression. Specific antibody markers used to uniquely identify hepatocytes, LSECs and KCs, respectively, are defined in parentheses. (b) LNPs contained mCherry-mRNA. Functional mRNA delivery was assessed based on mCherry reporter gene expression levels at 24 hpi. (c) Heatmap of mCherry expression in different liver cell types enabled by mRNA delivery using DSPC-LNP and srLNP. *Injected dose:* 1 mg/kg mRNA. srLNPs led to enhanced gene expression in hepatic RES cells, predominantly in LSECs. (d) Cell specific mCherry expression normalized to DSPC-LNP for each cell type. In all cases, $n = 6$ represents 3 separate liver tissue samples from 2 mice sorted into individual cell types. Bars and error bars in c and e represent mean \pm s.e.m. Statistical significance was evaluated using a two-tailed unpaired Student's t-test. * $p < 0.05$, ** $p < 0.01$, *** $p < 0.001$. Exact P values for d: Hepatocytes $P = 0.00018$, LSECs $P = 0.0083$, KCs $P = 0.025$

Formulation	mRNA	Fluorescent lipid	% of Fluorescent Lipid	Avg. Size (nm)	PDI	Zeta Potential (mV)	EE (%)	n
DSPC-LNP	eGFP	DOPE-LR	0.2	82.5 ± 2.0	0.085 ± 0.027	-5.5 ± 1.2	95 ± 2	3
srLNP	eGFP	DOPE-LR	0.2	89.2 ± 5.7	0.094 ± 0.023	-21.9 ± 2.5	88 ± 3	3
DSPC-LNP	eGFP	DiD	0.1	82.5 ± 3.4	0.081 ± 0.026	-4.1 ± 1.6	95 ± 1	3
srLNP	eGFP	DiD	0.1	94.7 ± 4.0	0.102 ± 0.016	-17.5 ± 2.4	91 ± 2	3
DSPC-LNP	eGFP	-	-	82.5 ± 4.0	0.103 ± 0.037	-4.0 ± 0.9	93 ± 1	2
srLNP	eGFP	-	-	86.6 ± 6.7	0.108 ± 0.006	-19.0 ± 1.1	91 ± 4	2
DSPC-LNP	mCherry	DiD	0.1	79.9 ± 5.2	0.072 ± 0.038	-3.7 ± 1.8	94 ± 3	2
srLNP	mCherry	DiD	0.1	92.7 ± 3.5	0.102 ± 0.012	-18.8 ± 2.1	89 ± 4	2
DSPC-LNP	Cy5-mRNA	DOPE-LR	0.2	87.0 ± 3.5	0.090 ± 0.016	-3.9 ± 0.9	95 ± 3	2
srLNP	Cy5-mRNA	DOPE-LR	0.2	94.1 ± 2.3	0.096 ± 0.01	-16.2 ± 1.2	91 ± 2	2
DOPC	-	DOPE-LR	0.2	96.3 ± 4.0	0.095 ± 0.011	-6.1 ± 1.1	-	2
DOPC+ApoE-peptide	-	DOPE-LR	0.2	104.7 ± 3.8	0.075 ± 0.012	14.7 ± 1.6	-	2

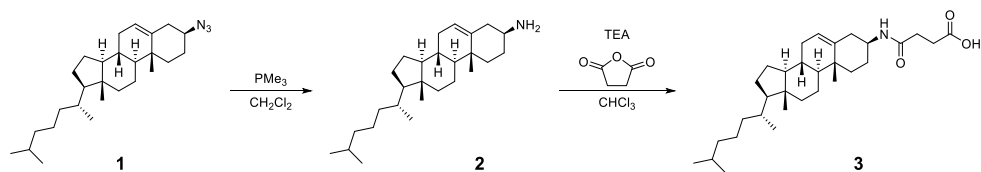
Table S1. Composition, size (as measured by DLS), polydispersity (PDI), surface charge (as measured by zeta potential), RNA encapsulation efficiency (as measured by RiboGreen assay) and reproducibility of all LNP and liposome formulations used in this study.

2. Materials and Methods

Reagents

Dimethylformamide (DMF), piperidine, acetic anhydride, pyridine, trifluoroacetic acid (TFA) and acetonitrile (MeCN) were purchased from Biosolve (Valkenswaard, The Netherlands). N,N-diisopropylethylamine (DIPEA), and Oxyma were obtained from Carl Roth GmbH & Co (Karlsruhe, Germany). Dichloromethane (DCM) and diethyl ether were supplied by Honeywell (Amsterdam, The Netherlands). Fmoc-Rink Amide AM resin was obtained from IRIS Biotech GmbH (Marktredwitz, Germany). All amino acids were supplied by NovaBioChem, (Zwijndrecht, The Netherlands), a subsidiary of Merck. 1,2-distearoyl-*sn*-glycerol-3-phosphocholine (DSPC), 1,2-distearoyl-*sn*-glycero-3-phospho-(1'-rac-glycerol) (DSPG), 1,2-dioleoyl-*sn*-glycerol-3-phosphocholine (DOPC) and 1,2-dimyristoyl-rac-glycero-3-methoxypolyethylene glycol-2000 (DMG-PEG2k) were purchased from Avanti Polar Lipids (Alabaster, USA) or Lipoid GmbH (Ludwigshafen, Germany). All other chemicals were purchased from Merck (Zwijndrecht, The Netherlands). (6Z,9Z,28Z,31Z)-heptatriaconta-6,9,28,31-tetraen-19-yl-4-(dimethylamino) butanoate (DLin-MC3-DMA) was synthesized as described.³ 3-azido-5-cholestene (1) was synthesized as described.⁴ CleanCap eGFP (5moU) mRNA, CleanCap mCherry (5moU) mRNA and CleanCap Cyanine 5 eGFP (5moU) mRNA were purchased from TriLink Biotechnologies (San Diego, USA) or Tebu-bio (Heerhugowaard, The Netherlands).

Synthesis of N-succinyl-3-amino-5-cholestene (3)⁵



3-azido-5-cholestene (**1**, 1240 mg, 3 mmol) was dissolved in 30 mL dry DCM and the flask placed under a nitrogen atmosphere. A 1M solution of trimethylphosphine (12 mL, 12 mmol, 4 eq.) in toluene was added and the mixture was stirred for 21 hours. The reaction was quenched by the addition of 25 mL 1M sodium hydroxide solution, followed by vigorous stirring for 30 minutes. The mixture was transferred to a separating funnel, organic phase collected and the aqueous phase further extracted with 25 mL dichloromethane. The organic phases were combined and washed with 100 mL water (2x), 100 mL brine, and the organic phase dried over anhydrous magnesium sulfate. After concentration *in vacuo*, the resulting white powder was dried under high vacuum overnight to yield cholesteryl-amine (**2**) in quantitative yield.

Cholesteryl-amine **2** (440 mg, 1.14 mmol) was combined with succinic anhydride (342 mg, 3.4 mmol, 2.98 eq.) in 30 mL CHCl₃ and warmed to dissolve the mixture. Triethylamine (315 μ L, 2.3 mmol, 2 eq.) was then added and the solution stirred for 16 hours. The reaction mixture was then washed with 50 mL 5% acetic acid solution in water (2x), 50 mL water (2x), 50 mL brine, and the organic phase dried over anhydrous magnesium sulfate. The mixture was concentrated *in vacuo* and filtered through a silica gel plug (eluent; 1:1 dichloromethane/ethyl acetate + 1% acetic acid). Concentration *in vacuo* yielded cholesteryl-4-amino-4-oxobutanoic acid (**3**) as a white powder (408 mg, 0.84 mmol, 74%).

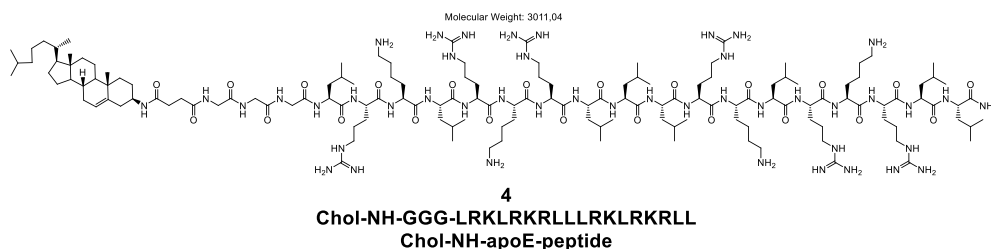
¹H NMR (400 MHz, DMSO): δ 12.05 (s, 1H), 7.76 (d, J = 7.8 Hz, 1H), 5.34 – 5.20 (m, 1H), 3.45 – 3.38 (m, 1H), 2.39 (t, J = 6.9 Hz, 2H), 2.26 (t, J = 6.9 Hz, 2H), 2.09 (d, J = 8.2 Hz, 2H), 2.00 – 1.86 (m, 2H), 1.80 (d, J = 12.3 Hz, 2H), 1.65 – 1.27 (m, 13H), 1.16 – 0.78 (m, 24H), 0.65 (s, 3H).

Peptide synthesis

Solid-phase peptide synthesis was performed at a 0.1 mmol scale with Fmoc-Rink Amide AM resin (0.64 mmol/g) on a Liberty Blue™ Automated Microwave Peptide Synthesizer. Fmoc-deprotection was achieved using 20% piperidine in DMF, and coupling reactions using DIC as activator and Oxyma as base. The final Fmoc-group was deprotected and the

resin was washed with DMF (3x) and DCM (3x) respectively and stored at 4 °C prior to further use.

Chol-NH-ApoE₃ peptide synthesis and purification



To the synthesized peptide on solid support (0.025 mmol) in a fritted syringe was added cholesteryl-4-amino-4-oxobutanoic acid (**3**, 0.1 mmol, 4 eq.), HATU (0.1 mmol, 4 eq.), DIPEA (0.5 mmol, 20 eq.) and dimethylformamide (5 mL) and the mixture agitated overnight at room temperature. The liquids were filtered from the resin and the resin was washed with dimethylformamide (3 x 5 mL) and dichloromethane (3 x 5 mL). Cleavage from the resin was performed by the addition of a mixture of TFA : TIPS : water (95 : 2.5 : 2.5 vol%, 5 mL) and agitation at room temperature for 2 hours. The reaction was precipitated using ice-cold diethyl ether (45 mL) and the precipitate was collected by centrifugation (3000 g, 30 min), suspended in water and lyophilized. Purification was performed by reversed-phase HPLC on a Kinetix® Evo C18 column (5 μ m, 100 Å, 150 mm x 21.2 mm) with a Shimadzu system comprising two LC-8A pumps and an SPD-10AVP UV-vis detector (operating at 220 nm). The cholesterol peptide-conjugate was purified using a gradient of 30–90% B, (where B is MeCN containing 0.1% TFA, and A is water with 0.1% TFA) over 20 minutes with a flow rate of 10 ml min⁻¹, eluting at 11.3–12.0 minutes. The collected fractions were analyzed using LC-MS, pooled and freeze-dried. LC-MS was performed on a Kinetix® Biphenyl column (2.6 μ m, 100 Å, 100 mm x 4.6 mm) using a Thermo Scientific™ Dionex™ Ultimate 3000 UHPLC (with a UV-VIS detector operating at 220 nm) coupled to a TSQ Quantum access MAX electron spray ionization (ESI) mass spectrometer operating with a ionization range of 140–2000 Da. Identification was performed using a gradient of 30–90% B, (where B is MeCN containing 0.1% TFA, and A is water with 0.1% TFA) over 13 minutes with a flow rate of 1 ml min⁻¹. Calculated mass: [M+H]⁺ = 1506.0 Da ; [M+2H]²⁺ = 1004.3 Da, Detected mass: [M+H]⁺ = 1505.44 Da [M+2H]²⁺ = 1003.1 Da.

Liposome Formulation

DOPC liposomes (with and without incorporated Chol-NH-ApoE-peptide, 5 mol%) were formulated in 20 mM HEPES buffer (pH = 7.3) at a total lipid concentration of 5 mM. DOPC and Chol-NH-ApoE-peptide, as stock solutions in chloroform (10 mM), were combined to the desired molar ratios and dried to a film, first under a stream of N₂ followed by the removal of trace solvents *in vacuo* for >1 h. Lipid films were hydrated and large unilamellar vesicles formed through extrusion at room temperature (Mini-extruder, Avanti Polar Lipids, Alabaster, US). Hydrated lipids were passed 11 times through a 100 nm polycarbonate (PC) membrane (Nucleopore Track-Etch membranes, Whatman). All liposome formulations were stored at 4°C and used within 2 days.

Lipid Nanoparticle (LNP) Formulation

Lipid nanoparticles entrapping mRNA were formulated as previously described.⁶ In brief, lipid components (MC3, cholesterol, DSPC or DSPG, and PEG-lipid) were dissolved in ethanol. For biodistribution studies, the non-exchangeable tracer DiD or DOPE-LR was added to lipid mixtures at a concentration of 0.1 mol% or 0.2 mol% respectively. The mRNA was dissolved in 25 mM sodium acetate or sodium citrate buffer (pH 4). The two solution were rapidly mixed (N/P ratio of 6) using a T-junction mixer (total flow rate of 20 mL/min, flow rate ratio of 3:1 v/v). The resulting LNP formulation was dialyzed overnight against PBS (pH 7.4), sterile filtered, and concentrated using 10K MWCO centrifugal filters (Amicon® Ultra, Merck). Entrapment efficiency and mRNA concentration were analyzed using the Quant-iT Ribogreen RNA assay (Life Technologies, Burlington, ON). Total lipid concentrations were measured using the Cholesterol E Total-Cholesterol assay (Wako Diagnostics, Richmond, VA). mRNA doses within embryonic zebrafish were calculated using an estimated average weight of 1 mg per embryo, independent of developmental stage, and an injection volume of 1 nL.

LNP and liposome biophysical characterization

LNP and liposome sizes and zeta potentials were measured using a Malvern Zetasizer Nano ZS (software version 7.13, Malvern Panalytical). For DLS (operating wavelength = 633 nm), measurements were carried out at room temperature in 20 mM HEPES buffer (pH = 7.3) for liposomes, and in 1x PBS (pH = 7.4) for LNPs, at a total lipid concentration of approx. 100 µM. Zeta potentials were measured at 500 µM total lipid concentration, using a dip-cell electrode (ZEN1002, Malvern) for liposomes and in a folded capillary cell (DTS1070,

Malvern) for LNPs, at room temperature. All reported DLS measurements and zeta potentials are the average of three measurements.

Cryo-electron Microscopy Imaging and Quantification

Vitrification of concentrated (~10 mM) LNPs was performed using a Leica EM GP operating at 21°C and 95% humidity. Sample suspensions were placed on glow discharged 100 µm lacey carbon films supported by 200 mesh copper grids (Electron Microscopy Sciences). Optimal results were achieved using a 60 second pre-blot and a 1 second blot time. After vitrification, sample grids were maintained below -170 °C and imaging was performed on a Tecnai T12 (ThermoFisher) with a biotwin lens and LaB6 filament operating at 120 keV equipped with an Eagle 4K x 4K CCD camera (ThermoFisher). Images were acquired at a nominal underfocus of -2 to -3 µm (49,000× magnification) with an electron dose of ~2000 e⁻·nm⁻². Images were processed and particle size was quantified using the Fiji distribution of ImageJ.⁷ For quantification, particle sizes were determined on particles present in amorphous vitrified water and obtained from a triplicate of assemblies (~150-200 particles per assembly per formulation). Generation of frequency distribution graphs was performed using GraphPad Prism (v 6.0).

Zebrafish Husbandry and Injections

Zebrafish (*Danio rerio*, strain AB/TL) were maintained and handled according to the guidelines from the Zebrafish Model Organism Database (<http://zfin.org>) and in compliance with the directives of the local animal welfare committee of Leiden University. Fertilization was performed by natural spawning at the beginning of the light period, and eggs were raised at 28.5 °C in egg water (60 µg/ mL Instant Ocean sea salts). In addition to wild-type (AB/TL) embryos, previously established *Tg(mpeg1:mCherry)^{gl23}*⁸ and *stab2^{ibl2}stab1^{ibl3}* zebrafish lines were also used in this study. Fluorescently labelled LNPs or liposomes were injected into 54-96 hours post fertilization (hpf) zebrafish embryos using a modified microangiography protocol.⁹ Embryos were anesthetized in 0.01% tricaine and embedded in 0.4% agarose containing tricaine before injection. To improve reproducibility of microangiography experiments, 1 nL volume were calibrated and injected into the common cardinal vein (2-3 dpf) or primary head sinus (4 dpf). A small injection space was created by penetrating the skin with the injection needle and gently pulling the needle back, thereby creating a small pyramidal space in which the liposomes or LNPs were injected. Successfully injected embryos were identified through the backward translocation of venous erythrocytes and the absence of damage to the yolk ball. Selected zebrafish embryos

successfully injected were kept in egg water at 28.5 degrees until later imaging (1.5 or 24 hours post injection, hpi).

Zebrafish confocal imaging acquisition and processing

Zebrafish embryos were randomly picked from a dish of 10-30 successfully injected embryos to be imaged after 1.5 or 24 hpi. Confocal z-stacks were captured on a Leica TCS SPE or SP8 confocal microscope, using a 10x air objective (HCX PL FLUOTAR), a 40x water-immersion objective (HCX APO L) or 63x water-immersion objective (HC PL APO CS). For whole-embryo views, 3 or 4 overlapping z-stacks were captured to cover the complete embryo. Laser intensity, gain and offset settings were identical between stacks and when comparing samples per experiment. Images were processed using the Fiji distribution of ImageJ.⁷ Confocal image stacks (raw data) are available upon reasonable request.

Mouse husbandry, injection protocol and cell isolation

All mouse protocols were approved by the Canadian Animal Care Committee and conducted in accordance with relevant guidelines and regulations. Mice were maintained on a regular 12-hour light/12-hour dark cycle in a specific pathogen-free animal facility at UBC. C57Bl6 male mice aged between 8 to 10 weeks were used throughout. These mice were divided into groups of 2 and either received intravenous (*i.v*) injection of LNP-mRNAs (either DSPC-LNPs or srLNPs) or PBS as a negative control. For biodistribution studies, LNPs entrapping luciferase mRNA were labelled with 0.5 mol% DiD as fluorescent lipid marker. Injections were performed at 42.75 mg/kg total lipid and mice were sacrificed at 2 hpi. For gene expression studies, LNPs encapsulating mRNA coding for the fluorescent reporter gene mCherry were used, injections were performed at 0.25 mg/kg mRNA dose, and mice were sacrificed at 24 hpi. Mice were anesthetized using a high dose of isoflurane followed by CO₂. Trans-cardiac perfusion was performed as follows: once the animals were unresponsive, a 5 cm medial incision was made through the abdominal wall, exposing the liver and heart. While the heart was still beating, a butterfly needle connected to a 30 mL syringe loaded with pre-warmed Hank's Balanced Salt Solution (HBSS, Gibco) was inserted into the left ventricle. Next, the liver was perfused with perfusion medium (HBSS, supplemented with 0.5 mM EDTA, Glucose 10mM and HEPES 10mM) at a rate of 3 mL/min for 10 min. Once liver swelling was observed, a cut was performed on the right atrium and perfusion was switched to digestion medium (DMEM, Gibco supplemented with 10% fetal bovine serum (FBS, Gibco) and 1% penicillin streptomycin (Gibco) and 0.8 mg/mL Collagenase Type IV, Worthington) at 3 mL/min for another 10 min. At the end of the

perfusion of the entire system, as determined by organ blanching, the whole liver and spleen were dissected and transferred to 50 mL Falcon tubes containing 10 mL ice cold (4°C) perfusion media and placed on ice. Next, isolation of hepatic cell types (*i.e.* hepatocytes, Kupffer cells (KCs) and liver sinusoid endothelial cells (LSECs)) was performed following density gradient-based separation. Briefly, the liver was transferred to a Petri dish containing digestion medium, minced under sterile conditions, and incubated for 20 min at 37°C with occasional shaking of the plate. Cell suspensions were then filtered through a 40 µm mesh cell strainer to eliminate any undigested tissue remnants. Primary hepatocytes were separated from other liver residing cells (LRCs) by low-speed centrifugation at 500 rpm with no brake. The supernatant containing mainly LRCs was pelleted using low speed (3000 rpm) centrifugation at 4°C, aliquoted and washed twice with ice cold PBS containing 2% FBS. The pellet containing mainly hepatocytes was collected, washed at low speed and placed on ice. Phenotypic detection using monoclonal antibodies, assessment of LNP delivery and mRNA expression on cells liver cells was performed immediately after isolation to avoid changes in gene regulation, polarization and dedifferentiation.¹⁰ LNP biodistribution across individual RES cell types of the spleen (*i.e.* endothelial cells and macrophages) were also characterized. Here, the spleen was also dissected and placed into a 40 µm mesh cell and mashed through the cell strainer into the petri dish using the plunger end of the syringe. The suspended cells were transferred to a 15 mL Falcon tube and centrifuged at 1000 rpm for 5 minutes. The pellet was resuspended in 1 mL ACK lysis buffer (Invitrogen) to lyse the red blood cells, aliquoted in FACS buffer and stained with antibodies as described below to identify splenic endothelial cells and macrophages.

FACS analysis

Cell aliquots were resuspended in 300 µL FACS staining buffer (FBS 2%, sodium azide 0.1% and ethylenediaminetetraacetic acid (EDTA 1mM)) followed by staining with fluorescence tagged antibodies. Prior to staining, cells were first labeled with anti-mouse CD16/CD32 (mouse Fc blocker, Clone 2.4G2) (AntibodyLab, Vancouver, Canada) to reduce background. Hepatocytes were identified following staining with primary mouse antibody detecting ASGR1 (8D7, Novus Biologicals) followed by goat polyclonal secondary antibody to mouse IgG2a labeled to PE-Cy7 (BioLegend). Kupffer cells were identified with CD11b – FITC or PE (Invitrogen) and F4/80high labeled to APC. LSECs were identified with CD146-VioBlue (Miltenyi Biotec) and CD31-PE-Cy7 (Abcam). Spleen macrophages and endothelial cells were detected using appropriate antibodies and identified as CD11bhigh and CD31+ve cells following antibody labeling as described. The data were acquired using a LSRII flow cytometer and the FACSDiva software and analyzed by FlowJo following acquisition of at

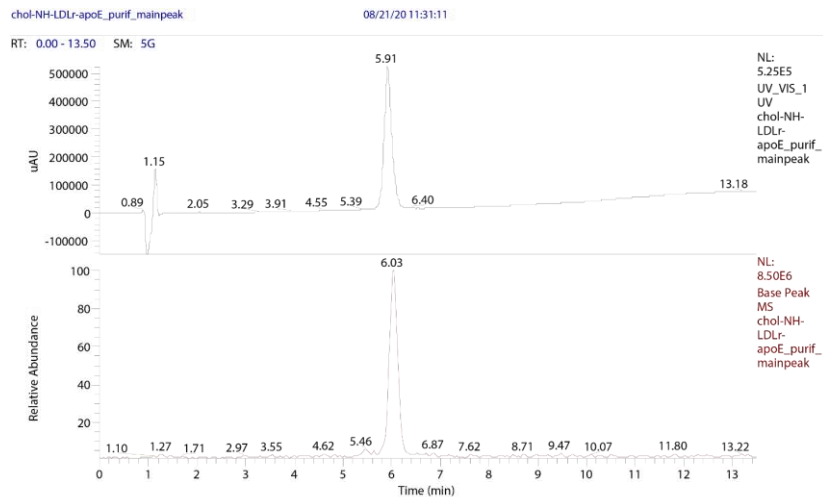
least 10,000 events after gating on viable cell populations. LNP-mRNA delivery or transfection efficacy were assessed based on the relative mean fluorescence intensity of DiD or mCherry positive cells, respectively, measured on histograms obtained from gated cell populations.

Statistics and Reproducibility

Frequency distributions for LNP size, derived from cryo-EM micrographs, and mean \pm standard deviation was obtained using Prism (v8.1.1, GraphPad Software, Inc.). All zebrafish experiments were repeated at least twice, with the exception of Supporting Figure 3 (performed once). All replicate experiments were performed using freshly prepared LNPs or liposomes. All replicate experiments were successful and confirmed the presented data. For all experiments performed in embryonic zebrafish, at least four embryos were randomly selected (from a pool of 10-30 successfully injected embryos) and analyzed (low resolution microscopy). All selected embryos showed consistent results and confirmed the presented data. From these embryos, at least one embryo was selected for high resolution, confocal microscopy. No statistical analysis was performed on acquired zebrafish data. Statistical analysis for mouse studies was performed by a Student's t-test with a correction for multiple comparisons using the Holm-Sidak method using Prism (v8.1.1, GraphPad Software, Inc.). All data represent at $n \geq 2$ independent measurements. Comparisons were considered significant at $P < 0.01$.

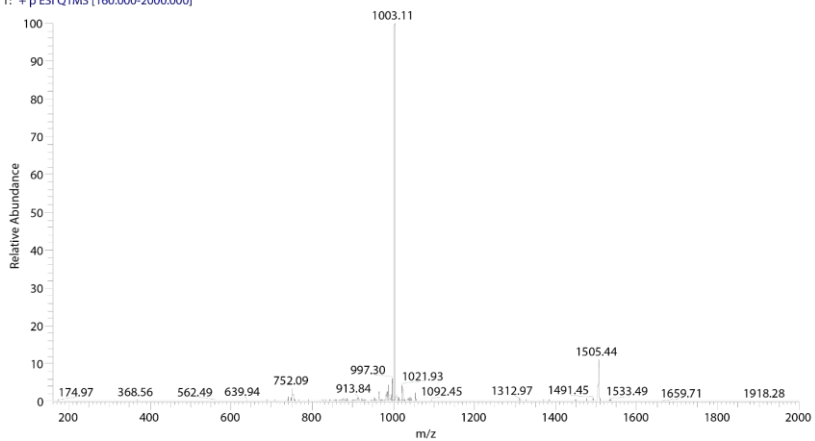
3. LC-MS spectra

LC-MS spectrum of Chol-NH-ApoE_peptide



chol-NH-LDLr-apoE_purif_mainpeak
Type: Unknown ID: RA1 Row: 1
Sample Name:
Study:
Client:
Laboratory:
Company:

chol-NH-LDLr-apoE_purif_mainpeak #208-213 RT: 5.97-6.12 AV: 6 SM: 7G NL: 5.94E6
T: + p ESI Q1MS [160.000-2000.000]



4. References

1. Arias-Alpizar, G. *et al.* Stabilin-1 is required for the endothelial clearance of small anionic nanoparticles. *Nanomedicine Nanotechnology, Biol. Med.* **34**, 102395 (2021).
2. Miller, C. M. *et al.* Stabilin-1 and Stabilin-2 are specific receptors for the cellular internalization of phosphorothioate-modified antisense oligonucleotides (ASOs) in the liver. *Nucleic Acids Res.* **44**, 2782–2794 (2016).
3. Jayaraman, M. *et al.* Maximizing the potency of siRNA lipid nanoparticles for hepatic gene silencing in vivo. *Angew. Chemie - Int. Ed.* **51**, 8529–8533 (2012).
4. Sun, Q., Cai, S. & Peterson, B. R. Practical Synthesis of 3 β -Amino-5-cholestene and Related 3 β -Halides Involving i-Steroid and Retro-i-Steroid Rearrangements. *Org. Lett.* **11**, 567–570 (2009).
5. Daudey, G. A., Zope, H. R., Voskuhl, J., Kros, A. & Boyle, A. L. Membrane-Fusogen Distance Is Critical for Efficient Coiled-Coil-Peptide-Mediated Liposome Fusion. *Langmuir* **33**, 12443–12452 (2017).
6. Kulkarni, J. A. *et al.* Fusion-dependent formation of lipid nanoparticles containing macromolecular payloads. *Nanoscale* **11**, 9023–9031 (2019).
7. Schindelin, J. *et al.* Fiji: an open-source platform for biological-image analysis. *Nat. Methods* **9**, 676–682 (2012).
8. Ellett, F., Pase, L., Hayman, J. W., Andrianopoulos, A. & Lieschke, G. J. mpeg1 promoter transgenes direct macrophage-lineage expression in zebrafish. *Blood* **117**, e49–56 (2011).
9. Weinstein, B. M., Stemple, D. L., Driever, W. & Fishman, M. C. Gridlock, a localized heritable vascular patterning defect in the zebrafish. *Nat. Med.* **1**, 1143–1147 (1995).
10. Severgnini, M. *et al.* A rapid two-step method for isolation of functional primary mouse hepatocytes: cell characterization and asialoglycoprotein receptor based assay development. *Cytotechnology* **64**, 187–195 (2012).

Appendix 3

Supplementary Information to Chapter 4

1. Supplementary Figures and Tables

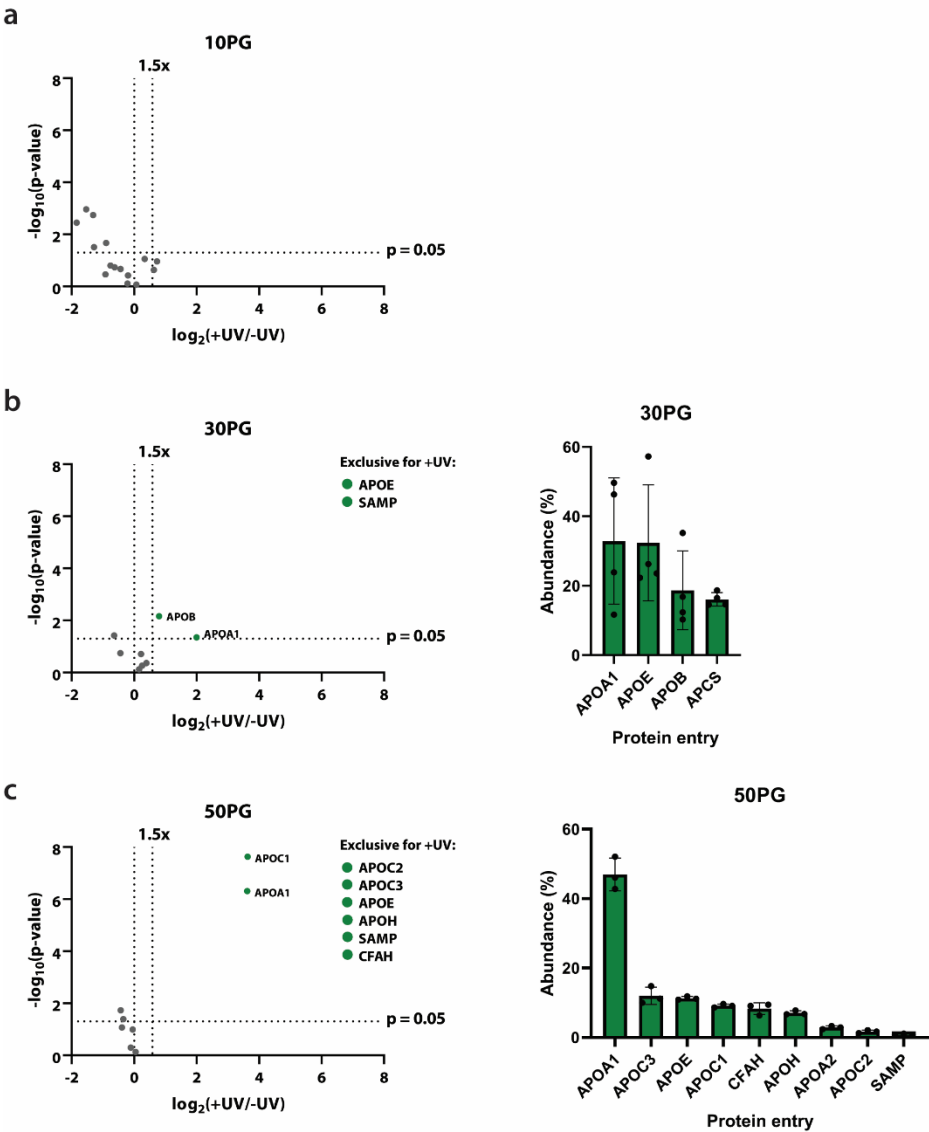


Figure S1. Volcano plots showing the enrichment of proteins in “+UV” over “-UV” samples as $\log_2(+\text{UV}/-\text{UV})$ against the statistical significance between the two groups ($n \geq 3$) as $-\log_{10}(\text{p-value})$. Selection threshold is set at 1.5-fold enrichment and a $\text{p-value} < 0.05$. Abundance plots only show proteins that meet selection criteria. (a) 10PG (b) 30PG (c) 50PG.

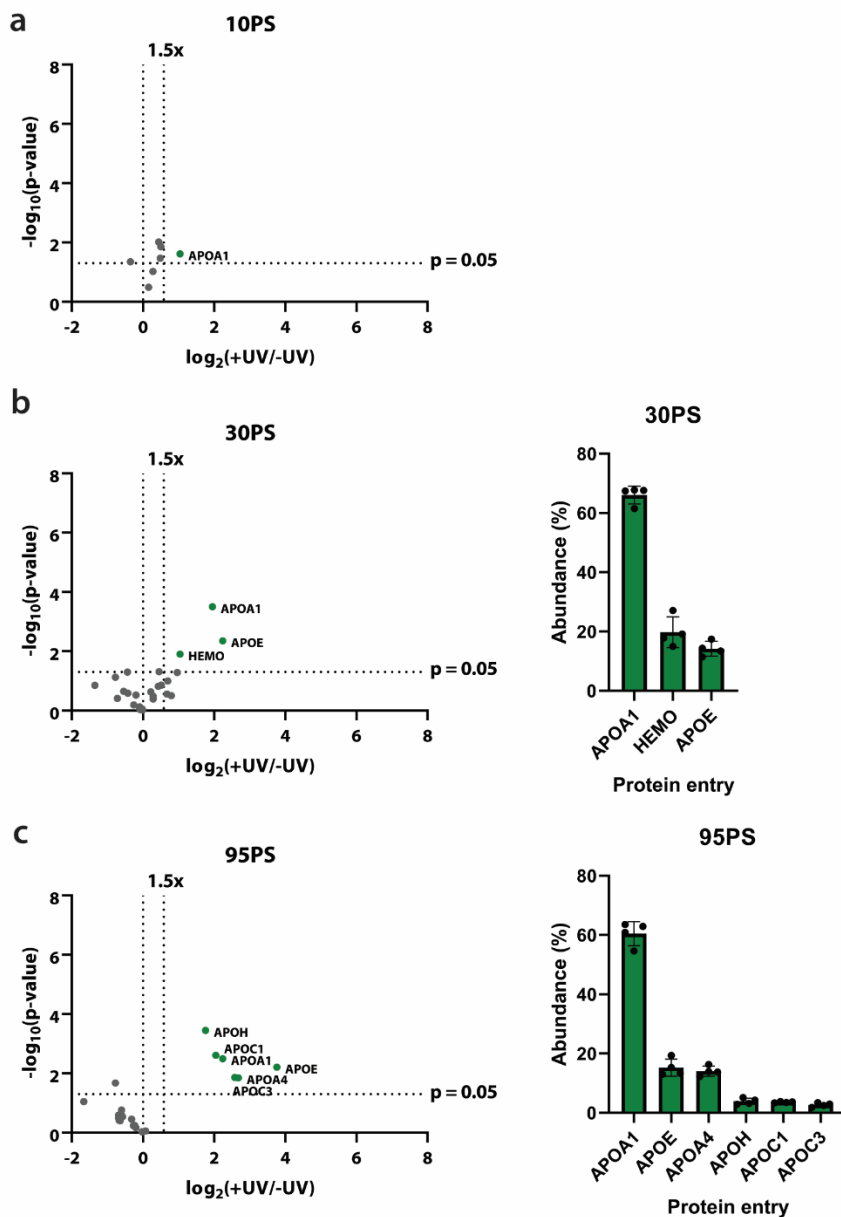


Figure S2. Volcano plots showing the enrichment of proteins in "+UV" over "-UV" samples as $\log_2(+UV/-UV)$ against the statistical significance between the two groups ($n \geq 3$) as $-\log_{10}(p\text{-value})$. Selection threshold is set at 1.5fold enrichment and a $p\text{-value} < 0.05$. Abundance plots only show proteins that meet selection criteria. (a) 10PS (b) 30PS (c) 95PS.

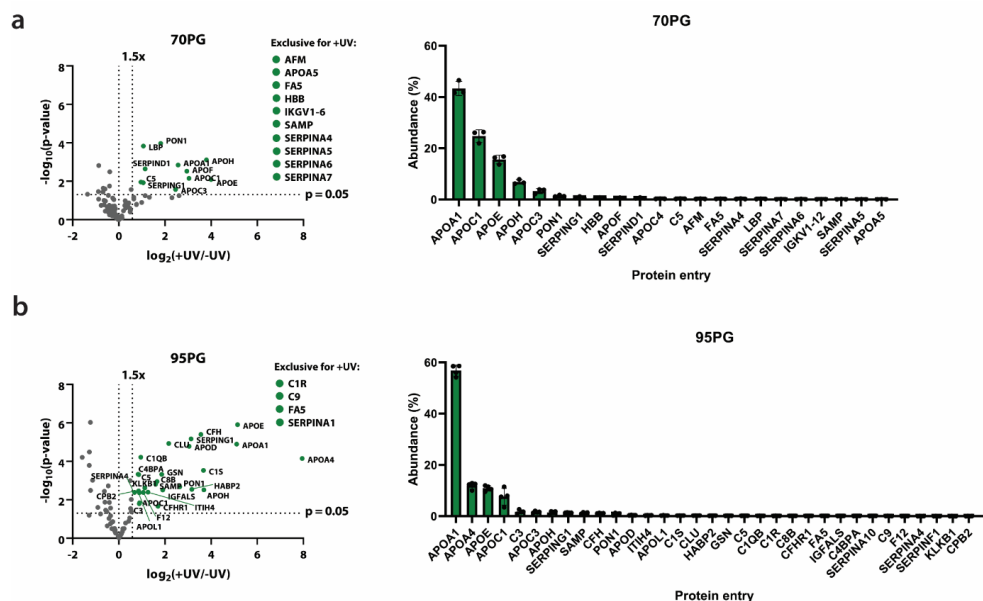
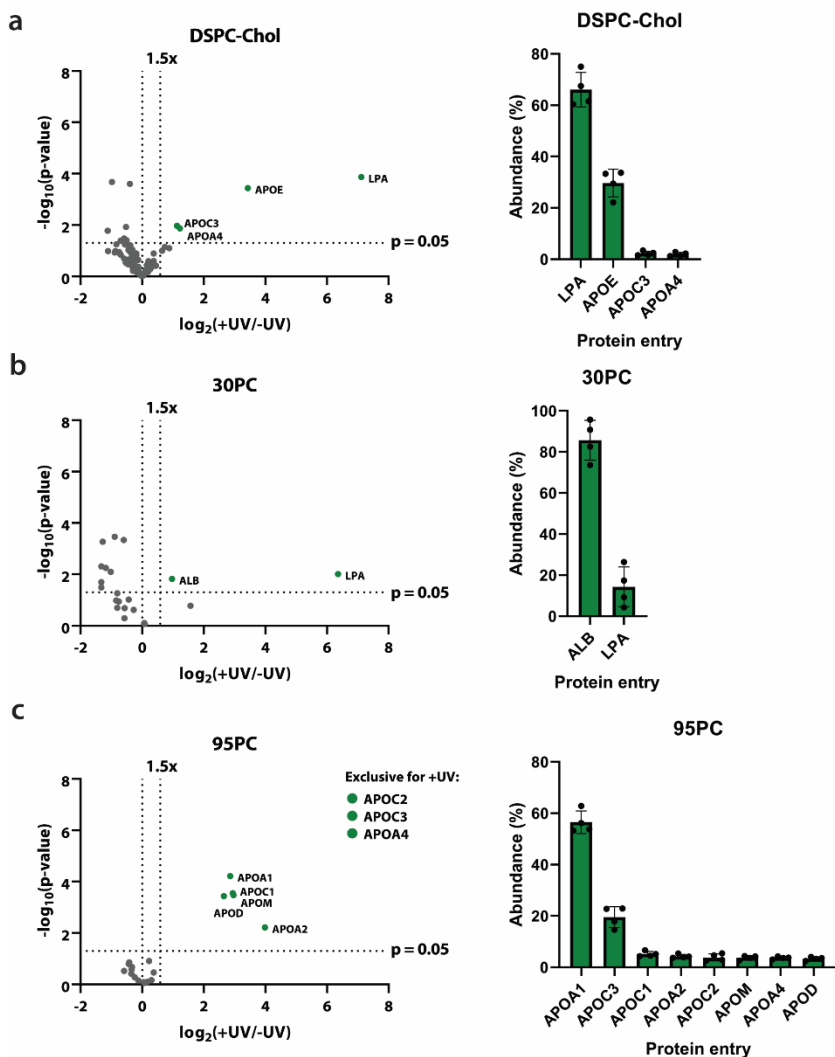
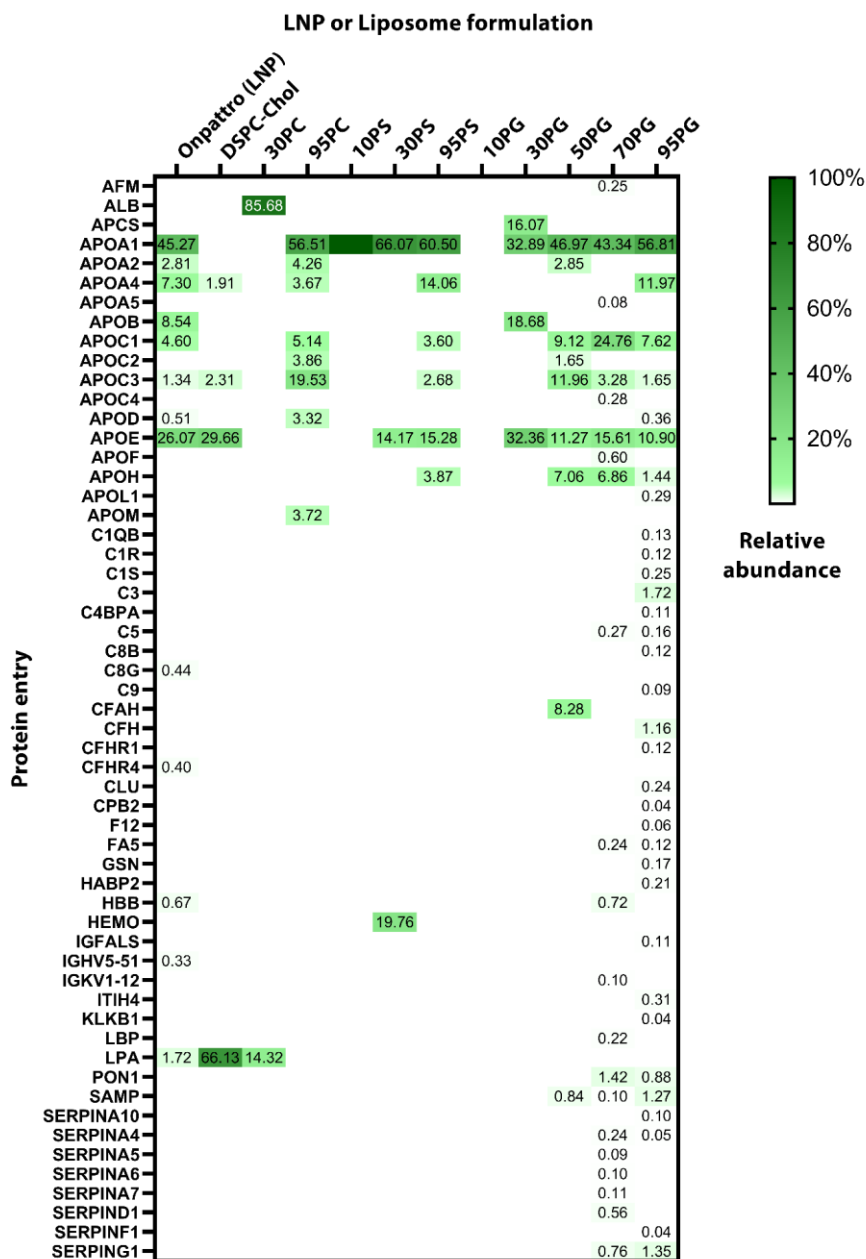
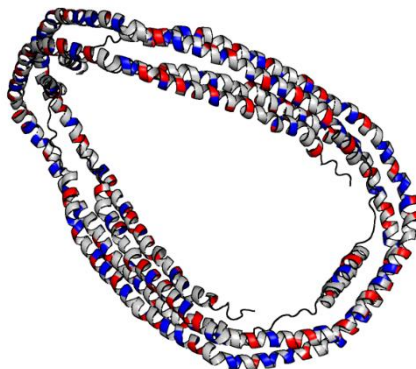


Figure S3. Volcano plots showing the enrichment of proteins in “+UV” over “-UV” samples as $\log_2(+UV/-UV)$ against the statistical significance between the two groups ($n \geq 3$) as $-\log_{10}(p\text{-value})$. Selection threshold is set at 1.5-fold enrichment and a $p\text{-value} < 0.05$. Abundance plots only show proteins that meet selection criteria. (a) 70PG (b) 95PG.





Supplementary Figure 5. Complete heatmap containing the proteins identified across all protein coronas and their average relative abundance in % (denoted by values).



Supplementary Figure 6. The structure of APOA1 (PDB entry 1AV1)¹ in which cationic residues (Lysine, Arginine and Histidine) are colored in blue and anionic residues (Glutamic acid and Aspartic acid) in red.

Formulation (+IKS02)	Avg. Size (nm)	PDI	ζ-potential (mV)
Onpattro	78	0.098	-3.9
DSPC-Chol	115	0.109	-2.5
30PC	105	0.074	-3.4
95PC	110	0.099	-1.3
10PS	99	0.085	-12.5
30PS	104	0.079	-25.4
95PS	101	0.113	-48.6
10PG	111	0.109	-13.9
30PG	96	0.100	-21.4
50PG	105	0.088	-33.8
70PG	109	0.079	-45.0
95PG	101	0.071	-50.3
Formulation (-IKS02)	Avg. Size (nm)	PDI	ζ-potential (mV)
Onpattro	75	0.111	-2.5
DSPC-Chol	109	0.106	-1.2
30PC	106	0.108	-4.7
30PG	108	0.092	-23.5

Supplementary Table 1. Size and surface charge measurements of all formulations used in this study. PDI = Polydispersity Index.

siRNA name	Sequence
Patisiran®	Sense: 5' GU _m AAC _m C _m AAGAGU _m AU _m U _m C _m C _m AU _m T _d T _d 3' Antisense: 3' T _d T _d CAU _m UGGU _m U _m CUCAU _m AAGGU _m A 5'

Supplementary Table 2. siRNA sequence of Patisiran® used in this study. U_m and C_m are ribonucleotides with a 2'-OMe functionalization on the ribose ring. T_d, G_d and A_d are DNA ribonucleotides.

2. Materials and methods

General

All solvents and reagents were obtained from general commercial sources (Sigma Aldrich, Acros Organics, Alfa Aesar, Fluka, Merck) and used as received without further purification, unless stated otherwise. Dynamic light scattering and zeta potential measurements were performed on a Malvern Zetasizer Nano ZS. For light irradiation, a CaproBox™ (Caprotec Bioanalytics GmbH) was used with a wavelength of 350 nm and applying a 300 nm light filter. Cholesterol (C8667), Heparin (H3149), Cy5-alkyne (777358) and Biotin-PEG4-alkyne (764213) were purchased from Merck (Zwijndrecht, The Netherlands). IKSo₂ was synthesized as described before.² DLin-MC3-DMA was synthesized as described before.³ 1,2-dioleoyl-*sn*-glycero-3-phosphocholine (DOPC), 1,2-dioleoyl-*sn*-glycero-3-phospho-L-serine (DOPS, sodium salt), 1-palmitoyl-2-oleoyl-glycero-3-phosphocholine (POPC), 1,2-distearoyl-*sn*-glycero-3-phosphocholine (DSPC), 1,2-dioleoyl-*sn*-glycero-3-phospho-(1'-*rac*-glycerol) (DOPG, sodium salt) and 1,2-dimyristoyl-*rac*-glycero-3-methoxypolyethylene glycol-2000 (DMG-PEG2000) were purchased from Avanti Polar Lipids through Merck. Patisiran siRNA was purchased from Integrated DNA Technologies (Leuven, Belgium) through custom synthesis, exact sequence can be found in Supplementary Table 2. Human Plasma (citrated) was purchased from Merck (P9523). Albumin from human serum (SRP6182), Human transferrin (T3309) and recombinant human apolipoprotein E3 (SRP4696) were purchased from Sigma-Aldrich. Human prothrombin (RP-43087) was purchased from Thermo-Fisher Scientific. Recombinant human Apolipoprotein A1 (ab50239) was purchased from Abcam B.V. (Amsterdam, The Netherlands). Evaporation of solvents with a vacuum centrifuge was performed using an Eppendorf speedvac (Eppendorf Concentrator Plus 5301). Sequencing grade modified trypsin was purchased from Promega (product code = V5111). Acetonitrile (LC-MS grade) and methanol (LC-MS grade) were purchased from Biosolve. Formic acid (LC-MS grade) was purchased from

Actu-All Chemicals. BioSpin columns were purchased from Bo-Rad. The Empore C18 47-mm extraction disks (model 2215) were purchased from 3M™ Purification. Enolase digest standard was purchased from Waters MassPREP™.

Liposome assembly

Liposome assembly was done as described before.² Briefly, lipids were combined from stocks in chloroform, dried under a nitrogen flow and trace solvents were removed *in vacuo* for at least 1 hour. The lipid films were hydrated with phosphate buffered saline (PBS, pH = 7.4) and extruded through double stacked 100 nm polycarbonate membrane filters (Nucleopore Track-Etch, Whatman) at 60 °C (Mini-extruder, Avanti Polar Lipids, Alabaster, US).

Lipid Nanoparticle assembly

Lipid Nanoparticles (LNPs) were assembled as described previously.⁴ Briefly, lipid films were generated similarly as for liposome assembly and dissolved in absolute ethanol. A solution of siRNA in 50 mM citrate buffer (pH = 4, RNase free) was prepared to resemble a nitrogen:phosphate ratio of 3 of siRNA to DLin-MC3-DMA. The solutions were mixed in a T-junction mixer at a 3:1 flow ratio of siRNA:lipids and afterwards directly loaded in 20k MWCO dialysis cassettes (Slide-A-Lyzer™, Thermo Scientific) and dialyzed against PBS (1x). LNPs were concentrated to the appropriate lipid concentration using 100k MWCO centrifugal filters (Amicon® Ultra, Merck).

Photoaffinity based chemoproteomic workflow

The photoaffinity based chemoproteomic workflow was performed as described before with minor modifications,² which are described in the following paragraphs.

Incubation, photo crosslinking and click chemistry

Liposomes or LNPs containing the photoaffinity probe IKS02 (50 µL, 5 mM for liposomes, 10 mM for LNPs) were added to pre-warmed human plasma (37 °C, 50 µL) and incubated in the dark at 37 °C for 1 hour. Half of the replicates were irradiated with 350 nm light for 15 minutes, while cooling. The other replicates were kept at room temperature in the dark for 15 minutes. Afterwards, the liposomes or LNPs were solubilized by addition of 20 µL 0.1% Triton X-100 in ultrapure water and incubated for 10 minutes. The proteins were precipitated according to Wessel and Flügge,⁵ by addition of water (up to 400 µL), methanol (650 µL), chloroform (200 µL) and ultrapure water (150 µL) sequentially with

vigorous vortexing in between. The mixture was centrifuged (3000 g, 15 min, 4 °C) and the liquid layers were removed, followed by resuspension of the pellet in methanol (600 µL) and centrifugation (14,000 g, 5 min, 4 °C). The supernatant was discarded and the pellet was dissolved in HEPES buffer with 0.5% SDS (200 µL, 100 mM, pH 8.0). For each protein sample, click reagent mixture (50 µL) was added from a 10x concentrated stock to obtain a final concentration of 100 µM CuSO₄, 1000 µM sodium ascorbate, 500 µM THPTA, 5000 µM aminoguanidine and 25 µM Biotin-PEG₄-alkyne, followed by incubation at room temperature for 1 hour at room temperature. After the reaction, the protein precipitation protocol described above was repeated. The pellet dissolved in freshly prepared denaturing buffer (250 µL, 6 M urea, 25 mM NH₄HCO₃) and used for enrichment. Alternatively, samples were snap-frozen with liquid nitrogen and stored for no longer than 2 weeks at -80 °C.

Reduction-alkylation, enrichment and on-bead digestion

To lipid-protein samples conjugated to biotin was added 5 µL 1 M DTT (20 mM final concentration). Samples were vortexed, centrifuged and incubated at 56 °C while shaking (600 rpm) for 30 minutes. The samples were allowed to cool down to room temperature, after which 40 µL 0.5 M iodoacetamide (80 mM final concentration) was added and the samples incubated at room temperature in the dark for 30 minutes. Afterwards, 20 µL 1 M DTT (100 mM final concentration) was added and the samples were vortexed and incubated at 56 °C for 5 minutes. Reduced and alkylated proteins were used directly for avidin bead enrichment. Avidin agarose beads (50% slurry, 100 µL per sample, Thermo Fisher Scientific) were washed three times with PBS (10 mL PBS per 400 µL slurry), centrifuging at 2500 g for 3 minutes. The beads were resuspended in PBS (1 mL PBS per 100 µL slurry) and divided over 15 mL tubes in 1 mL fractions. An additional 2 mL PBS and 5 µL of SDS (10% in water) was added to each tube, after which the denatured and alkylated protein samples were added and the samples were shaken gently in an overhead shaker at RT for at least 3 hours. Beads were pelleted (2,500 g, 5 min) and the supernatants were discarded. The beads were washed twice with SDS in PBS (0.5% w/v, 10 mL), three times with PBS (10 mL) and twice with ultrapure water (10 mL). In between each washing step, the samples were vortexed, centrifuged (2,500 g, 5 min) and the supernatants were discarded. The washed beads were resuspended in 250 µL on-bead digestion buffer (100 mM TRIS pH 8.0, 100 mM NaCl, 1 mM CaCl₂ and 2% v/v acetonitrile (LC-MS grade)) and transferred to 1.5 mL low-binding Eppendorf tubes. Next, 10 µL 0.1 µg/µL trypsin was added and the samples were incubated at 37 °C while shaking (950 rpm) overnight. To the samples was added 12.5 µL formic acid and loaded onto Bio-Spin columns (Bio-Rad), the flow-

through was collected by centrifugation (2,500 g, 2 min) in low-binding Eppendorf tubes. The samples were desalted using the StageTips procedure described below.

Protein validation and competition assay

Incubation, photo crosslinking and click chemistry

Proteins from concentrated stock solutions were mixed and pre-warmed (37 °C) to generate a composition of Albumin (ALBU, 50 µg), Transferrin (TRFE, 16 µg), apolipoprotein A1 (APOA1, 3 µg), apolipoprotein E3 (APOE, 3 µg) and prothrombin (THRB, 3 µg) in a total volume of 25 µL (1x PBS) for each replicate. To each replicate was added liposomes or LNPs containing IKSO₂ (25 µL, 1 mM for liposomes, 2 mM for LNPs). For competition experiments, liposomes without IKSO₂ or heparin was added according to the competitive ratio. The mixture was incubated at 37 °C for 1 hour followed by UV irradiation (15 min, 350 nm) lysis with 1% Triton X-100 (5 µL). Proteins were precipitated by addition of water up to a volume of 400 µL, methanol (400 µL) and chloroform (100 µL), followed by vigorous vortexing and centrifugation (3000 g, 10 min, 4 °C). The liquid layers were removed, the pellet resuspended with methanol (200 µL) and centrifuged (14,000 g, 5 min, 4 °C). The supernatant was discarded and the pellet was dissolved in HEPES buffer (90 µL, 100 mM, pH 8.0). For each protein sample, click reagent mixture (10 µL) was added from a 10x concentrated stock to give a final concentration of 100 µM CuSO₄, 1000 µM sodium ascorbate, 500 µM THPTA, 5000 µM aminoguanidine and 25 µM Cy5-alkyne, followed by incubation at room temperature for 1 hour. Protein precipitation was repeated as prior to the click reaction and the pellet was dissolved in 0.1% SDS in PBS (100 µL).

SDS-PAGE, In-gel fluorescence and Coomassie blue imaging

Protein concentration was determined by BCA assay prior to loading samples for in-gel fluorescence. To a volume corresponding to 7.5 µg of protein was added Laemmli buffer (4x stock) and the proteins were heated at 70 °C for 10 minutes followed by resolving on 4–15% Mini-PROTEAN® TGX™ Precast Protein Gel (Bio-Rad) at 180 V. The subset of fluorescent proteins was imaged on a Typhoon FLA 9500 (GE Healthcare), followed by staining of all the proteins with Coomassie Brilliant Blue R-250 staining solution (Bio-Rad) and imaging on a ChemiDoc MP system (Bio-Rad). Images were processed using the Fiji package of ImageJ.⁶

StageTips desalting

The protein digest desalting procedure was conducted as previously described.⁷ Briefly, C₁₈ extraction disks (47 mm) were placed in 200 µL pipette tips. These StageTips were conditioned, loaded, washed and eluted, following the scheme below. The eluted fractions were collected into low-binding Eppendorf tubes, dried using a vacuum centrifuge and stored at -20 °C or immediately prepared for UPLC-MS/MS measurements.

STAGE	BUFFER
Conditioning 1	50 µL MeOH (LC-MS grade)
Conditioning 2	50 µL StageTip solution B: 0.5% (v/v) formic acid, 80% (v/v) acetonitrile and 19.5% ultrapure water
Conditioning 3	50 µL StageTip solution A: 0.5% (v/v) formic acid in ultrapure water
Loading	Sample
Washing	100 µL StageTip solution A
Elution	100 µL StageTip solution B

NanoUPLC-MS/MS analysis

Peptide samples were dissolved in 50 µL LC-MS sample solution (ultrapure water:acetonitrile:formic acid 97:3:0.1) containing 10 fmol/µL enolase digest as an internal standard for label-free quantification. LC-MS/MS measurements were performed on a Synapt G2Si mass spectrometer (Waters) operating with Masslynx as described before without any modification,^{2,8} or on an UltiMate 3000 RSLCnano system with a HQExactive mass spectrometer. The latter was set in a trap-elute configuration with a nanoEase M/Z Symmetry C18 100Å, 5µm, 180µm x 20 mm (Waters) trap column for peptide loading/retention and nanoEase M/Z HSS C18 T3 100Å, 1.8µm, 75 µm x 250 mm (Waters) analytical column for peptide separation. The column was kept at 40°C in a column oven. Flow gradient used for analysis was a steep (45 min) gradient of mobile phase A (0.1% formic acid (FA) in ULC-MS grade water (Biosolve)) and mobile phase B (0.1% FA in ULC-MS grade acetonitrile (ACN, Biosolve)) controlled by a flow sensor at 0.3µl/min with average pressure of 400-500 bar (5500-7000 psi). Samples were injected (5 µL) on the trap column at a flow rate of 15 µl/min for 9 min with 99%A, 1%B eluent. The gradient was programmed with linear increment to 1% B from t₀ to t₂ min, 10%B to t₅ min, 30%B at t₂₅, 90%B at t₂₆ to t₃₃ and 1%B at t₃₄ to t₄₅ min. The eluent was introduced by electro-spray

ionization (ESI) via the nanoESI source (Thermo) using stainless steel Nano-bore emitters (40 mm, OD 1/32", ES542, Thermo Scientific). The QExactive HF was operated in positive mode with data dependent acquisition without the use of lock mass, default charge of 2+ and external calibration with LTQ Velos ESI positive ion calibration solution (88323, Pierce, Thermo) every 3-5 days to less than 2 ppm. The tune file for the survey scan was set to scan range of 350 – 1400 m/z, 60,000 resolution, 1 microscan, automatic gain control (AGC) of 1e6, max injection time of 50 ms, no sheath, aux or sweep gas, spray voltage ranging from 1.7 to 3.0 kV, capillary temp of 250°C and a S-lens value of 80. The sensitive MS method settings were: the survey scan was taken at 120,000 resolution, AGC target of 3e6, maximum IT time of 100 ms, and scan range of 350 to 1400 m/z. For the 10 data dependent MS/MS events the loop count was set to 10 and the general settings were resolution to 15,000, AGC target 1e5, max IT time 50 ms, isolation window of 1.6 m/z, fixed first mass of 120 m/z and normalized collision energy (NCE) of 28 eV. For individual peaks the data dependent settings were 1.00e3 for the minimum AGC target yielding an intensity threshold of 2.0e4 that needs to be reached prior of triggering an MS/MS event. No apex trigger was used, unassigned, +1 and charges >+8 were excluded with peptide match mode preferred, isotope exclusion on and dynamic exclusion of 10 sec. In between experiment samples routine wash and control runs were done by injecting 5 µl 97.3.0.1 solution, 5 µl of 10 fmol/µl BSA or enolase digest and 1 µl of 10 fmol/µl angiotensin III (Fluka, Thermo)/oxytocin (Merck) to check the performance of the platform on each component (nano-LC, the mass spectrometer (mass calibration/quality of ion selection and fragmentation) and the search engine).

Proteomic analysis

The resulting proteomics data from the Synapt and HQExactive Mass spectrometers were processed using ISOQuant or MaxQuant software respectively.^{9,10} In both cases, label-free quantification (LFQ) was applied using a TOP3 approach. Limitations for peptides was set a minimum length of 6 amino acids and positive identification of at least 2 different peptides. Protein identification was done using the reviewed proteins from the PLGS or Uniprot databases (Human, reviewed, downloaded on 1st of June, 2020) to which Trypsin, Enolase, Avidin, Streptavidin and Bovine Serum Albumin were added manually. Processing of proteins into volcano plots and the selection of “hits” were subject to certain criteria and statistical processing. First, proteins had to be present in all replicates of “+UV” samples. Second, self-introduced proteins were excluded for volcano plots and further analysis. Third, sufficient enrichment over background was set at 1.5-fold. Fourth, the maximum p-value for a hit was set at $p = 0.05$. P-values were determined by multiple t-tests comparing the replicates of each group with a Benjamini-Hochberg approach using the

GraphPad Prism software (v8.0). If proteins did not have any background signal or not enough replicates in the background in order to perform a t-test, the proteins were labeled as “exclusive” and were directly selected as hits. Abundance plots were generated by plotting the average LFQ intensity values, subtracted by the background, for each protein and calculating their relative abundance.

Cryogenic transmission electron microscopy

CryoTEM was performed as described previously.⁴ Briefly, LNPs (~10–15 mM) were vitrified using a Leica EM GP operating at 22°C or 37°C and 95% relative humidity. Sample suspensions were placed on glow discharged 150 µm lacey carbon films supported by 200 mesh copper grids (Electron Microscopy Sciences). Sample grids were maintained below –170 °C and imaging was performed on a Tecnai T12 (ThermoFisher) with a biotwin lens and LaB6 filament operating at 120 keV equipped with an Eagle 4K x 4K CCD camera (ThermoFisher). Images were acquired at a nominal underfocus of –2 to –3 µm (49,000× magnification) with an electron dose of ~2000 e[–]·nm^{–2}. Image processing was performed using the Fiji distribution of ImageJ.⁶

3. References

1. Borhani, D. W., Rogers, D. P., Engler, J. A. & Brouillette, C. G. Crystal structure of truncated human apolipoprotein A-I suggests a lipid-bound conformation. *Proc. Natl. Acad. Sci.* **94**, 12291–12296 (1997).
2. Pattipeiluhu, R. *et al.* Unbiased Identification of the Liposome Protein Corona using Photoaffinity-based Chemoproteomics. *ACS Cent. Sci.* **6**, 535–545 (2020).
3. Jayaraman, M. *et al.* Maximizing the potency of siRNA lipid nanoparticles for hepatic gene silencing in vivo. *Angew. Chemie - Int. Ed.* **51**, 8529–8533 (2012).
4. Pattipeiluhu, R. *et al.* Paracrystalline Inverted Lipid Phases Encapsulating siRNA Enhance Lipid Nanoparticle Mediated Transfection. *Chapter 5, This Thesis* (2021).
5. Wessel, D. & Flügge, U. I. A method for the quantitative recovery of protein in dilute solution in the presence of detergents and lipids. *Anal. Biochem.* **138**, 141–143 (1984).
6. Schindelin, J. *et al.* Fiji: an open-source platform for biological-image analysis. *Nat. Methods* **9**, 676–682 (2012).
7. Rappsilber, J., Mann, M. & Ishihama, Y. Protocol for micro-purification, enrichment, pre-fractionation and storage of peptides for proteomics using StageTips. *Nat. Protoc.* **2**, 1896–1906 (2007).
8. van Rooden, E. J. *et al.* Mapping in vivo target interaction profiles of covalent inhibitors using chemical proteomics with label-free quantification. *Nat. Protoc.* **13**, 752–767 (2018).
9. Distler, U. *et al.* Drift time-specific collision energies enable deep-coverage data-independent acquisition proteomics. *Nat. Methods* **11**, 167–170 (2014).
10. Tyanova, S., Temu, T. & Cox, J. The MaxQuant computational platform for mass spectrometry-based shotgun proteomics. *Nat. Protoc.* **11**, 2301–2319 (2016).

Appendix 4

Supplementary Information to Chapter 5

1. Supplementary Figures and Tables

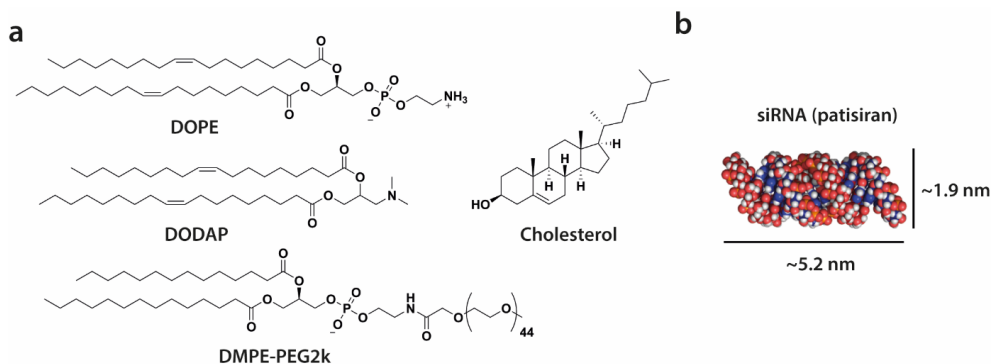


Figure S1. LNP components used in this study. (a) Chemical structures of lipid components used in LNP assembly. (b) RNA A-form structure of Patisiran®, model was created using UCSF Chimera. Width and length were determined in PyMol.

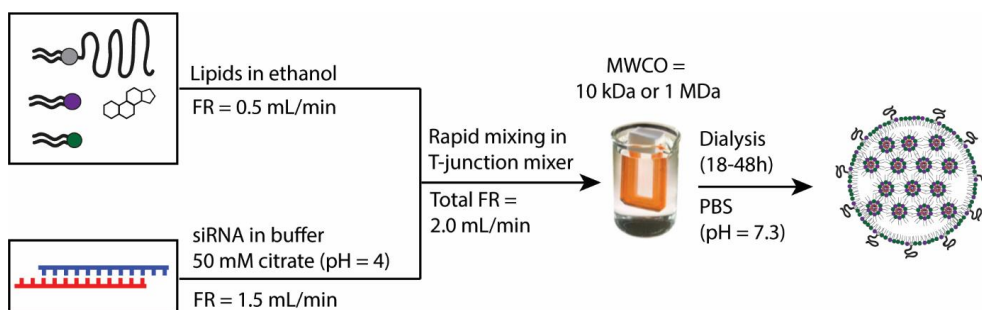


Figure S2. Schematic of LNP assembly. Lipids in ethanol were mixed through a T-junction mixture with siRNA in 50 mM citrate buffer (pH = 4.0) at respective flow rates (FRs) of 0.5 mL/min and 1.5 mL/min. The acquired suspension was dialyzed against PBS to obtain the fully assembled LNPs.

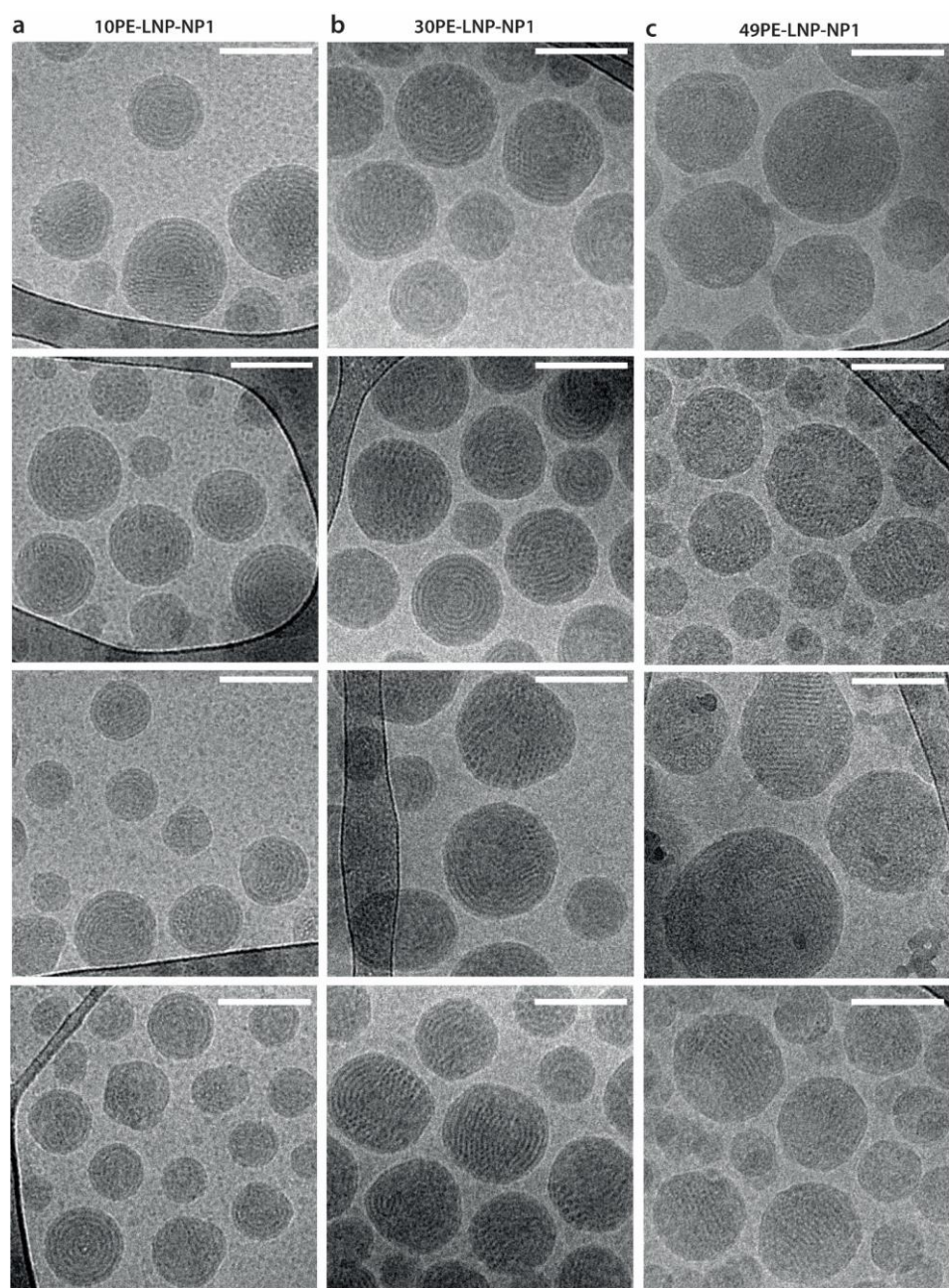


Figure S3. Additional cryoTEM images of 10PE-LNP-NP1, 30-PE-LNP-NP1 and 49PE-LNP-NP1. (a-c) Imaging was performed on a 120 kV Tecnai T12 as described in the Materials and Methods section. All scale bars are 100 nm.

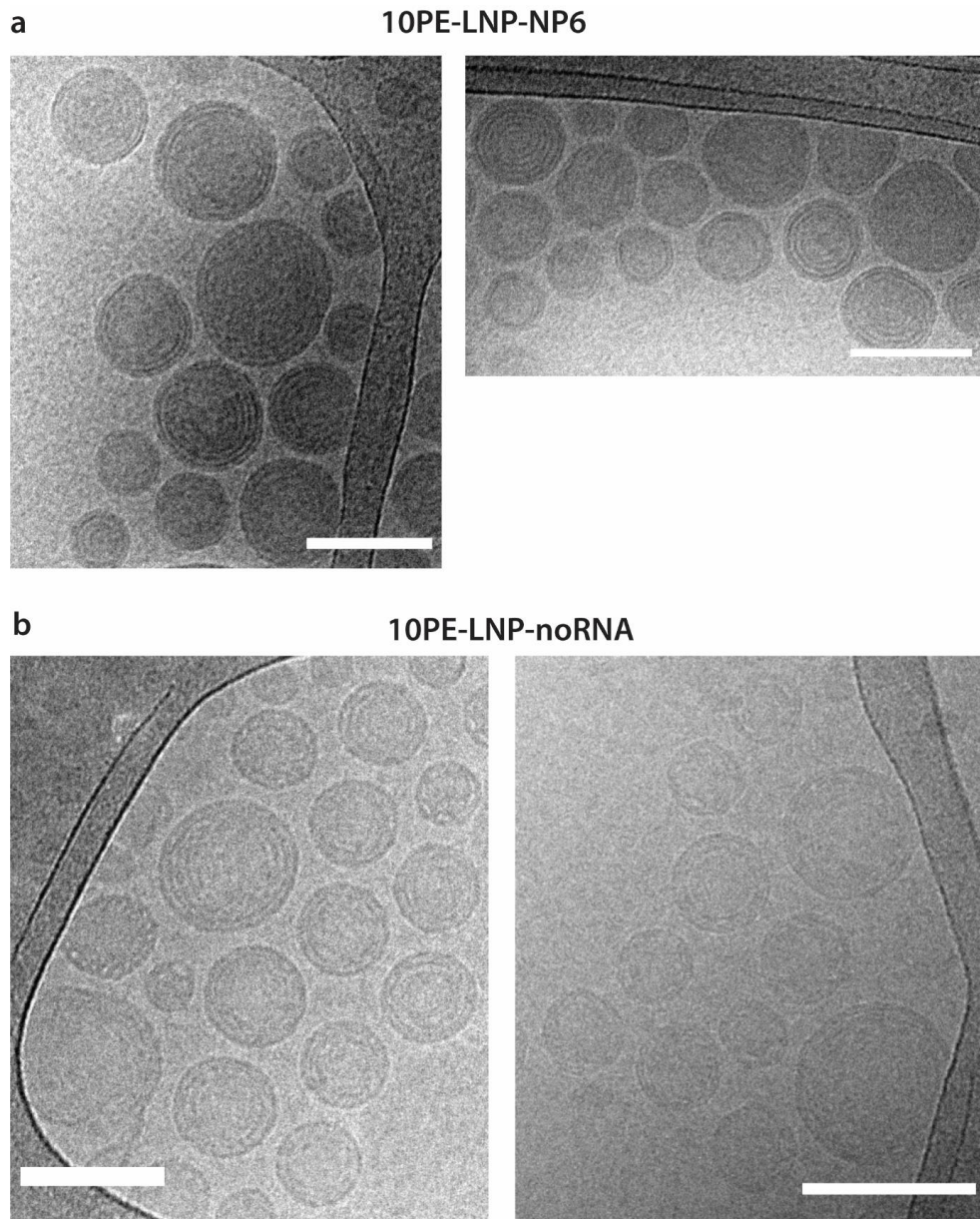


Figure S4. CryoTEM images of 10PE-LNP-NP6 and 10PE-LNP-noRNA. (a-b) Imaging was performed on a 120 kV Tecnai T12 as described in the Materials and Methods section. All scale bars are 100 nm.

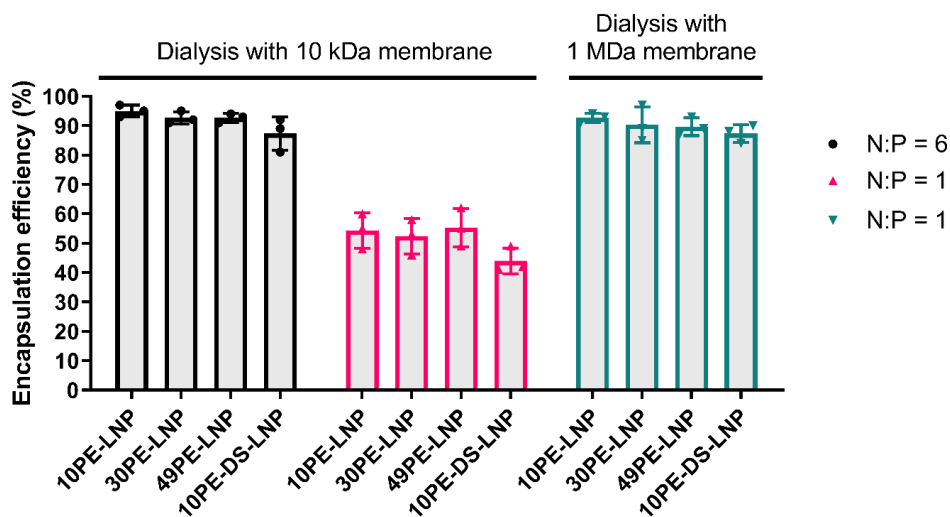


Figure S5. Encapsulation efficiency (%) of all formulations formulated at NP ratios of 6 and 1. For the NP ratio of 1, dialysis performed with 1 MDa membranes (Spectra-Por® Float-A-Lyzer® G2, Thermo Scientific) shows the efficient removal of non-encapsulated siRNA over dialysis with 10 kDa membranes (Slide-A-Lyzer™, Thermo Scientific). Dialysis time was 48 hours in all cases. Bar plots and error bars represent the average and standard deviation from a triplicate of independent assemblies.

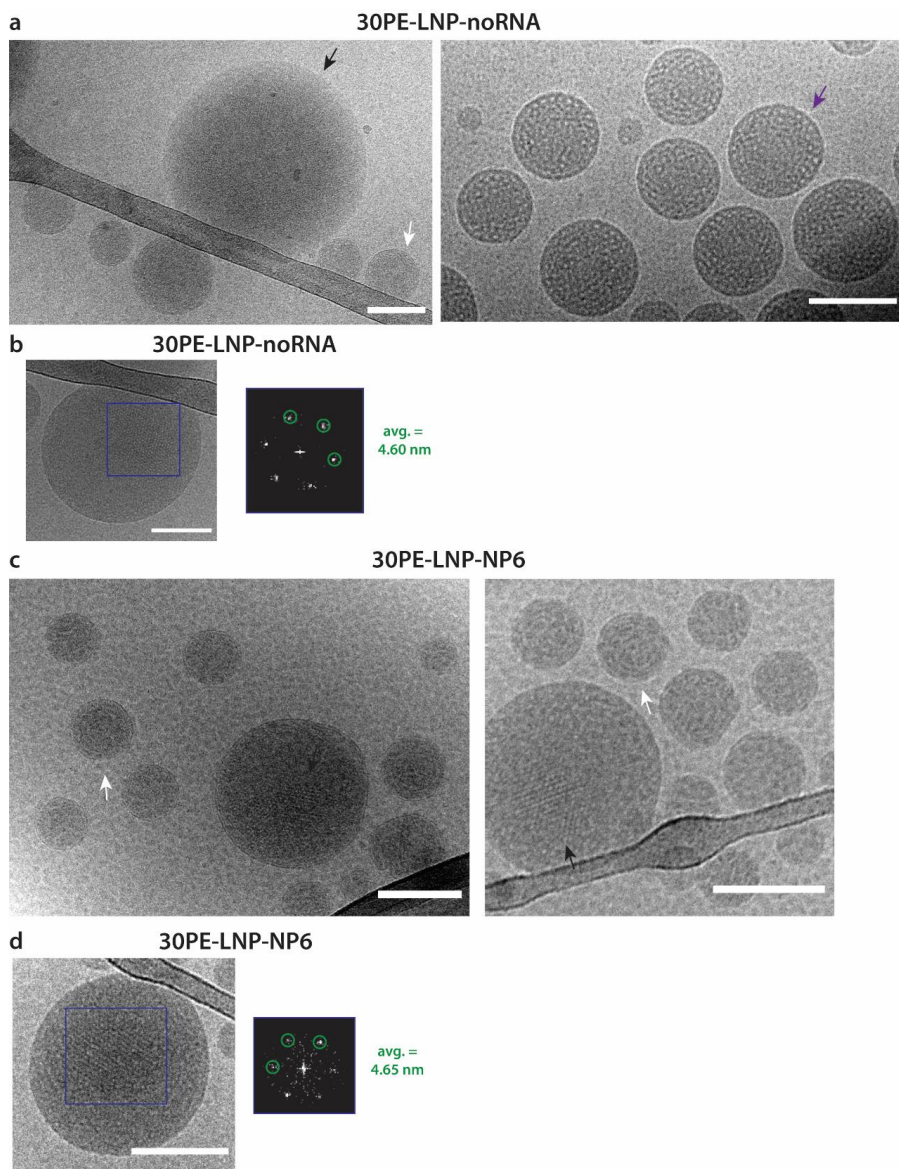


Figure S6. CryoTEM images of 30PE-LNP-NP6 and 30PE-LNP-noRNA. (a-d) Imaging was performed on a 120 kV Tecnai T12 as described in the Materials and Methods section. All scale bars are 100 nm. Black arrows indicate the presence of tubular inverse hexagonal structures. White arrows indicate the presence of concentric lamellar structures. Purple arrows indicate the presence of undefined lipid structures. FFT values represent the average of the [001] structure of the selected areas in individual particles.

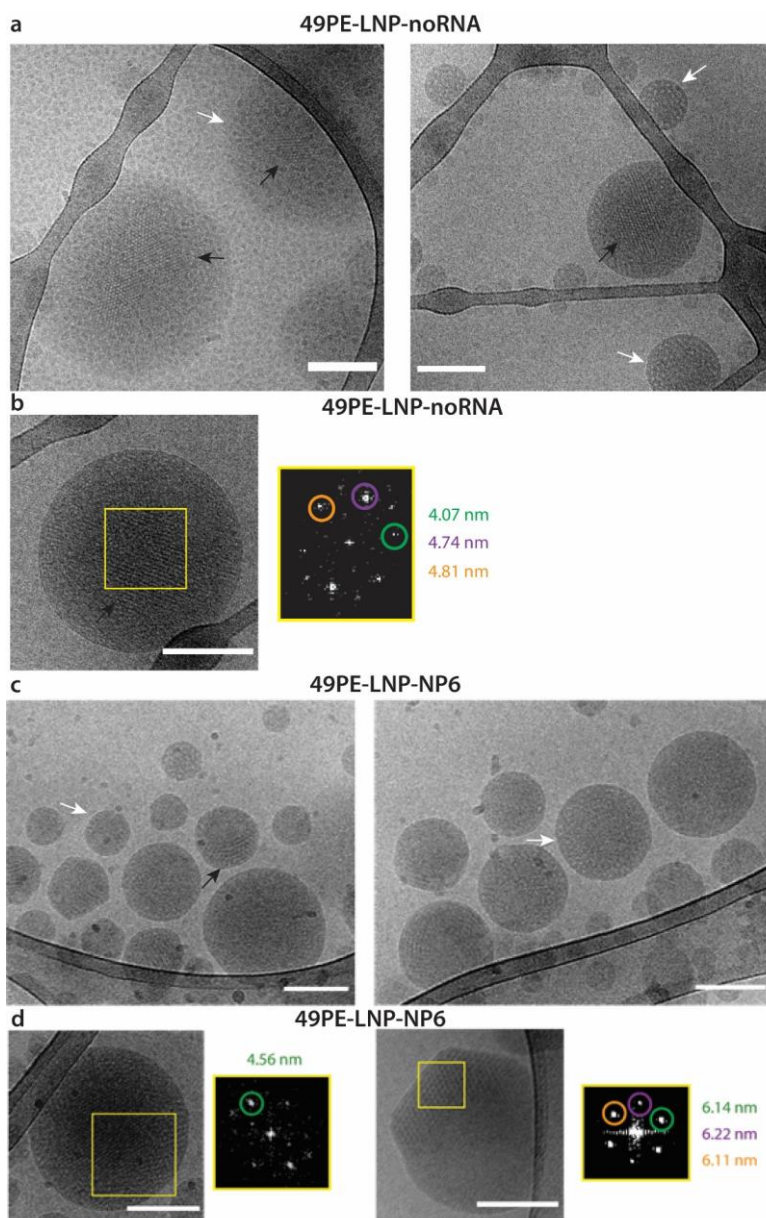


Figure S7. CryoTEM images of 49PE-LNP-NP6 and 49PE-LNP-noRNA. (a-d) Imaging was performed on a 120 kV Tecnai T12 as described in the Materials and Methods section. All scale bars are 100 nm. FFT values are matched by color in the selected areas in individual particles. Black arrows indicate the presence inverse hexagonal structures throughout the LNP core. White arrows indicate the presence of spherical structures described in Supplementary Figure 10.

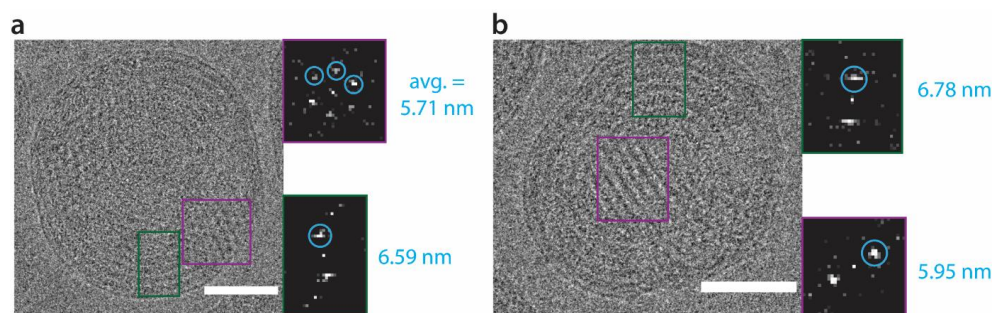


Figure S8. Co-existence of lamellar, straight line and hexagonal structures in 30PE-LNP-NP1. (a,b) cryoTEM images of 30PE-LNP-NP1 particles, showing the co-existence of structures within the same particle, along with FFT analysis of the color coded selections. Purple selections represent hexagonal or straight line structures of inverse hexagonal structures, green selections represent lamellar structures. Imaging was performed on a 300 kV Titan Krios 2 as described in the Materials and Methods section. All scale bars are 50 nm.

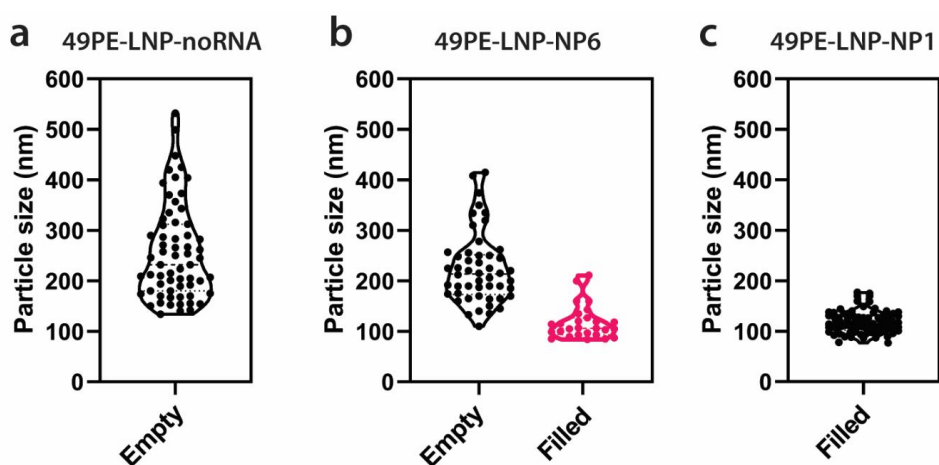


Figure S9. Correlation of filled paracrystalline inverse hexagonal phases with LNP particle size. Relation between lattice spacings show in **Figure 3b** to particle size for 49-LNP variants at different siRNA amounts. (a) 49PE-LNP-noRNA ($n = 63$, $257 \text{ nm} \pm 95 \text{ nm}$), (b) 49PE-LNP-NP6, empty ($n = 50$, $224 \text{ nm} \pm 70 \text{ nm}$) NP = 6 filled ($n = 27$, $117 \text{ nm} \pm 33 \text{ nm}$) and (c) 49PE-LNP-NP1 ($n = 81$, $118 \text{ nm} \pm 22 \text{ nm}$).

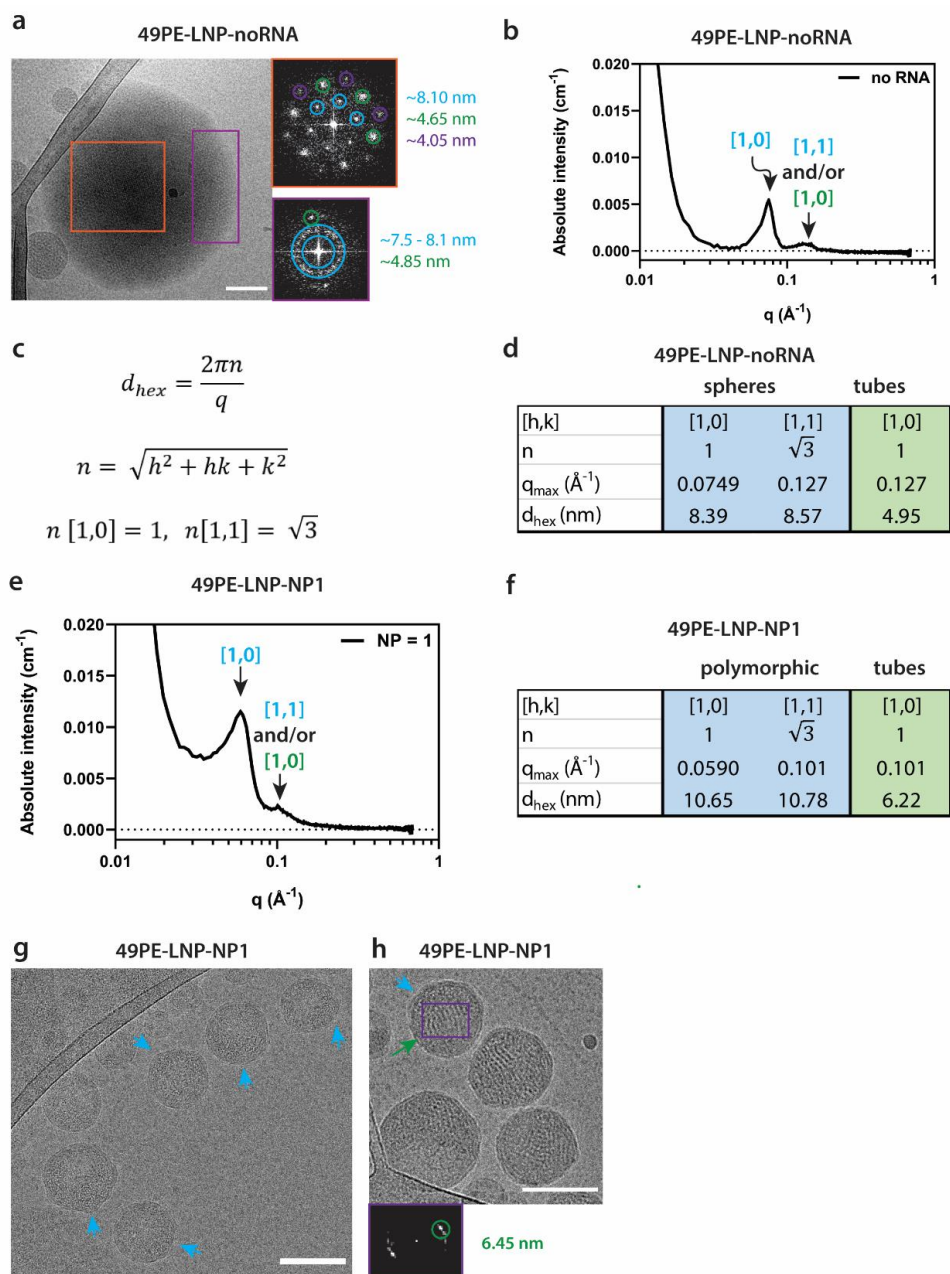


Figure S10. Comparison of identified structures in cryoTEM of 49PE-LNP to SAXS profiles. (a) CryoTEM image of large 49PE-LNP-noRNA particle showing both hexagonally packed spheres and inverse hexagonal tubular structures. (b) SAXS profile of 49PE-LNP-noRNA derived from **Figure 1f**,

with indications of Bragg peaks with Miller indices. (c) Formulas used for the calculation of the d-spacing assuming a hexagonally packed structure. (d) d-spacing calculations for 49PE-LNP-noRNA (e) SAXS profile of 49PE-LNP-NP1 derived from **Figure 1f**, with indications of Bragg peaks with Miller indices. (f) Formulas used for the calculation of the d-spacing assuming a hexagonally packed structure. (g-h) cryoTEM images of 49PE-LNP-NP1 showing polymorphic (blue arrows) and inverse hexagonal tubular structures (green arrow).

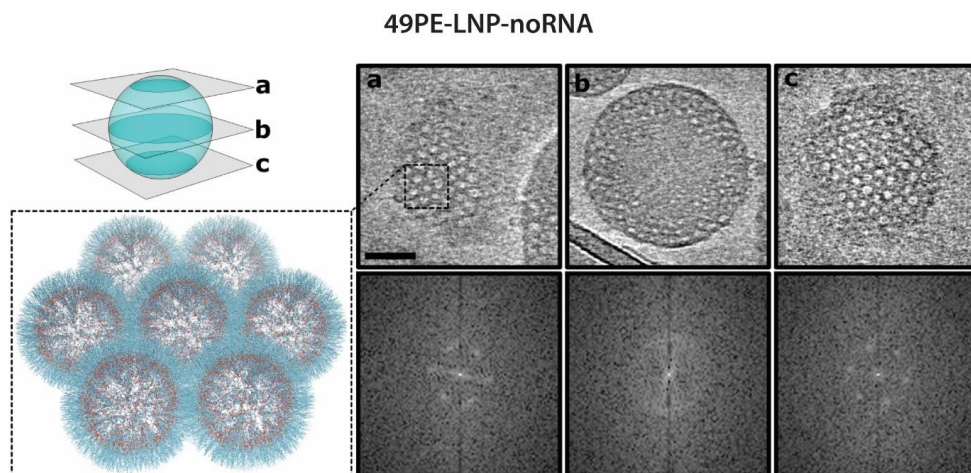


Figure S11. CryoET slices of an individual 49PE-LNP-noRNA particle. Tomographic slices through an individual 49PE-LNP-noRNA particle (cyan) at the heights indicated with (a,b,c), revealing the hexagonally packed spheres through the LNP, with an amorphous core. Model displays spheres with lipid tails pointed outwards and an average size of ~8 nm. Scale bar = 50 nm.

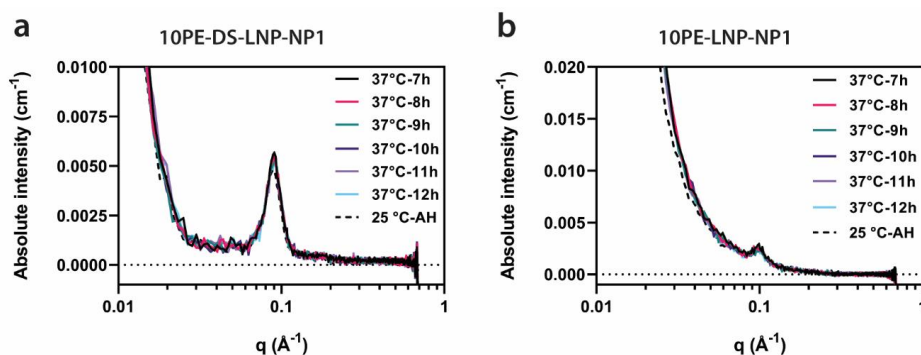


Figure S12. SAXS profiles after incubation at 37 °C for 7-12 hours. SAXS profiles at additional points of incubation at 37 °C and 25 °C after heating (AH) for (a) 10PE-DS-LNP-NP1 and (b) 10PE-LNP-NP1.

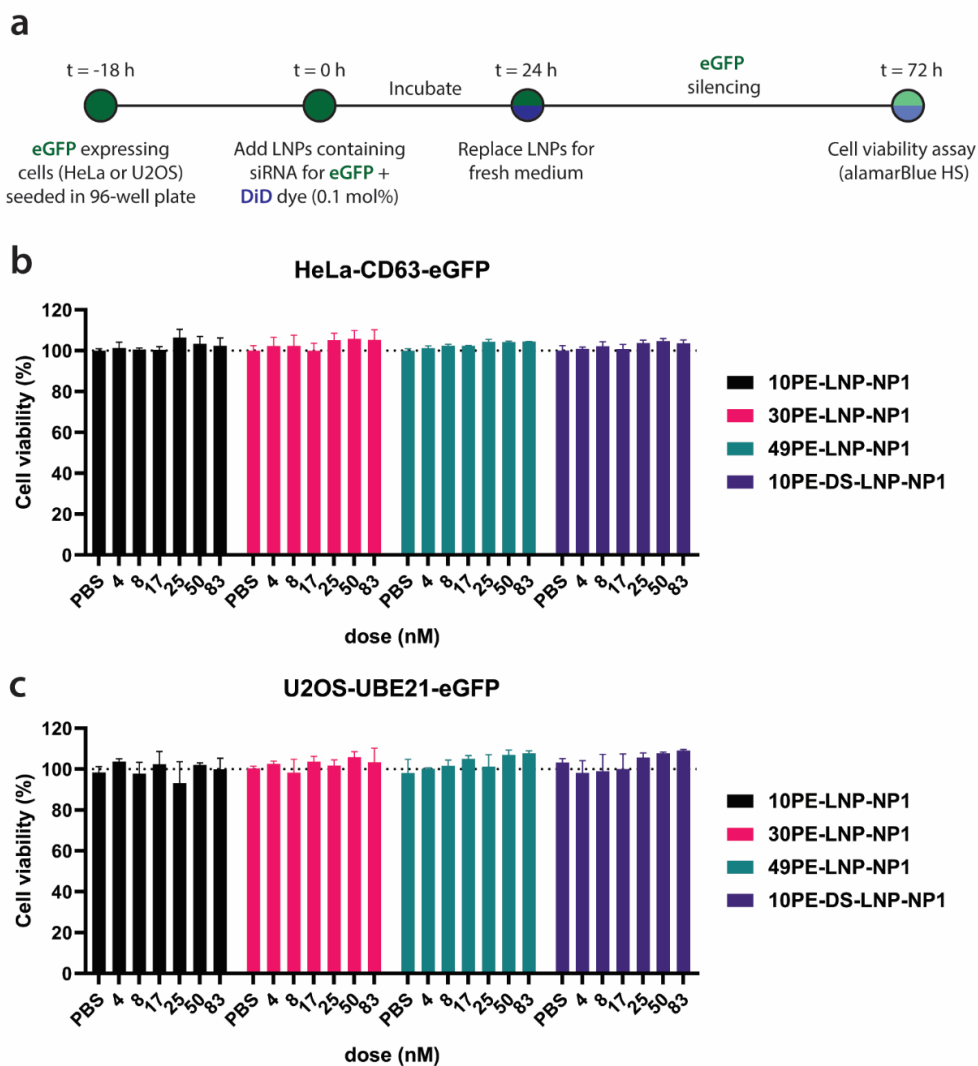


Figure S13. Cell viability study of cell lines treated with LNPs. (a) Schematic showing the timeline of the cell viability study conducted. (b-c) Results of the cell-viability assay (AlamarBlue HS) of the HeLa and U2OS cell lines.

Anionic LUVs

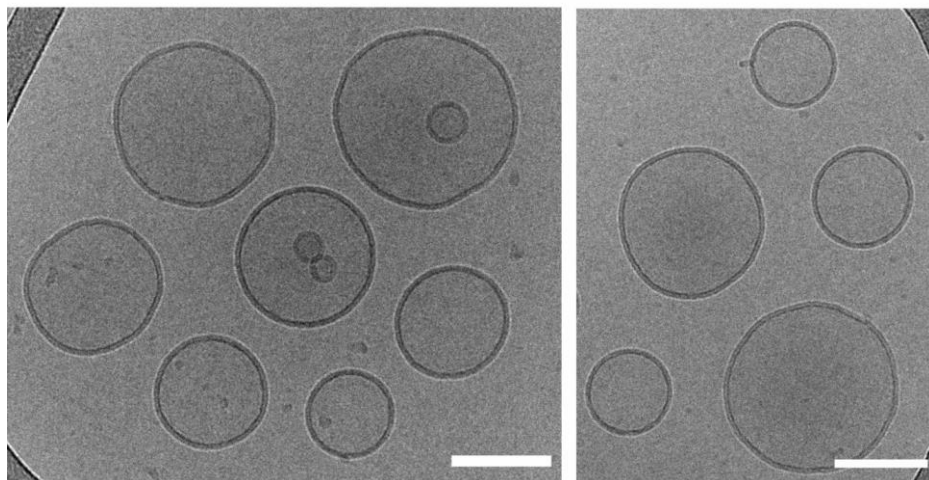


Figure S14. CryoTEM images of anionic LUVs. LUVs are composed of PC:PE:PS:Chol:PI at a ratio of 50:27:10:10:3 mol%. Sample vitrification in the mixture of 100 mM citrate buffer and PBS (1:2 vol:vol) at 37 °C as described in the Materials and Methods section. All scale bars are 100 nm.

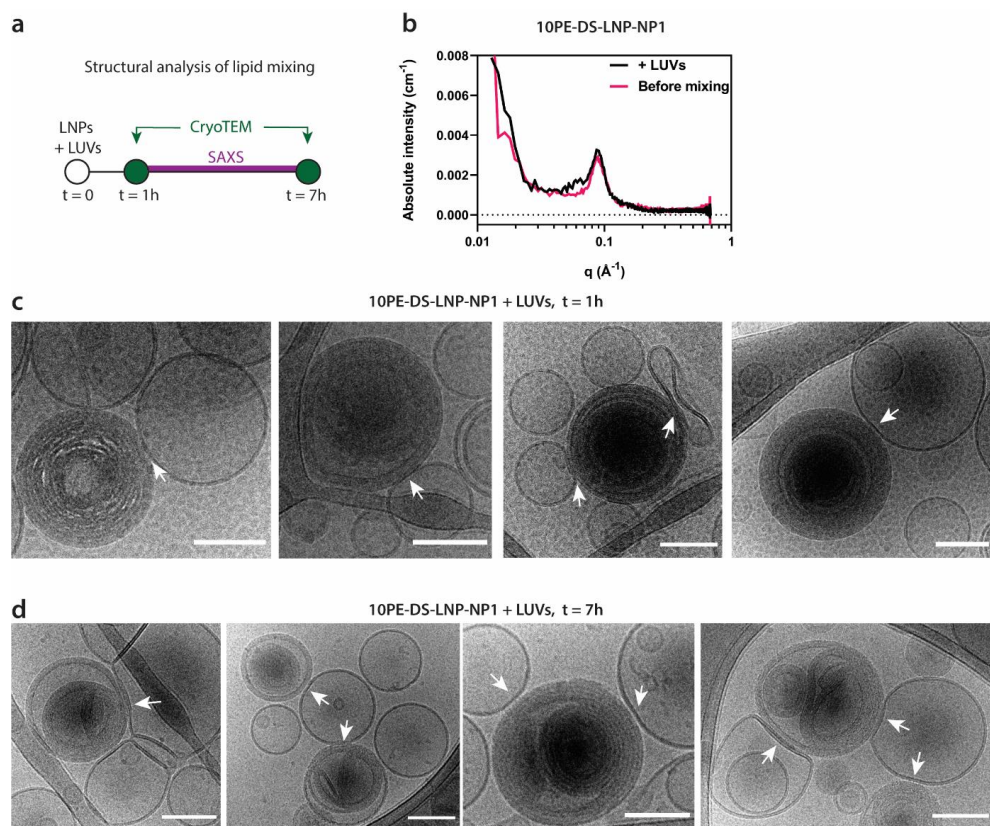


Figure S15. Interaction of 10PE-DS-LNP-NP1 with anionic LUVs. (a) Schematic representation depicting the experiments for the structural analysis of the LNP-LUV interaction. (b) SAXS profile of 10PE-DS-LNP-NP1 incubated with anionic LUVs. (c,d) CryoTEM images of 10PE-DS-LNP-NP1 incubated with anionic LUVs at pH 6 after 1 hour ($t = 1\text{h}$) and after 7 hours ($t = 7\text{h}$). White arrows indicate positions where docking between LNPs and LUVs is observed. All scale bars are 100 nm.

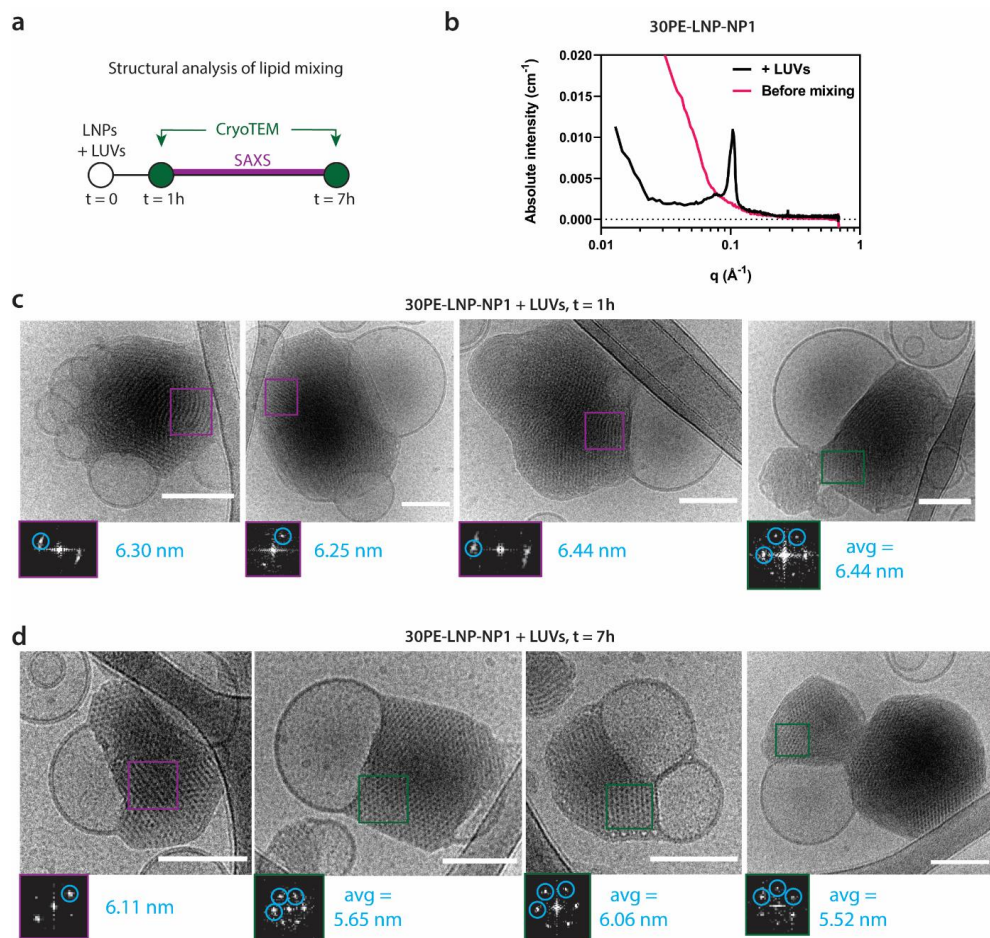


Figure S16. Interaction of 30PE-LNP-NP1 with anionic LUVs. (a) Schematic representation depicting the experiments for the structural analysis of the LNP-LUV interaction. (b) SAXS profile of 30PE-LNP-NP1 incubated with anionic LUVs. (c,d) CryoTEM images and FFTs of selected areas of 30PE-LNP-NP1 incubated with anionic LUVs after 1 hour ($t = 1h$) and after 7 hours ($t = 7h$). All scale bars are 100 nm.

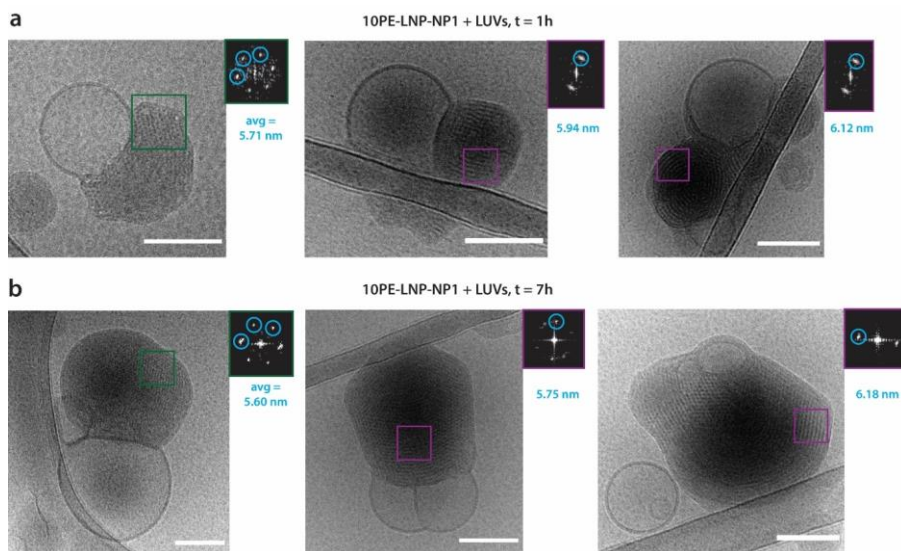


Figure S17. Additional cryoTEM images of 10PE-LNP-NP1 interaction with anionic LUVs. (a,b) Additional CryoTEM images and FFTs of selected areas of 10PE-LNP-NP1 incubated with anionic LUVs after 1 hour (t = 1h) and after 7 hours (t = 7h). All scale bars are 100 nm.

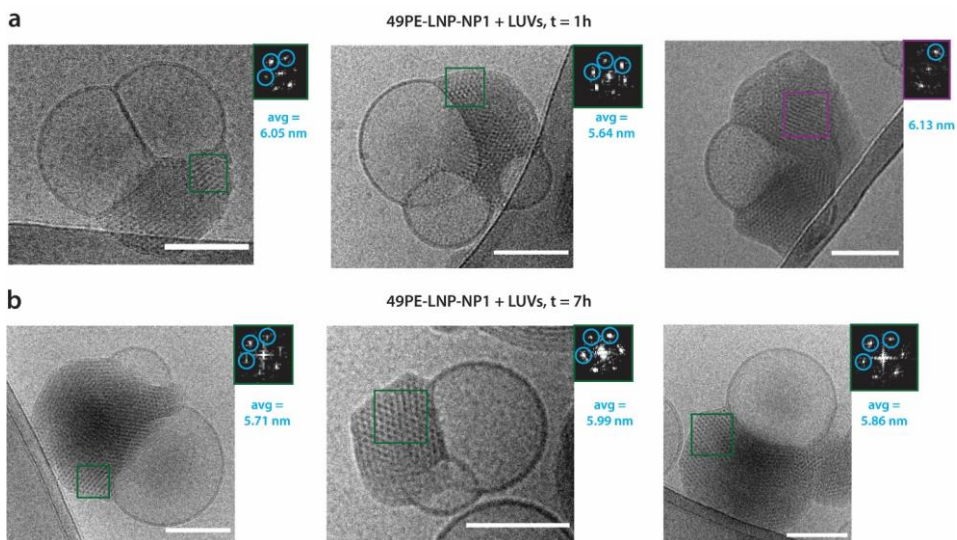


Figure S18. Additional cryoTEM images of 49PE-LNP-NP1 interaction with anionic LUVs. (a,b) Additional CryoTEM images and FFTs of selected areas of 49PE-LNP-NP1 incubated with anionic LUVs after 1 hour (t = 1h) and after 7 hours (t = 7h). All scale bars are 100 nm.

2. Materials and methods

Reagents

Cholesterol was purchased from Sigma-Aldrich (Zwijndrecht, The Netherlands). 1,1'-Diocadecyl-3,3,3',3'-Tetramethylindodicarbocyanine (DiD) was purchased from Thermo Fisher Scientific (Landsmeer, The Netherlands). L- α -phosphatidylserine (Brain, Porcine, PS), L- α -phosphatidylcholine (Brain, Porcine, PC), L- α -phosphatidylethanolamine (Brain, Porcine, PE), L- α -phosphatidylinositol (Brain, Porcine, PI), 1,2-dioleoyl-*sn*-glycero-3-phosphoethanolamine-N-(7-nitro-2-1,3-benzoxadiazol-4-yl) (PE-NBD), 1,2-dioleoyl-*sn*-glycero-3-phosphoethanolamine-N-(lissamine rhodamine B sulfonyl) (PE-LR), 1,2-dioleoyl-*sn*-glycero-3-phosphoethanolamine(DOPE), 1,2-dimyristoyl-*sn*-glycero-3-phosphoethanolamine-N-methoxypolyethylene glycol-2000 (DMPE-PEG2k), 1,2-dioleoyl-3-dimethylammonium-propane (DODAP) and 1,2-distearoyl-3-dimethylammonium-propane (DSDAP) were purchased from Avanti Polar Lipids through Merck. All siRNA molecules were purchased from Integrated DNA Technologies (Leuven, Belgium) either through custom synthesis or from the catalog, exact sequences can be found in Supplementary Table 1. HeLa-CD63-eGFP, U2OS-UBE21-eGFP cell line were cultured in DMEM growth medium (Sigma Aldrich) containing sodium bicarbonate, without sodium pyruvate and HEPES, was supplemented with 10% fetal bovine serum (Sigma), 1% of L-glutamine (Thermo Fisher Scientific) and 1% penicillin/streptomycin (Thermo Fisher Scientific), at 37 °C in the presence of 5% CO₂. Opti-MEM reduced serum medium (Thermo Fisher Scientific) was applied among transfection experiments.

Self-assembly of Lipid Nanoparticles (LNPs)

Lipids were combined at the desired molar ratios and concentrations from stock solutions (1-10 mM) in chloroform:methanol (1:1). Solvents were evaporated under a nitrogen flow and residual solvent was removed *in vacuo* for at least 30 minutes. The lipid film was dissolved in absolute ethanol and used for the assembly. A solution of siRNA was made by dissolving siRNA in 50 mM citrate buffer (pH = 4, RNase free). The solutions were loaded into two separate syringes and connected to a T-junction microfluidic mixer. The solutions were mixed in a 3:1 flow ratio of siRNA against lipids (1.5 mL/min for siRNA solution, 0.5 mL/min for lipids solution). After mixing, the solution was directly loaded in a 10k MWCO dialysis cassette (Slide-A-Lyzer™, Thermo Scientific) or a 1 MDa MWCO dialysis cassette (Spectra-Por® Float-A-Lyzer® G2, Thermo Scientific) and dialyzed against Phosphate Buffered Saline (PBS, 137 mM NaCl, 2.7 mM KCl, 8 mM Na₂HPO₄, and 2 mM KH₂PO₄) overnight. After overnight dialysis, siRNA encapsulation efficiency was determined by

Quant-iT™ RiboGreen™ RNA Assay Kit as described below. If necessary, LNPs were concentrated using 100k MWCO centrifugal filters (Amicon® Ultra, Merck). Adjustment and dilution of LNPs was done with Dulbecco's PBS (Merck).

RNA encapsulation and dose determination assay

Encapsulation efficiency (EE%) defined as the amount of siRNA encapsulated versus the free siRNA in solution after dialysis was determined using a Quant-iT™ RiboGreen™ RNA Assay Kit (Invitrogen). For the determination of non-encapsulated siRNA, LNPs after dialysis were diluted with the supplied 1 x TE buffer (RNase free) and treated with the RiboGreen™ reagent. For the determination of the complete amount of siRNA in the sample, LNPs after dialysis were treated with 1% Triton X-100 in TE buffer (RNase free) and incubated for 15 minutes followed by dilution with TE buffer and treatment with the RiboGreen™ reagent. Both conditions were performed in triplicate to ensure proper lysis of the LNPs. Change in fluorescence was measured in 96-well plates using a TECAN Infinite M1000 Pro microplate reader and the percentage of siRNA encapsulation (EE%) was determined using the fraction of $(F_{\text{total RNA}} - F_{\text{free RNA}}) / F_{\text{total RNA}} \times 100\%$. Quantification of the dose was determined using a similar protocol, in which the RiboGreen™ fluorescence was determined of concentrated LNPs. The supplied RNA standards were used to generate a standard curve and the concentration of encapsulated mRNA was determined by inserting $(F_{\text{total RNA}} - F_{\text{free RNA}})$ in the standard curve.

Cryogenic Transmission Electron Microscopy (cryoTEM)

Vitrification of concentrated LNPs (~10-15 mM) was performed using a Leica EM GP operating at 22°C or 37°C and 95% relative humidity. Sample suspensions were placed on glow discharged 150 µm lacey carbon films supported by 200 mesh copper grids (Electron Microscopy Sciences). In general, optimal results were achieved using a 30-60 second pre-blot and a 1 second blot time. After vitrification, sample grids were maintained below -170 °C and imaging was performed on a Tecnai T12 (ThermoFisher) with a biotwin lens and LaB6 filament operating at 120 keV equipped with an Eagle 4K x 4K CCD camera (ThermoFisher). Images were acquired at a nominal underfocus of -2 to -3 µm (49,000x magnification) with an electron dose of ~2000 e⁻·nm⁻².

For higher resolution cryoEM, grids were loaded into a Titan Krios transmission electron microscope (FEI Company) equipped with a field emission gun operating at 300 kV and were imaged using a Falcon 3 direct electron detector (FEI). Images were acquired a

calibrated magnification of 75,000 \times with a nominal underfocus of -1 to -2 μm and an electron dose of $\sim 2000\text{ e}^- \cdot \text{nm}^{-2}$.

Single particle analysis of cryoTEM data

Single particles were chosen based on the presence of structure formation from a collection of 2D cryoTEM images, divided over three independent assemblies of the same LNP formulation. Only particles present in vitreous ice were considered for analysis. Regions of interest from individual particles and the fast Fourier transform (FFT), as well as the determination of particle size was performed using the Fiji distribution of ImageJ.¹

Cryogenic Electron Tomography (cryoET)

Samples for cryoET were prepared as described for 2D cryoTEM, but with the addition of BSA coated 10 nm gold beads immediately prior to vitrification to act as fiducial markers for tomogram reconstruction. Tilt series were collected using Tomo 4.0 (FEI) on a Titan Krios at a magnification of 75,000 \times , for a final pixel size 1.87 $\text{\AA}/\text{pixel}$, using a continuous tilt series from -60° to $+60^\circ$ with increments of 2° and an electron dose of $\sim 200\text{--}250\text{ e}^-/\text{nm}^2$ per tilt image. Focusing to -4 to $-5\text{ }\mu\text{m}$ was performed every second image acquisition using a low-dose routine. Tomograms were processed using IMOD software,² using fiducial tracking and reconstructed with both weighted back-projection and 5 iterations of a SIRT-like filter within IMOD to enhance contrast. Tomograms were visualised and analysed using a combination of IMOD and UCSF Chimera.³

Model building

DOPE and DODAP lipids were built using PyMOL,⁴ before parametrization in eLBOW within Phenix.^{5,6} Lipids were relaxed into varied appropriate geometries using ISOLDE within UCSF ChimeraX.^{7,8} UCSF Chimera was used to build models of siRNA and lipid-siRNA structures.

Small Angle X-Ray Scattering (SAXS)

SAXS measurements were performed in transmission mode on a SAXSLAB GANESHA system with a Pilatus 300K solid-state photon-counting 2D detector using a high brilliance Microfocus Cu Source, Xenocs Genix3D, wavelength 1.54184 \AA . The LNPs ($\sim 12\text{ mM}$) were loaded into 2mm lockable thin wall capillaries and measured at a q -range of $0.0129\text{--}0.6870\text{ }\text{\AA}^{-1}$ with an exposure time of 6 hours. Prior to each measurement series, a silver behenate standard was used to correct for deviations in the sample to detector distance. For

temperature dependent experiments, the temperature was equilibrated to 25 °C or 37 °C for 30 minutes prior to measurement. The measured SAXS profiles are displayed as the average intensity $I(q)$ vs. the q -range. For kinetic temperature experiments, the measurement time was divided into the average intensity of 1-hour sections.

Assembly of large unilamellar vesicles (LUVs)

LUVs were assembled using a combination of freeze-thaw cycles and extrusion. Lipids were combined from stock solutions (2-10 mM) in chloroform to achieve a lipid composition of PC:PE:PS:Chol:PI of 50:27:10:10:3 mol% or PC:PE:PS:Chol:PI:PE-NBD:PE-LR of 50:24:10:10:3:1.5:1.5 mol%. The solvent was evaporated from the mixture under a nitrogen flow, followed by removal of trace solvents *in vacuo* for at least 1 hour. The resulting lipid film was hydrated with either 100 mM citrate buffer (pH = 5.5) or phosphate buffered saline (PBS, pH = 7.3), to achieve the desired total lipid concentration (10-20 mM) and vortexed until the entire lipid film was fully suspended in solution. The suspension was subjected to seven freeze-thaw cycles. In each cycle, the mixture was frozen completely with liquid nitrogen and left to thaw at room temperature, followed by vigorous mixing to ensure complete thawing. After these cycles, the mixture was extruded at 40 °C (Mini-extruder, Avanti Polar Lipids, Alabaster, US). The mixture was passed 11 times through a 200 nm polycarbonate (PC) membrane (Nucleopore Track-Etch membranes, Whatman). All liposome formulations were stored at 4 °C and used within 2 days.

Lipid mixing determined by Fluorescence Resonance Energy Transfer (FRET)

For the determination of lipid mixing efficiency by FRET, LUVs with a composition of PC:PE:PS:Chol:PI:PE-NBD:PE-LR of 50:24:10:10:3:1.5:1.5 mol% were prepared in 100 mM citrate buffer (pH = 5.5) or PBS (pH = 7.4) as described above. The LUVs were diluted with their respective buffers to 250 μ M and 100 μ L was transferred to black F-bottom chimney 96-well plates (Greiner®). The LUVs were heated to 37 °C prior to further use. For the control serving as 100% lipid mixing, 20 μ L of 1% Triton X-100 in H₂O was added followed by the addition of 80 μ L PBS. For the control serving as 0% lipid mixing, 100 μ L PBS was added to the LUVs. LNPs were assembled and diluted in PBS (pH = 7.4) to 500 μ M and 100 μ L was added to the acceptor LUVs, yielding a final concentration 125 μ M LUVs and 250 μ M LNPs. In the case where 100 mM citrate buffer was used for the LUVs, the final pH was ~6.0. All of the conditions were performed in triplicate. After addition of the LNPs, the dequenching of the PE-NBD signal was measured every 15 seconds for 25 minutes using a TECAN Infinite M1000 Pro microplate reader (λ : excitation = 460 nm \pm 10 nm, emission = 535 nm \pm 10 nm).

CryoTEM and SAXS analysis of lipid mixing

For the assessment of lipid mixing with cryoTEM and SAXS analysis, LUVs with a composition of PC:PE:PS:Chol:PI of 50:27:10:10:3 mol% were prepared in 100 mM citrate buffer (pH = 5.5) at a concentration of 20 mM as described above. LNPs were prepared as described before and concentrated to ~20 mM. The LUVs and LNPs were mixed at a volumetric ratio of 1:2 respectively, and incubated at 37 °C. For cryoTEM, samples were vitrified after 1 hour of incubation as described above. In the case of SAXS measurements, the mixture of LUVs and LNPs were loaded into capillaries and equilibrated at 37 °C for 1 hour prior to the start of the measurement, as described above. The presented data is of the mixed samples minus the background of LUVs in citrate buffer mixed with PBS (without LNPs) at the same final concentration.

Cell transfection and FACS experiments

HeLa-CD63-eGFP, U2OS-UBE21-eGFP were seeded in 96-well plate at the density of 1×10^4 cells/well on the day before, different concentrations of siRNA-GFP encapsulated LNPs (0 – 83 nM) in 100 μ L Opti-MEM medium were added to the cells and incubated for 24 h, then the medium was removed and refreshed with new Opti-MEM for continuous 48 h culturing. After 72h incubation, cells were digested, collected and resuspended in PBS for FACS measurements (Guava easyCyte Flow Cytometers). DiD mean fluorescence intensities (Red-R channel) was quantified as the uptake of LNPs into cells. The eGFP expression (GFP MFI, Green-B channel) of all LNP treated cells are relative to PBS treated cells, for which the values are set as 100%.

Cell viability assay

HeLa-CD63-eGFP, U2OS-UBE21-eGFP cells were seeded 96-well plate at a density of 1×10^4 cells per well the day before, then followed with the same procedure as the transfection with different concentrations of LNPs determined by the Ribogreen RNA assay. After 72 h incubation, cell viability reagent alamarBlue HS solution (10 μ L, ThermoFisher) was added to the medium (100 μ L) and incubated for another 4 h at 37°C. After 4 h, the absorbance at 570 nm (using 600 nm as a reference wavelength) was measured at room temperature using a Tecan infinite M1000, which was shaken for 60 s before measurement (2 mm linearly, 654 rpm). The cell viability was normalized with control (blank HeLa-CD63-eGFP, U2OS-UBE21-eGFP cells), which was set at 100% cell survival. All conditions were performed in triplicate.

3. References

1. Schindelin, J. *et al.* Fiji: an open-source platform for biological-image analysis. *Nat. Methods* **9**, 676–682 (2012).
2. Mastronarde, D. N. & Held, S. R. Automated tilt series alignment and tomographic reconstruction in IMOD. *J. Struct. Biol.* **197**, 102–113 (2017).
3. Pettersen, E. F. *et al.* UCSF Chimera--a visualization system for exploratory research and analysis. *J. Comput. Chem.* **25**, 1605–1612 (2004).
4. Schrodinger LLC. The PyMOL Molecular Graphics System, Version 1.8. (2015).
5. Afonine, P. V. *et al.* Real-space refinement in PHENIX for cryo-EM and crystallography. *Acta Crystallogr. Sect. D, Struct. Biol.* **74**, 531–544 (2018).
6. Moriarty, N. W., Grosse-Kunstleve, R. W. & Adams, P. D. electronic Ligand Builder and Optimization Workbench (eLBOW): a tool for ligand coordinate and restraint generation. *Acta Crystallogr. D. Biol. Crystallogr.* **65**, 1074–1080 (2009).
7. Croll, T. I. ISOLDE: a physically realistic environment for model building into low-resolution electron-density maps. *Acta Crystallogr. Sect. D, Struct. Biol.* **74**, 519–530 (2018).
8. Pettersen, E. F. *et al.* UCSF ChimeraX: Structure visualization for researchers, educators, and developers. *Protein Sci.* **30**, 70–82 (2021).

